REPORT NO. 632-3-170
CONTRACT NAS 8-27419

DICA

DESIGN AND DEVELOPMENT OF PRESSURE AND REPRESSURIZATION PURGE SYSTEM FOR REUSABLE SPACE SHUTTLE MULTILAYER INSULATION SYSTEMS

PHASE REPORT

GENERAL DYNAMICS
Convair Aerospace Division

CR-123942

(NASA-CR-123942) DESIGN AND DEVELOPMENT OF PRESSURE AND REPRESSURIZATION PURGE SYSTEM FOR REUSABLE SPACE SHUTTLE MULTILAYER INSULATION (General Dynamics/Convair) 31 Oct. 1972 96 p CSCL 22A G3/31
N73-12914
Unclas 16765

PRECEDING PAGE BLANK NOT FILMED

FOREWORD

This report describes the work completed by the Convair Aerospace Division of General Dynamics on Tasks 3 and 4 of Contract NAS8-27419. The work was administered under the technical direction of Mr. J. Walters, S&E-ASTN-ESV of the George C. Marshall Space Flight Center.

In addition to the project leader Mr. A. B. Walburn, the following Convair Aerospace personnel were major contributors to the study.

R. Adset	Materials Research
J. Bodle	Design
H. Brittain	Engineering Test
G. Copeland	Engineering Test
J. Dyer	Stress Analysis
B. Ganoe	Engineering Test
R. Jennings	Thermodynamics
L. Siden	Design
I. Tubb	Manufacturing Research

TABLE OF CONTENTS

TABLE OF CONTENTS, Contd

LIST OF FIGURES

LIST OF FIGURES, Contd

LIST OF FIGURES

LIST OF FIGURES, Contd

LIST OF TABLES

PRECEDING PAGE BLANK NOT FILMED

NOMENCLATURE

A	area, m^2 (ft^2)
f	seam width to depth ratio function = 0.0182
$\mathcal{F}$	radiation interchange factor
K	thermal conductivity, watts/cm- K (Btu/hr-ft- R)
ℓ	conduction path length, m (ft)
M	molecular weight
n	number of radiation shields
P	pressure, Torr
Q	heat transfer rate, watts (Btu/hr)
R	Universal gas constant
T	temperature, K (R)
α	accommodation coefficient (0.8)
γ	specific heat ratio
δ	seam depth, m (ft)
ϵ	emittance
σ	Stefan-Boltzmann Constant

Subscripts

c	cold layer
cond	conduction
EF	effective
h	hot layer
rad	radiation
s	seam
t	tuft
tot	total
1	unflocked layer
2	flocked layer

PRECEDING PAGE BLANK NOT FILMED

SUMMARY

This report covers the work performed under Task 3, Component and Material Evaluation and Task 4, Purge System Design, of NASA/MSFC Contract NAS8-27419 by Convair Aerospace Division of General Dynamics, San Diego, California. The accomplishments of each task are summarized below.

TASK 3 - COMPONENT AND MATERIAL EVALUATION

The component and material evaluation task has been completed. The task consisted primarily of the experimental determination of purge bag materials properties, development of purge bag manufacturing techniques, experimental evaluation of a subscale purge bag under simulated operating conditions and the experimental evaluation of the purge pin concept . r MLI purging.

The basic purge bag material, epoxy fiberglass bounded by skins of FEP Teflon, showed no significant permeability to helium flow under normal operating conditions. The tensile strength of the bag material at room temperature averaged 262 MN/m^2 and was degraded a maximum of 17% when exposed to a boiling water environment and subsequently tested at 450K. Two adhesive systems (Crest 7343 and Epon 934) were tested in both peel and shear for use in joining purge bag sections. It was found that the Crest adhesive had virtually no strength in an environment of 450K. The shear strength of the Epon 934 adhesive exceeded 1.52 MN/m^2 (220 psi) at 450K and it was selected for use in purge bag fabrication. Additional property test data were also obtained for a new experimental DuPont material, PRD-49, being investigated for possible future use as an improved purge bag material. The tensile strength of the PRD-49 was 24% higher than the epoxy fiberglass at elevated temperature (450K). The total linear thermal expansion coefficient of the Epoxy impregnated PRD-49 averaged less than $-1.5 \times 10^{-6}\ K^{-1}$.

Purge bag small scale manufacturing tests were conducted to develop tooling and fabrication techniques for use in full scale bag manufacture. A purge bag material layup technique was developed whereby the two plys of epoxy fiberglass enclosed between skins of FEP Teflon are vacuum bag cured in an oven in a single operation. The material is cured on a tool with the shape of a purge bag half. Plastic tooling was selected for use in bag fabrication. A model purge bag 0.6 m in diameter was fabricated and subjected to a series of structural and environmental tests simulating various flight type environments. Pressure cycling tests at high (450K) and low (200K) temperature as well as acoustic loading tests were performed. The purge bag concept proved to be structurally sound and was used for the full scale bag detailed design model.

A series of tests were run to demonstrate and verify the purge pin gas injection concept for purging MLI of condensable gases. Purge pin radial gas flow injection, the effects of purge pin spacing along the MLI blanket, and the effects of purge gas flow rates were evaluated. Tests were conducted using Superfloc and perforated aluminized Mylar/Dacron netting MLI blankets. Data resulting from each of the tests were used to obtain purge gas concentration profiles, blanket purge gas equilibrium concentration values, MLI blanket purging histories and comparison with previously predicted purge values. The profile test results demonstrate that the radial flow distribution around a purge pin is uniform for both the Superfloc and aluminized Mylar/Dacron net MLI blanket systems. Neither insulation purged to less than 1% residual condensable gases at the edges or ends of the blankets when the blankets were not enclosed by a simulated purge bag. The use of a simulated purge bag allowed complete purging to occur, however, the aluminized Mylar/Dacron net MLI required a minimum of twice the purge gas volumetric flow rate as the Superfloc to achieve 1% residual condensable gas concentration in the MLI blanket. Three purge pins per gore blanket configuration was selected as most applicable to use on the full scale tank test program.

It was concluded from the test results that approximately 5 minutes will be required to purge the full scale test tank prior to cryogen filling. A comparison of the purging test results with previously obtained analytical predictions indicates a very good agreement between prediction and test.

TASK 4 - PURGE SYSTEM DESIGN

The completed purge system design task includes both the development of purge system detailed designs and the performance analysis of the test article design. The analyses conducted include a parametric MLI gold thickness requirement study, a purge and repressurization gas flow rate analysis, a purge plenum venting and repressurization analysis and a complete test system thermal performance analysis. The amount of gold required on each MLI sheet was calculated to be 400 Å per side. The study showed that the gold thickness requirement was not extremely sensitive to modest changes in average blanket temperature or allowable radiation transmittance. The test article helium purge or repressurization gas flow rate requirement was established by the re-entry repressurization condition at 9.0 Kg/hr minimum. This number with a factor of safety was then used to size fluid loop hardware. Analysis of the pressure loads on the existing test tank purge plenums during repressurization indicated that additional stiffness was required to withstand the transient pressure loads. Rework designs were thus made for the fiberglass plenums.

The helium pressurization fluid loop hardware is designed to operate in a manual purge mode, a manual vent mode or an automatic repressurization mode. The design of the MLI purge and repressurization system consists of details of the MLI and purge bag, hardware description, assembly procedures, weights, materials, operating conditions, area and volume determinations and operating procedures. The design consists of the cryogenic test tank, fiberglass purge plenums, the Superfloc MLI layup applied in 24 gore sections (2 blankets) and flat end blankets, the fiberglass purge bag, a rigid penetration panel which mounts the fluid loop hardware and instrumentation fittings and acts as a tank access door and the fiberglass support struts. The fairing is equipped with purge pins for distributing gas between the MLI layers. The general arrangement for the system as well as a tabular system description are shown below.

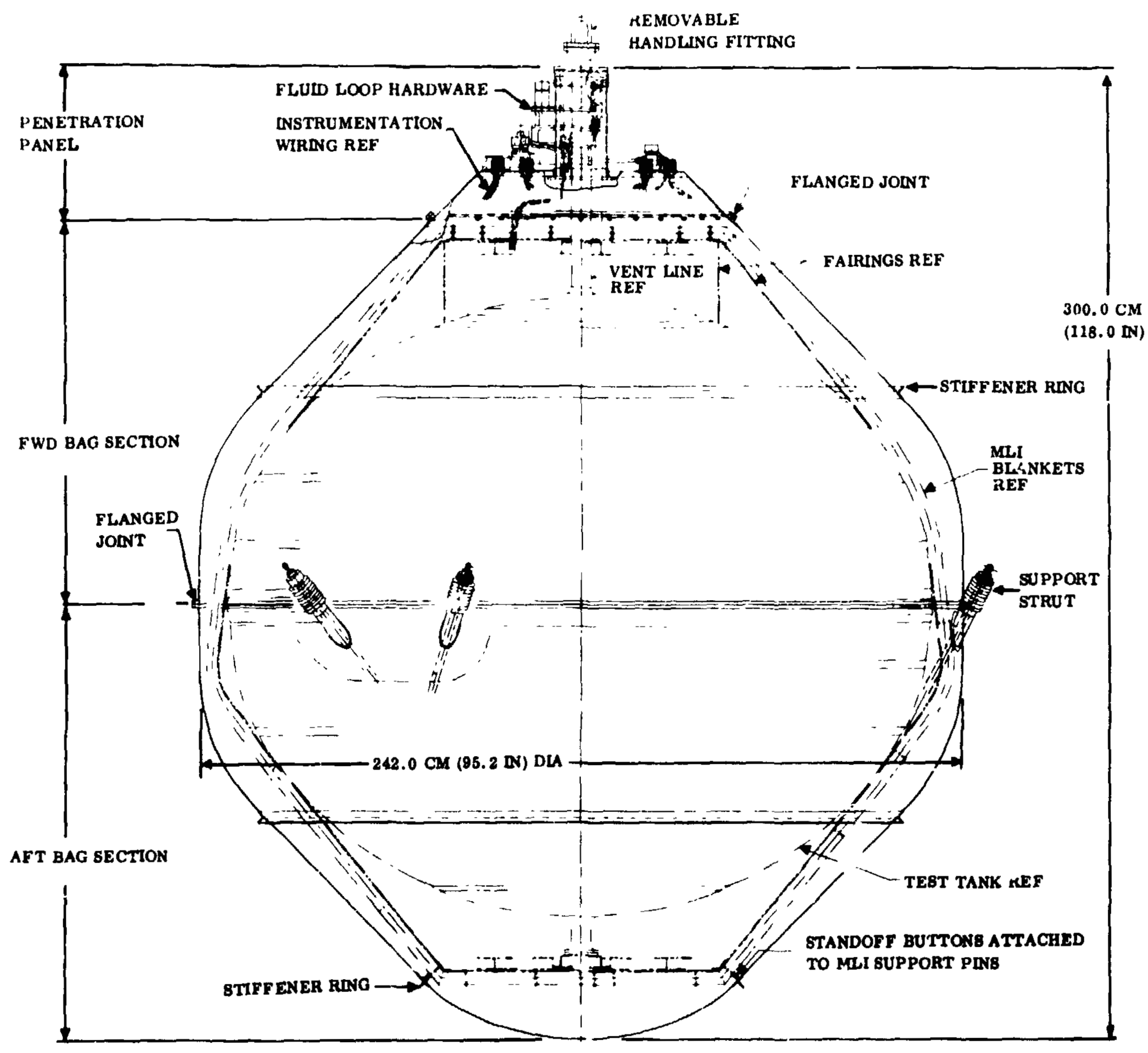

MLI Purge/Repressurization General Arrangement

In addition the details of the test tank thermal performance analysis are also shown. The system as designed predicts a 30% improvement in thermal performance over an aluminized Mylar Superfloc system of similar design which was previously tested at Convair.

Superfloc MLI System Design and Performance Data
221 cm (87 inch) Convair Aerospace Tank

DESIGN DATA

TANK

Surface Area:	14.12 sq meters (152 ft^2)
Capacity:	4.95 cubic meters (175 ft^3)
Support System:	3 pairs of Epoxy/Fiberglass tubular struts arranged in "V" patterns.
Material:	2219-T62 Al Aly
Thickness:	1.95 mm to 3.94 mm (0.077 in to 0.155 in)
Fill, Drain and Vent:	Co-axial tube assembly. 6.35 cm (2.50 in) O.D. outer tube. 3.81 cm (1.50 in) O.D. inner tube. Material; 6061-T4 al aly, 304L CRES and Epoxy/Fiberglass.

FAIRINGS

Configuration:	Frustrum of cone at forward and aft end with stiffened flat panel at small end of cone. Ring type section at girth area. Fairing at girth seals with struts.
Material:	Epoxy/Fiberglass
Accessories:	Removable forward flat panel for access. Incorporates MLI support pins and purge pins.

MLI SYSTEM

Type of MLI:	30 gauge (0.00076 cm) double goldized Kapton Superfloc. 12 layers/cm (30 layers/inch) lay-up density. 0.00971 kg/m^2 (0.001986 lb/ft^2) per layer.
Face Sheets:	Beta glass scrim coated with pyre M.L. (preformed). 0.0888 kg/m^2 (0.0182 lb/ft^2). 0.00173 cm (0.007 in) average thickness.
Blankets:	22 core sheets and 2 face sheets/blanket. 0.523 rad (30°) preformed gores. 12 gores per blanket layer.
Quantity of Blanket Support Pins:	48 Epoxy/Fiberglass material
Quantity of Twin Pin Fasteners:	158 for outer blanket layer. 86 for inner blanket layer. Polyphenylene oxide (PPO) material.
Quantity of Coupler Pin:	24 for inner blankets. 24 for outer blankets. Coupler pin is a twin pin adapted for interconnecting the MLI blankets to the support pins. Heat leak path for two coupler pins is equal to one twin pin.
Seam Lengths:	40 meters (131 ft) per blanket layer.
Total Lay-Up Thickness:	3.82 cm (1.50 in)
Weight (Incl. Fasteners):	14.0 kg (30.8 lb)
Average Area:	16.5 sq meters (178 ft^2)

PURGE DISTRIBUTION SYSTEM

Quantity of Purge Pins:	43 PPO material.
Type of Purge Pins:	Slotted tubular type.
Gas Flow Path:	Tubular manifold supplies plenum chambers formed between tank and fairings. Plenums feed purge pins.
Purge Volume Between Tank & Bag.	2.42 cu meters (85.5 ft^3)

PURGE BAG ASSEMBLY

Fwd and Aft Bag Sections:	2 plys of 181 Epoxy/Fiberglass sandwiched between two FEP films.
Penetration Panel:	Multi ply lay-up of Epoxy/Fiberglass with one FEP film layer on inboard surfaces.
Joints Between Sections:	Bolted flange types.
Weight:	43.23 kg (95.31 lbs)

PURGE AND REPRESSURIZATION FLUID LOOP HARDWARE

Vent:	15.25 cm (6.0 in) motorized butterfly valve.
Bleed:	5.08 cm (2.0 in) motorized gate valve.
Emergency Relief:	2.54 cm (1.00 in) spring loaded poppet valve.
Supply:	0.952 cm (0.375 in) solenoid poppet valve.
Controls:	Two diaphram type pressure switches.
Weight:	11.20 kg (24.65 lbs)

THERMAL PERFORMANCE DATA

292-22K	Heat Leakage (watts)	Percent of Total
MLI	3.01	32.6
Seams	2.68	29.0
Pins	2.37	25.6
Penetrations	0.50	5.4
Residual Gas	0.40	4.2
Struts	0.29	3.2
	9.25	100.0

Heat Flux:	.56 w/m^2 (.177 Btu/hr-ft^2)
Effective Conductivity, k_{eff}:	79.3 μw/m-k (4.56×10^{-5} Btu/hr-ft-R)
MLI System ρK Product:	1.65 mW-Kg/m^4-K (5.97×10^{-5} Btu-lb/hr-ft^4 R)

1

INTRODUCTION

The use of cryogens in spacecraft requires the incorporation of a thermal protection system to minimize propellant heating and thus, increase propellant storage capability. The effectiveness of these protection systems is achieved by a series of radiation shields of low emissivity which are separated by low heat conducting spacers. Integration of such a multilayer insulation (MLI) system with vehicle tankage offers an opportunity to optimize the total structural and thermal systems of the vehicle from the standpoints of performance as well as manufacturability and maintenance. The development of the MLI and its design is strongly dependent upon the environment in which the system must function. In recent years much effort has been expended toward the development of MLI materials and design concepts applicable to derivatives of the Saturn V type space launch vehicles. These systems are characterized by single usage and moderate temperature environment requirements.

Convair Aerospace has developed a complete cryogenic propellant space storage system of Saturn V type. The system, developed under a division IRAD project, consists of a 2.21 m (87 in) diameter oblate spheroid aluminum tank insulated with 44 layers (two blankets) of aluminized Mylar Superfloc MLI and suspended by low-conductive fiberglass struts from an enclosing shroud. The total system was designed to withstand the Saturn V launch environment. A complete structural and thermal experimental program has verified that the flightweight system will meet all ground hold, boost, and space storage structural and thermal requirements.

Small-scale component and complete system tankage structural tests were conducted, including vibration, thermal and structural cycling, acoustic, and rapid evacuation tests. The tests were climaxed by a combined-environment (acceleration, vibration, thermal gradient, and rapid depressurization) test of a complete blanket insulation system on a 0.63 m (25 in) tank in the Convair Aerospace CEVAT centrifuge test facility. The CEVAT test successfully scaled up insulation system stress levels from the full-scale Saturn V vehicle to the small-size tank for proper simulation of the complete boost trajectory. Visual inspection of the system after CEVAT testing and comparison of pre-test and post-test space equilibrium boiloff measurements indicated no insulation system damage caused by the boost trajectory testing.

The complete, large-scale propellant space storage system was designed and built on the basis of scale-model test program results. It was completely tested in the 3.66 m (12 ft) diameter space simulation chamber. Tests included ground MLI purge system testing and heat leak studies, and space equilibrium thermal performance testing. The ρk product for this system at temperatures between 300 and 22 K (540 and 40 R) is 2.5×10^{-3} W kg/m^4 - K (9.02×10^{-5} Btu-lb/hr-ft^4 R).

The present insulation system is made of aluminized Mylar, which tests have shown to be unsatisfactory for the entry thermal environment of the Space Shuttle. Convair Aerospace has developed a modified Superfloc MLI concept under MSFC Contract NAS8-26129 to meet the life and environmental requirements of the shuttle vehicle. This study determined that goldized Kapton was the optimum MLI shield material. Other structural modifications were made, including new blanket pin design and material, and a complete set of performance verification component tests to verify acceptability of the system for the shuttle.

Since the Mylar Superfloc MLI system cannot withstand shuttle environmental requirements, Convair Aerospace has designed, is fabricating, and will install a completely new goldized Kapton MLI system on the 2.21 m (87 in) test tank. The new MLI system will meet all performance and structural requirements for Space Shuttle application, as defined by the results of the Cryogenic Insulation Development effort, Contract NAS8-26129.

The new MLI system by itself, however, would not provide a completely reusable propellant storage system for the Space Shuttle tankage. Because of the requirement to withstand the re-entry environment, the MLI must be repressurized during entry to neutralize the crushing atmospheric pressure loads. In addition, the MLI must be protected from repeated exposure to moisture from condensable gases in the atmosphere. An additional system was thus developed to provide: (1) ground purging of the MLI to remove condensable gases before cryogenic tanking, (2) venting of the MLI during boost and (3) repressurization of the MLI during atmospheric entry. With these functions added, the previously developed cryogenic space storage system will be completely reusable for Space Shuttle type missions.

The objective of this program is the development of a purge/repressurization system for a representative MLI system, suitable for 30 days storage of approximately 10,000 gallons LH_2 and 3700 gallons of LOX propellants and applicable to the Space Shuttle. The development of the purge system includes a survey and identification of existing suitable materials and components, concept definition, material selection and evaluation component tests, detail system design fabrication, installation and quality plans, assembly, and demonstration testing of a purge/repressurization and MLI system with cryogens. The purge/repressurization system referred to herein is defined as a purge jacket, purging requirements, valves, ducting, tubing, regulators, ground hold, and storage provisions, repressurization and pressurization techniques, and requirements necessary for ground ascent, re-entry, and landing conditions.

The program is being accomplished by the performance of the following six major tasks:

TASK 1 - Literature Survey. Currently available literature, related to MLI material, property data, evacuation valves, repressurization and evacuation systems was reviewed. The survey determined the availability of all necessary flightworthy components for the system. The findings of the survey are documented in Reference 1.

TASK 2 - Purge System Concepts. Concepts for purge systems capable of evacuation, pressurization and repressurization for representative liquid hydrogen tankage onboard a space vehicle during extended life cycle including multiple reuse were defined in References 1 and 2.

TASK 3 - Component and Materials Evaluation. Exploratory data acquisition and design verification scale model thermal and structural tests will be conducted on purge system components, valves, joints, attachments and surface coatings to establish repeatability characteristics, materials compatibility to cyclic temperature environments, abrasive resistance of bag materials and/or coatings, and vent valve operations and seal characteristics.

TASK 4 - Purge System Design. Based on data from Tasks 1 through 3, the purge, repressurization, preconditioning and multilayer insulation systems will be selected and assembly and detail drawings prepared. The design evolved will represent a total integrated system design suitable for both the LOX/LH_2 tanks on the Space Shuttle and flightworthy in an environment up to 450 K (350 F).

Structural, weight, thermal, gas flow, and material analyses and tests will be performed to assure system compatibility with expected Space Shuttle environments.

TASK 5 - Manufacturing Development. Assembly sequence drawing and drawings for all tooling and fixtures required to fabricate the purge and repressurization system and the necessary provisons for cross-country shipments will be established. A manufacturing plan, including sequence, quality control and inspection provisions affecting the design for the installation of the purge and repressurization system onto the Convair Aerospace Division 2.21 m (87 in) diameter tank, will be developed.

TASK 6 - Fabrication, Test and System Evaluation. A preconditioning, purge and repressurization system will be fabricated in conjunction with a multilayer insulation concept as determined from the results of Tasks 1 through 5. Documentation for instrumentation, installation, and output location and function will be prepared for the proposed tank test of the total MLI system. A test plan will be formulated for the purge and repressurization system to include the test specimen definition, instrumentation definition and requirements, and data processing and correlation methods. A functional test will be performed on the test specimen proposed in Task 4 to demonstrate the total system's performance. The total system will be evaluated and a test report prepared. The evaluation shall include the system's performance penalties and a summary of its compatibility with the Space Shuttle environments.

The program master schedule is shown on Figure 1.

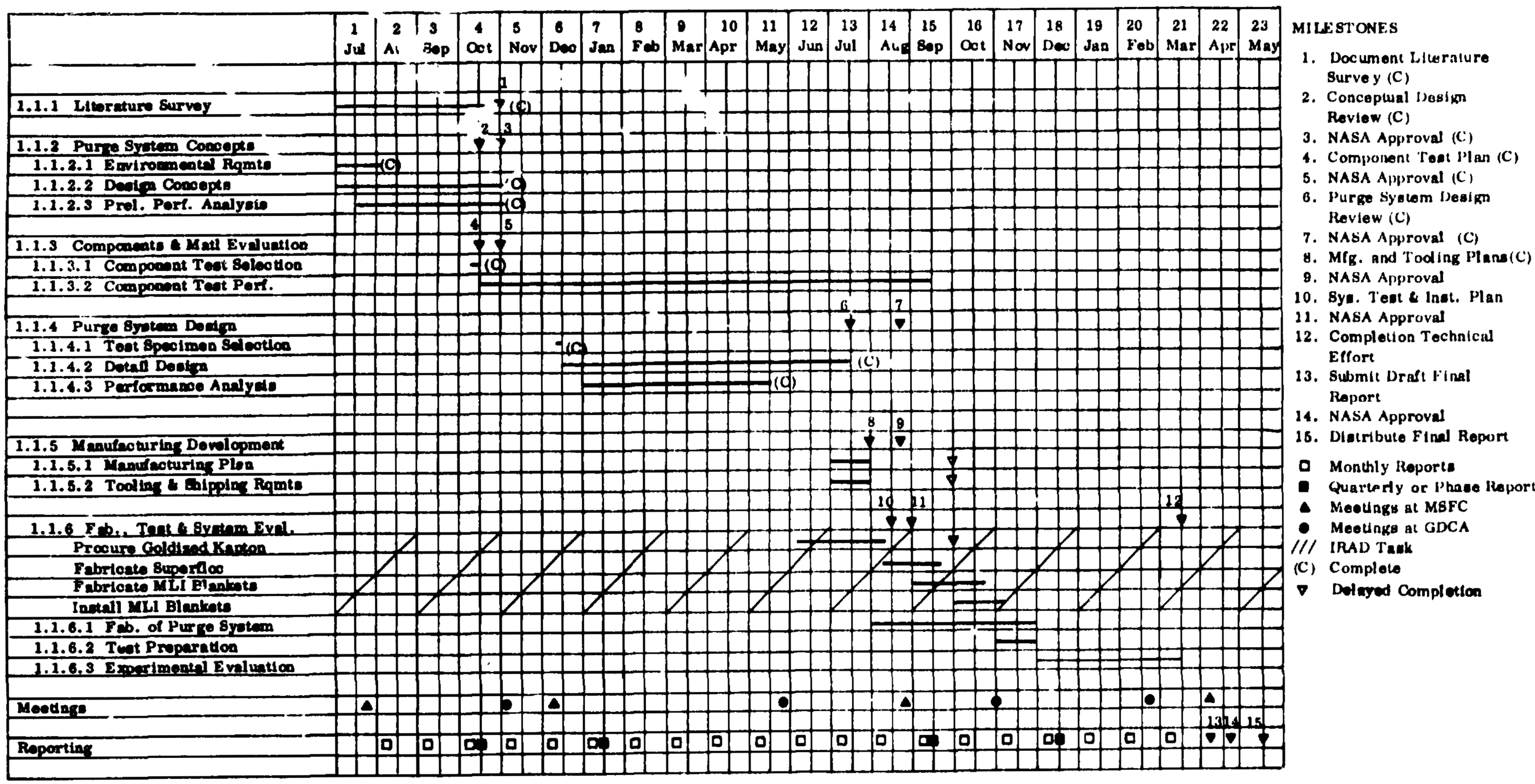

Figure 1. Pressure and Repressurization Purge System for Reusable Space Shuttle Multilayer Insulation Program Master Schedule

2

COMPONENT AND MATERIAL EVALUATION (TASK 3)

The component and material evaluation task has been completed. The task consisted primarily of the experimental determination of purge bag materials properties, development of purge bag manufacturing techniques, experimental evaluation of a subscale purge bag under simulated operating conditions and the experimental evaluation of the purge pin concept for MLI purging.

2.1 MATERIAL TESTS PROGRAM

Objectives of the material property test program were: (1) to evaluate the effects of combined stress and high temperature on bag material permeability, (2) to evaluate the effect of humidity and repeated temperature cycling on bag wall material strength at low and high temperatures, and (3) to evaluate the effects of humidity and repeated temperature cycling on the shear and peel strengths of two bag adhesive candidates.

2.1.1 PERMEABILITY TESTS. Purge bag material permeability tests were conducted in the apparatus shown schematically in Figure 2. The purge bag material is two plys of epoxy pre-impregnated 181 style fiber glass laminated with skins of two mil FEP Teflon. Three bag material samples were pressurized to 10.3 kN/m^2 differential (1.5 psid) with helium and the permeability (volumetric flow rate per unit cross sectional area) measured. Three identical samples were similarly measured after stressing to 60% of their apparent tensile strength at 450 K (350 F). Test results are presented in Table 1. As indicated, the permeability before and after high temperature stressing was negligible.

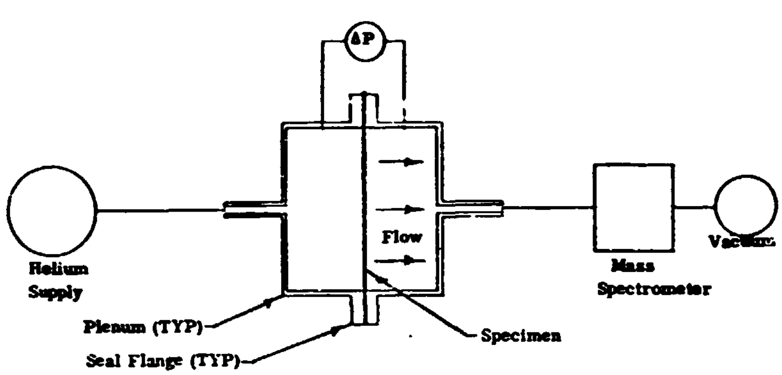

Figure 2. Purge Bag Material Permeability Test Apparatus

2.1.2 MATERIAL STRENGTH TEST. Purge bag material strength tests were conducted in order to measure the effect of temperature and humidity upon the shear and peel strength of bonded purge bag joints. Two candidate adhesives were tested on each type of joint, EPON 934 and silane modified Crest 7343 polyurethane. Non-bonded control samples of bag material were tensile tested in order to verify efficiency of the bonded joints as well as to determine the effect of temperature and humidity on tensile strength of the bag material. The control, shear, and peel samples are shown in Figure 3. Figure 4 presents a schematic of sample test configuration. Tests were conducted at ambient temperature, 450 K (350 F), or 200 K (-100 F), and after boiling water or temperature cycling. Sample description, test parameters and results are summarized in Table 2.

Results show that the modified 7343 polyurethane adhesive is unsatisfactory for bonding FEP Teflon to

Table 1. Purge Bag Material Permeability Test Results

Specimen Number		Condition	Permeability (scc He/sec-m^2)
1	a	As Received	< Sensitivity Limit
	b	As Received	< Sensitivity Limit
2	a	As Received	< Sensitivity Limit
	b	As Received	< Sensitivity Limit
3	a	As Received	< Sensitivity Limit
	b	As Received	$.43 \times 10^{-4}$
4	a	After Thermal/Stress	$.30 \times 10^{-4}$
	b	After Thermal/Stress	< Sensitivity Limit
5	a	After Thermal/Stress	< Sensitivity Limit
	b	After Thermal/Stress	< Sensitivity Limit
6	a	After Thermal/Stress	< Sensitivity Limit
	b	After Thermal/Stress	< Sensitivity Limit

NOTE:
Specimen 1a-3b - Sensitivity Limit=$.18\times10^{-4}$ scc He/sec-m^2
Specimen 4a-6b - Sensitivity Limit=$.28\times10^{-4}$ scc He/sec-m^2

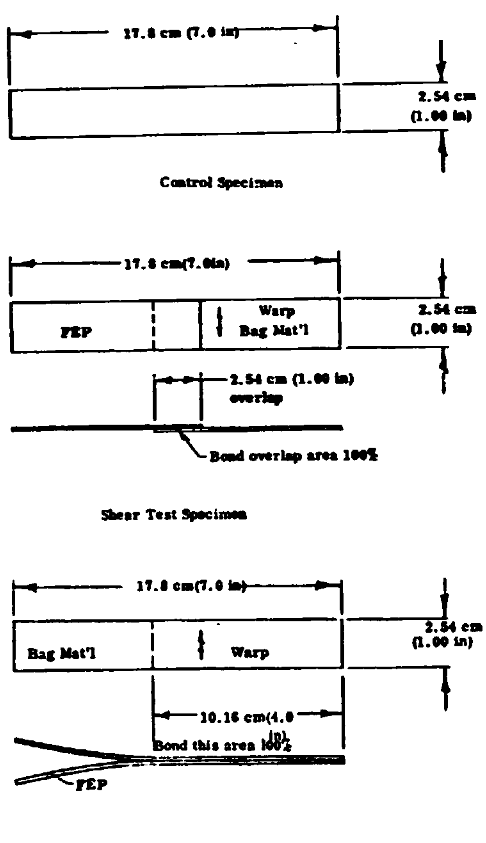

Figure 3. Purge Bag Material Test Sample Configurations

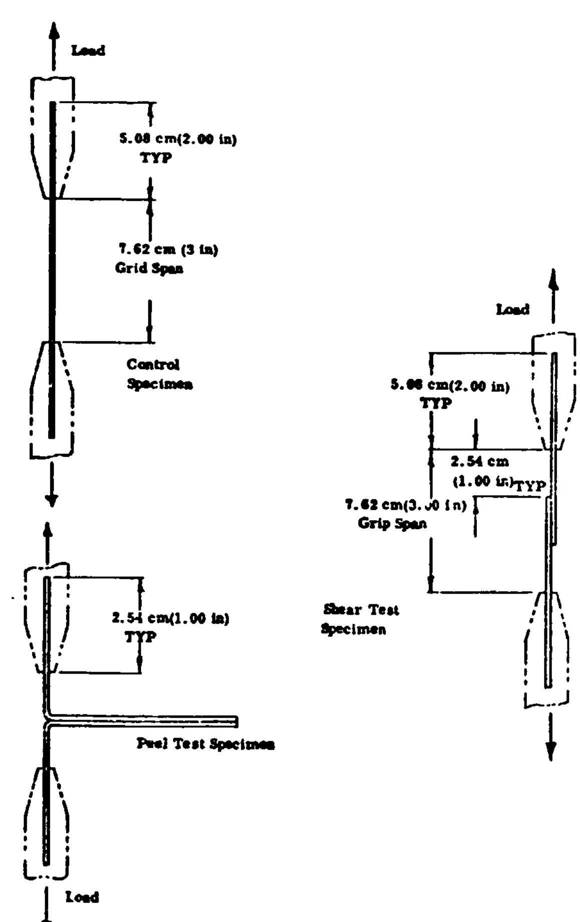

Figure 4. Purge Bag Material Strength Test Load Application Schematic

Table 2. Summary of Material Strength Tests

Test Specimens	Test No.	Chamber Temp. °K	(°F)	Pre-Test Condition	Ultimate Load kN	(lb)	F_{tu} MN/m^2	(psi)	Bond Effic.	Remarks
.064 cm (.025 in) gage FEP/181 glass	1	Ambient		-	3.60	(810)	263	(38,100)	-	Pull direction parallel
	2	450	(350)	-	3.31	(745)	261	(37,800)	-	to warp.
Control Specimens	3	450	(350)	Boil in H_2O 2 hrs	3.31	(743)	230	(33,300)	-	
	4	200	(-100)	-	6.52	(1465)	454	(65,700)	-	
	5	450	(350)	100 Temp. Cycles	3.12	(702)	223	(32,300)	-	
	6	200	(-100)	100 Temp. Cycles	7.27	(1635)	501	(71,500)	-	
.064 cm (.025 in) gage FEP/181 glass	1	Ambient		-	3.63	(815)	261	(37,800)	-	Pull direction normal
	2	450	(350)	-	3.21	(721)	223	(32,400)	-	to warp.
Control Specimens	3	450	(350)	Boil in H_2O 2 hrs	3.07	(690)	217	(31,400)	-	
	4	200	(-100)	-	5.85	(1315)	427	(62,000)	-	
	5	450	(350)	100 Temp. Cycles	3.08	(692)	219	(31,700)	-	
	6	200	(-100)	100 Temp. Cycles	6.16	(1385)	444	(64,500)	-	
.064 cm (.025 in) gage FEP/181 glass	1	Ambient		-	0.0867	(19.5)	-	-	100%	All specimens broke in
bonded to .025 cm (.010 in) FEP film	2	450	(350)	-	0.0222	(5.0)	-	-	100%	the FEP half.
with EPON 934 adhesive.	3	450	(350)	Boil in H_2O 2 hrs	0.0231	(5.2)	-	-	100%	
	4	200	(-100)	-	0.200	(45.0)	-	-	100%	
Shear Specimens	5	450	(350)	100 Temp. Cycles	0.0187	(4.2)	-	-	100%	
	6	200	(-100)	100 Temp. Cycles	0.240	(54.0)	-	-	100%	
.064 cm (.025 in) gage FEP/181 bonded to	1	Ambient		-	0.0565	(12.7)	-	-	65%	Peel separation between
.025 cm (.010 in) FEP film with EPON	2	450	(350)	-	0.0120	(2.7)	-	-	54%	FEP half and adhesive
934 adhesive.	3	450	(350)	Boil in H_2O 2 hrs	0.0102	(2.3)	-	-	44%	on all specimens.
	4	200	(-100)	-	0.0623	(14.0)	-	-	31%	
Peel Specimens	5	450	(350)	100 Temp. Cycles	0	(0)	-	-	100%	No peel, FEP half broke.
	6	200	(-100)	100 Temp. Cycles	0.0745	(16.75)	-	-	31%	Peel separation in fiberglass FEP laminant.
.064 cm (.025 in) gage FEP/181 glass	1	Ambient		-	0.0872	(19.6)	-	-	100%	FEP half broke.
bonded to .025 cm (.010 in) FEP film with	2	450	(350)	-	0.0013	(0.3)	0.002	(0.3)	6%	Adhesive separated.
Polyurethane 7343 (modified with silane	3	450	(350)	Boil in H_2O 2 hrs	0.0022	(0.5)	0.003	(0.5)	10%	Adhesive separated.
additive) adhesive.	4	200	(-100)	-	0.205	(46.0)	-	-	100%	FEP half broke.
Shear Specimens										
.064 cm (.025 in) gage FEP/181 glass	1	Ambient		-	0.0151	(3.4)	-	-	17.4%	Adhesive separated on
bonded to .025 cm (.010 in) FEP film with	2	450	(350)	-	0.0013	(0.3)	-	-	6%	all specimens.
Polyurethane 7343 (modified with silane	3	450	(350)	Boil in H_2O 2 hrs	0	(0)	-	-	0%	
additive) adhesive.	4	200	(-100)	-	0.0013	(0.3)	-	-	0.6%	
Peel Specimens										
.064 cm (.025 in) gage FEP/181 glass	1	450	(350)	-	1.326	(298)	-	-	-	Fiberglass delaminated
bonded to same (no FEP in bond area)	2	450	(350)	-	0.983	(221)	-	-	-	on all specimens.
with EPON 934 adhesive	3	450	(350)	-	0.992	(223)	-	-	-	
Shear Specimens										

the bag wall material. The 7343 adhesive has virtually no peel or shear strength at 450 K (350 F). Results indicate no degradation in bag wall material strength or shear and peel strength of the EPON 934 adhesive as a result of temperature cycling or humidity. The general condition of the material after temperature cycling was excellent. An increase in the shear strength by a factor of approximately 50 was obtained by removing the FEP Teflon film and bonding 181 glass to 181 glass with EPON 934. The purge bag bonding procedure has subsequently been modified to eliminate peel stressed bond joints and to bond all joints with EPON 934 after removal of the FEP layers in the bond area.

PRD-49 (a DuPont T.M.) material strength tests were also conducted in order to establish the acceptability of the material as an alternate to the 181 glass purge bag material. The tests were designed to measure the effect of temperature and humidity upon the basic PRD-49 material (control samples) and bonded lap (adhesive shear test) joints. EPON 934 was the adhesive used for all of the PRD-49 lap joints. The control and shear samples without FEP film layers are as shown in Figure 3. Separate specimen tests were conducted at ambient temperature, 450 K (350 F) and 200 K (-100 F). Further, selected samples were tested after two hour emersion in boiling water or after sample temperature cycling from 200 K to 45´ K. Test parameters and results are summarized in Table 3. Results show that no degradation occurs in PRD-49 material strength or lap joint shear strength as a result of temperature cycling or humidity exposure.

Table 3. Material PRD-49 Strength Tests - Result Summary

Test No.	Chamber Temp, °K(°F)		Pre-Test Condition	Ultimate Load kN	(lbs)	F_{tu} MN/m^2	(PSI)	Remarks
1	Room Temp.		-	5.59	(1260)	432	(62687)	
2	Room Temp.		-	4.82	(1085)	402	(58333)	
3	Room Temp.		100 Temp Cycles	4.13	(930)	328	(47497)	
4	Room Temp.		100 Temp Cycles	3.29	(742)	261	(37857)	
5	Room Temp.		100 Temp Cycles	3.94	(888)	322	(46737)	
6	Room Temp.		100 Temp Cycles	3.37	(758)	266	(38497)	
7	200	(-100)	-	5.82	(1310)	464	(67179)	
8	200	(-100)	-	5.26	(1185)	417	(60459)	
9	450	(+350)	-	4.00	(900)	320	(46325)	
10	450	(+350)	-	3.46	(780)	280	(40625)	
11	Room Temp.		100 Temp Cycles	2.85	(643)			Lap shear, bond line separated.
12	Room Temp.		100 Temp Cycles	3.24	(730)			Lap shear, PRD-49 broke.
13	Room Temp.		-	2.91	(655)			Lap shear, bond line separated.
14	200	(-100)	-	3.17	(715)			Lap shear, bond line separated.
15	450	(+350)	-	1.35	(305)			Lap shear, adhesive separated.
16	450	(+350)	2 hr water boil	1.69	(380)			Lap shear, adhesive separated.
17	450	(+350)	2 hr water boil	2.89	(650)	234	(3?854)	
18	450	(+350)	2 hr water boil	3.33	(750)	270	(39063)	

NOTE: All lap shear specimen joints were bonded with HYSOL EA 934 adhesive.

PRD-49 material linear thermal expansion tests were also conducted and the data have been evaluated. Tests were conducted after thermal cycling the material between 200 K (-100 F) and 450 K (+350 F) in order to establish stable linear expansion data. Measurements were made parallel and perpendicular to the material warp. Stable linear expansion test data results are presented in Figure 5. Results indicate that perpendicular to the warp, the linear coefficient of thermal expansion is -8.4×10^{-7} K^{-1} (-4.7×10^{-7} R^{-1}). Parallel to warp, the thermal expansion appears non-linear. The average value in the temperature range from 311 K (100 F) to 450 K (350 F) is approximately -1.5×10^{-6} K^{-1} (-8.3×10^{-7} R^{-1}). At temperatures below 311 K (100 F), the average coefficient is of a lower magnitude.

The PRD-49 material appears to be satisfactory structurally as an alternate purge bag material for future applications contingent upon successful completion of selected application tests (eg, vibration, machinability, etc).

2.2 MODEL PURGE BAG FABRICATION AND TEST PROGRAM

A subscale model of the purge bag was selected for fabrication and testing prior to full scale bag manufacture. This was accomplished in order to develop manufacturing and tooling techniques for the full scale bag and to provide experimental data on bag structural performance. The model purge bag manufacturing and testing provided the data, techniques, and confidence necessary to initiate the full scale program.

The purge enclosure model is shown in Figure 6. The bag model includes the major design features of the full scale enclosure which will be fabricated for the 2.2 m (87 in) test tank. The similarities between the model bag and the full scale bag as well as the model bag test objectives are described below.

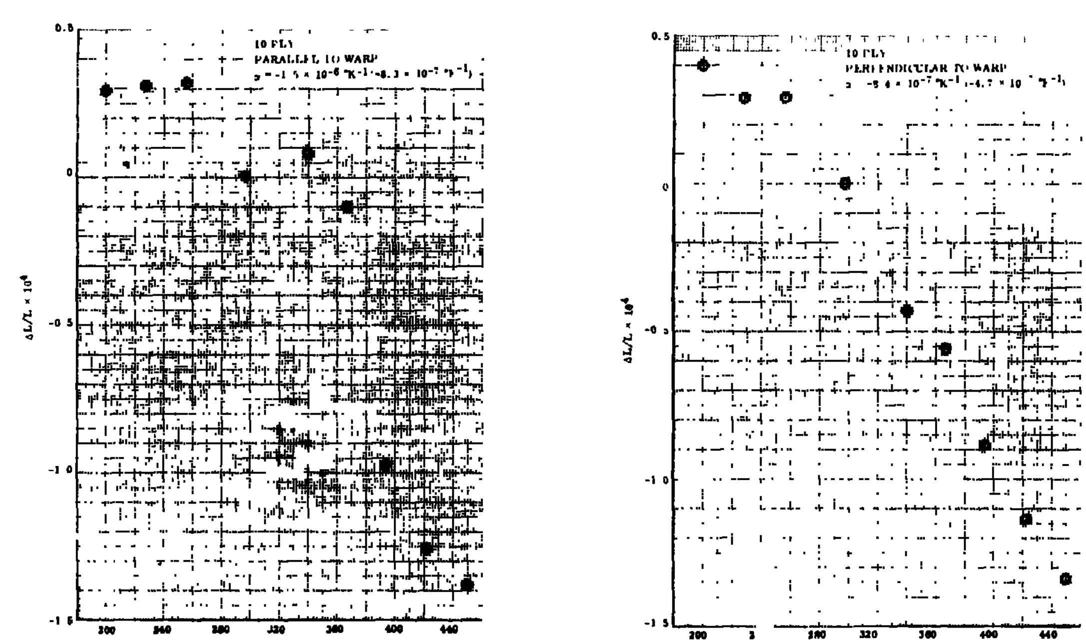

Figure 5. Total Linear Thermal Expansion of PRD-49 (DuPont), 181 Style Cloth/ 0-73009-2, Class II

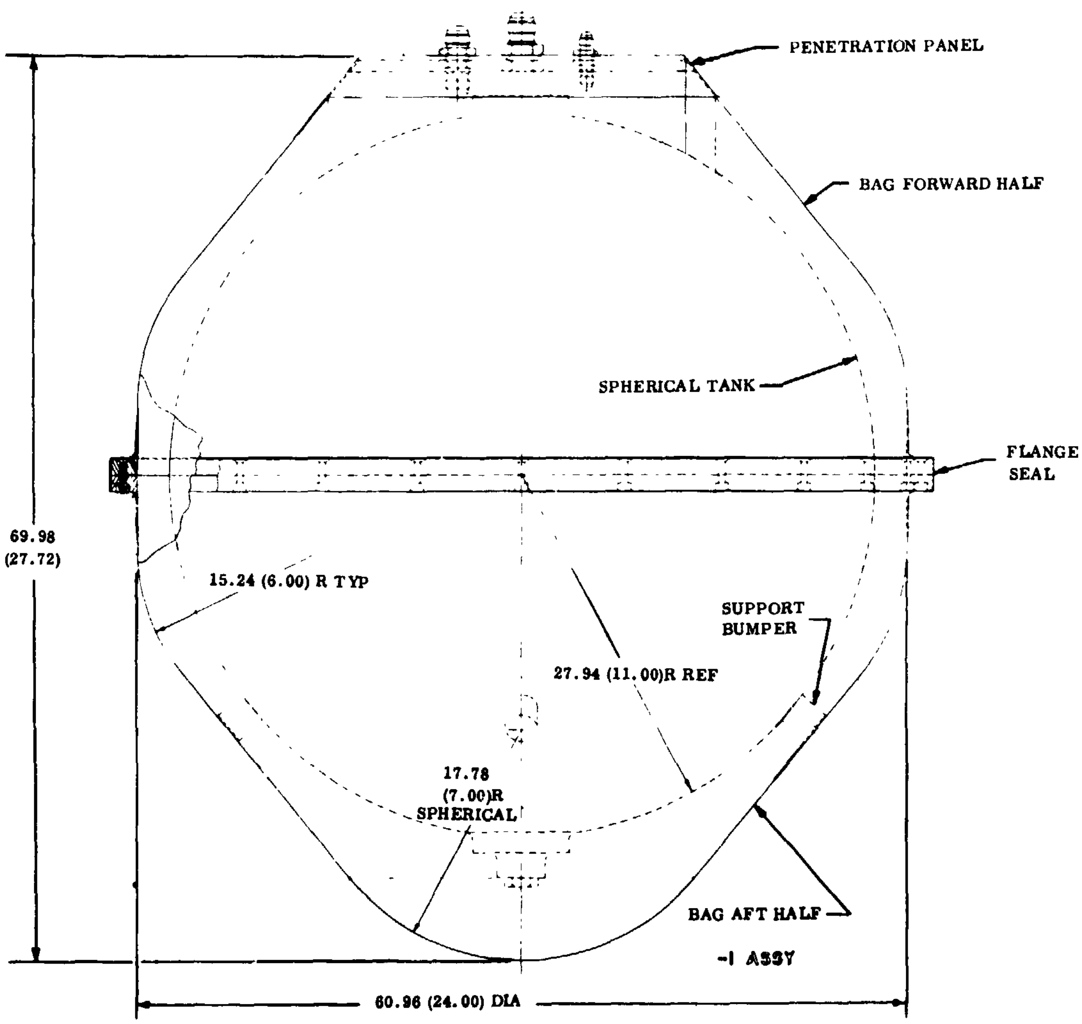

Figure 6. Purge Enclosure Model

Design features of the full scale bag described in Reference 2 and the subscale model of Figure 6 include the following:

a. A flat, rigid forward end piece is provided for equipment mounting and system penetrations. The entire bag is supported by this forward end. Standoff bumpers are provided near the aft end of the bag to maintain centering.

b. Each bag half is cylindrical at the mid-section with a conical transition to the ends. The aft bag end is spherical.

c. A bolted fiberglass flange is provided to allow separation of the bag halves.

Each bag half, including separation flange, was manufactured during a single layup operation. This procedure was deemed more reliable and economical than manufacturing separate gore sections and flanges and bonding them together.

The purge bag separation flanges were sealed after final torquing of the flange screws. The screw heads and flange seam were sealed by overlaying with two ply of epoxy impregnated glass cloth. The flange nuts were potted with epoxy resin to prevent leakage.

2.2.1 SMALL SCALE BAG FABRICATION. The small scale bag program offered an opportunity to examine low cost tooling methods for fabricating the epoxy-fiberglass bag. A high temperature plaster tool was selected for bag manufacture since the procedure is in common use within the industry and is one of the techniques used at Convair Aerospace.

A male tool, shown in Figure 7, was constructed from a framework of welded 1.9 cm (0.75 in) black pipe. The welds were normalized for 2 hours at 922°K (1200°F) to prevent possible distortion during cure. U.S. Gypsum Hydrocal B-11 plaster was applied and swept to form a wall 7.66 cm (3 in) thick. The plaster was dried for an accumulated time in excess of sixty hours in an air-circulating oven at a temperature of 339 to 350°K (150 to 170°F). The plaster mold was then coated with ten coats of Ram Chemical Company's Garalease 915 parting agent. Each coat was air dried a minimum of 15 minutes at ambient conditions before applying the next coat. The dry Garalease 915 film was then coated with six spray coats of Frekote 33.

The one stage lay-up and cure with FEP teflon barrier on both laminate surfaces was not practical. Forming and holding the FEP gore sections to the male tool proved to be time consuming and the film wrinkled before lay-up of prepreg began. Layup was accomplished by laying the prepreg next to the tool and placing a ply of 50.8 μ m (0.002 in) thick FEP over the prepreg. The part was then vacuum bagged and cured under 0.687 m (27 in) Hg vacuum for two hours at 450°K (350°F). Temperature was measured by a thermocouple in the laminate.

The cured half-shell presented in the photographs of Figures 8 and 9 show the resulting delaminations, resin wash-out and wrinkles which contained condensate from the plaster not having been completely dry or from the release of water of hydration or both. Release of moisture from plaster tooling at the required cure temperatures, prohibited the use of plaster for part fabrication on this program. Tooling constructed from high temperature epoxy fiberglass was substituted.

A female tool for the small scale bag was then constructed by modifying the outside dimensions of the male plaster tool to conform to the model bag dimensions, and fabricating the female epoxy tool from a male tool lay-up. The FEP Teflon bag skin material was cut to fit the female tool and the overlap joints were heat sealed. The entire FEP skin was held in place by vacuum during bag lay-up. The bag forward end enclosure which provides for equipment mounting was bonded to the bag using modified Crest 7343 polyurethane adhesive which was cured at room temperature. End closure fittings were installed using EPON 934 epoxy adhesive to provide a seal. The resulting successfully completed model purge bag is shown in Figure 10.

Figure 7. Plaster Tool for Small Scale Purge Bag Fabrication

Figure 8. External View of Cured Bag Half Shell Made on Plaster Tool

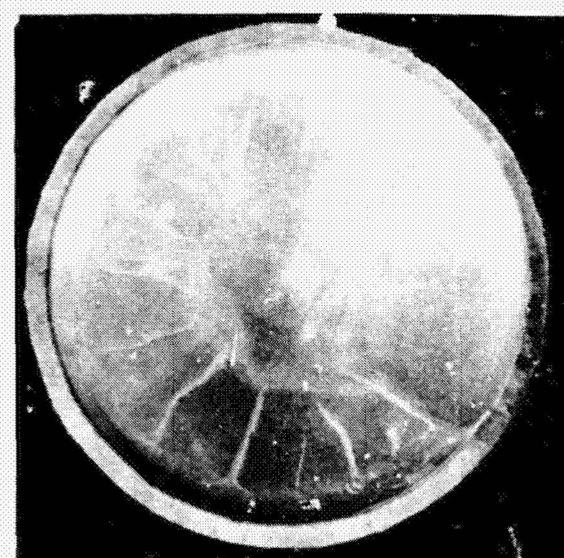

Figure 9. Internal View of Cured Bag Half Shell Made on Plaster Tool

2.2.2 MODEL PURGE BAG TEST PROGRAM. Environmental tests were conducted on the completed model purge bag to establish that the design would satisfy minimum life requirements. The overall objective of the test program was to demonstrate the ability of the purge bag design to meet minimum operational requirements for at least 100 mission cycles. Tests conducted were:

a. Repeated pressurization cycles (0-82.7 kN/m^2) at high (450 K) and low temperature (200 K) (pressure life cycling).

b. Acoustic loading at specified pressure levels.

SHELL HALVES

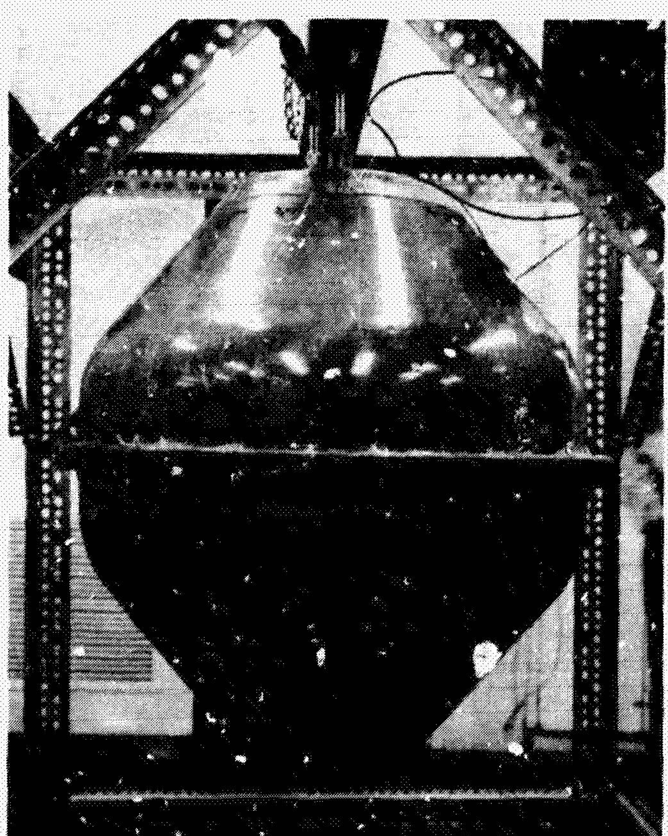

IN SUPPORT STRUCTURE

Figure 10. Completed Model Purge Bag

2.2.2.1 Model Bag Pressure Life Cycle Testing. Model purge bag pressure life cycle testing was conducted in the Convair Aerospace environmental laboratory temperature chamber shown in Figure 11. Figure 12 presents a schematic of the test configuration setup. The model bag was suspended from a support structure and installed within the chamber as shown in Figure 13. Proof pressure tests were conducted at a pressure of 124.1 kN/m^2 (18 psig). A pressure decay leakage rate of 41.37 N/m^2-sec (0.360 psi/min) was noted.

A total of 500 low temperature pressure cycles were performed at bag temperatures between 197K (-105F) and 207K (-88F). The pressurization rate was 82.7 kN/m^2 (12 psi) in one to two seconds. A typical pressurization rate profile is shown in Figure 14. The bag pressure leakage rate after 500 low temperature cycles was 41.02 N/m^2-sec (0.357

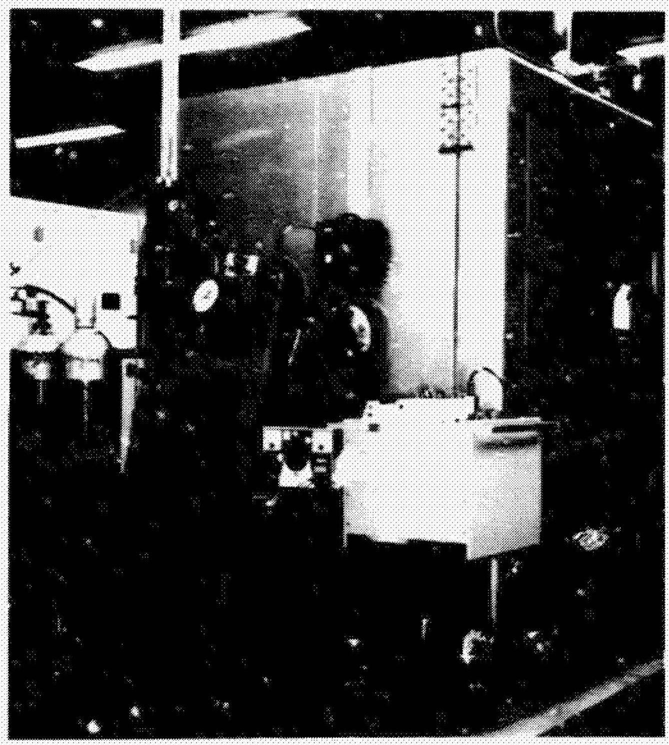

Figure 11. Model Bag Environmental Test Chamber and Pressure Test System

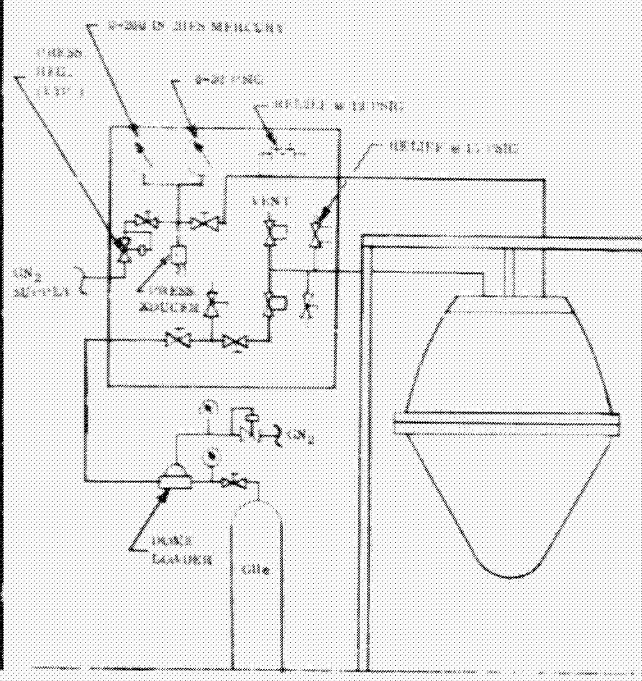

Figure 12. Pressure Test Set-up Schematic

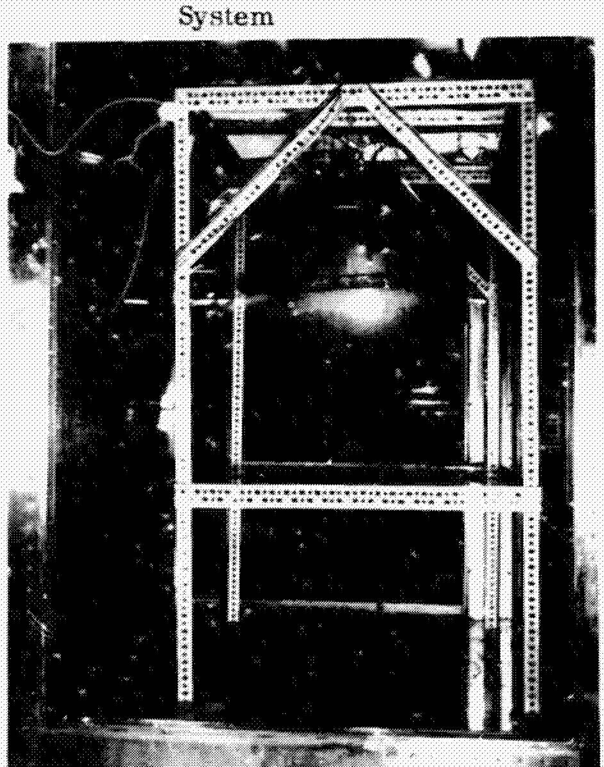

Figure 13. Support and Installation of Model Bag Inside Temperature Test Chamber

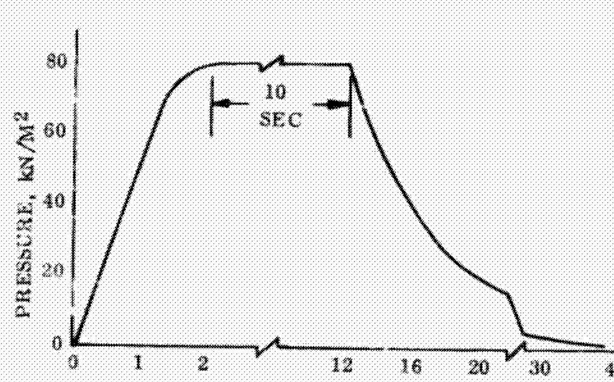

Figure 14. Typical Pressure Cycle - Model Purge Bag Pressure Test

psi/min) indicating no change in leakage rate due to low temperature pressure cycling.

During model bag temperature stabilization for the bag high temperature [450K (350F)] pressure cycling testing, the forward bag shell separated from the upper enclosure surface and the girth flange seal failed. The bag temperature was approximately 422K (300F). The separation is shown in Figure 15. The failures occured at joints bonded with Crest 7343 adhesive. Repairs were made by bonding one ply of epoxy fiber-glass cloth over the leakage areas with EPON-934 adhesive. Repairs are shown in Figure 16. The post repair bag pressure decay rate was reduced to 8.73 N/m^2-sec (0.076 psi/min) prior to high temperature testing. A total of 403 high temperature pressurization cycles were completed before inadvertent overpressurization [124.1 kN/m^2 (18 psig)] resulted in loss of pressure. The objective of the high temperature test was completion of 500 pressure cycles. However, sufficient data had been obtained from the completed tests to provide confidence in the successful application of bag design concepts to the full scale bag, and pressure testing was terminated.

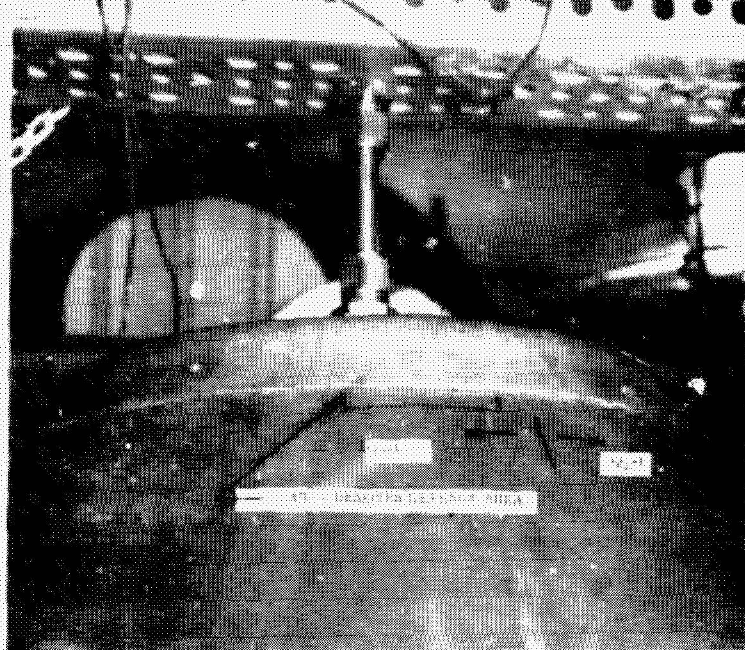

Figure 15. Separation of Model Bag Upper Surface From Forward Shell Half - QUAD 2

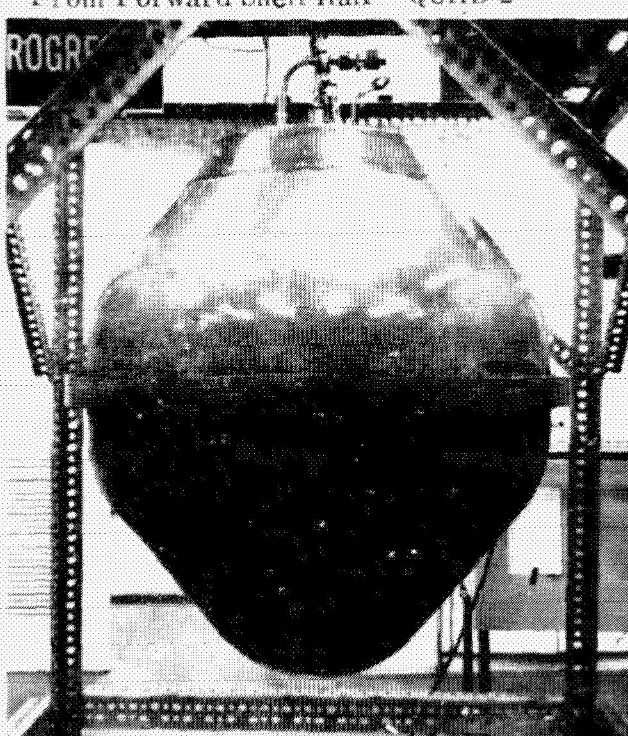

Figure 16. Shell Fwd Half and Girth Flange Glass Cloth/EPON 934 Seal Repairs

The bag temperature during high temperature pressure cycling ranged from 440K (332F) to 450K (350F). During the last 140 cycles of the high temperature testing, the bag pressure was permitted to exceed 89.63 kN/m^2 (13 psig) a total of nine times. The maximum pressure during these cycles was 110.3 kN/m^2 (16 psig). A test summary of the pressure life cycle testing is presented in Table 4.

Table 4. Model Purge Bag Testing Summary

Test Performed	Test Results	Conclusions
Ambient Temp. Leak and Proof Pressure Test	Bag wall had no evidence of leakage.	Leakage characteristics satisfactory.
Low Temp. Press. Cycling	500 cycles completed. No evidence of leaks or damage in bag wall.	Bag not affected by 200K exposure
High Temp. Press. Cycling	After 404 successful cycles, overpressurization of bag resulted in leakage failure. Separation flange seal failed in shear and hoop. Condition of bag wall was satisfactory.	Such failure will be avoided on large bag by inability to overpressurize. Higher factors of safety will be used on flange seal design to assure its integrity.

2.2.2.2 Model Bag Acoustic Loading. Acoustic loading testing of the model purge bag was conducted in the Convair Aerospace acoustic laboratory. The model bag was subjected to the simulated space shuttle acoustic environment as defined by the data specified in Reference 2. The test specimen was suspended in the 28.3 m^3 (1000 ft^3) acoustic reverberant chamber by elastic shock cords as shown in Figure 17. A calibrated microphone was placed approximately 0.457 m (18 in) from the bag at 90° to the acoustic horn.

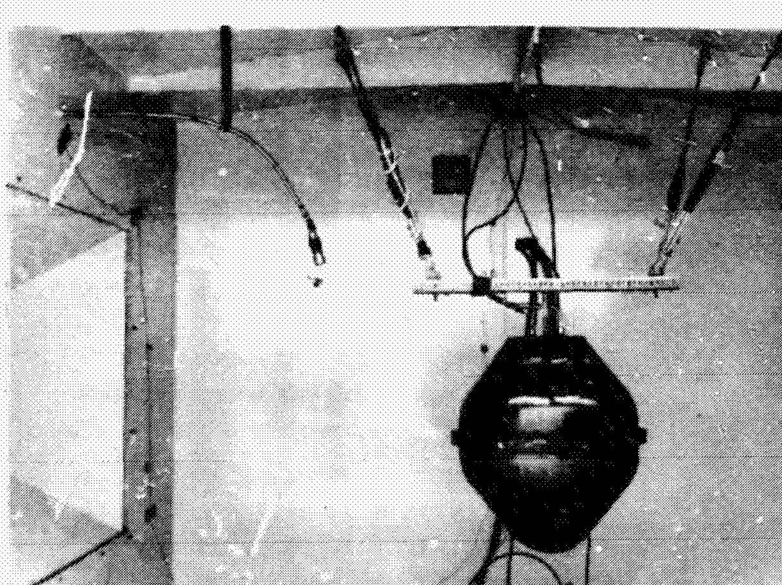

Figure 17. Installation of the Model Bag Inside the Convair Aerospace Acoustic Chamber

The chamber was secured, the bag vented, and acoustic excitation applied. Sound pressure was maintained for 10 minutes at the level shown in Reference 2. The bag was examined following excitation and no visible damage or deformation was observed.

The chamber was again secured, the bag pressurized to 82.7 kN/m^2 (12 psig) with GHe, and acoustic excitation was applied. Sound pressure was maintained for 10 minutes. Specimen pressure was reduced to ambient at end of test. The specimen was examined and no visible damage or deformation was observed. A leakage test following completion of all acoustic testing showed no increase in leakage rate.

2.3 MULTILAYER INSULATION PURGING TESTS

MLI purging tests using purge pin gas injection were conducted using two types of MLI. The objective of the tests was to demonstrate and verify the purge pin gas injection concept for purging MLI of condensable gases. Purge pin radial gas flow injection, the effects of purge pin spacing along the MLI blanket, and the effects of purge gas flow rates were evaluated. Tests were conducted using Convair Aerospace Superfloc MLI and perforated aluminized Mylar/Dacron net MLI systems, as described in Reference 3, both with and without a simulated purge bag. Three purge gas flow rates were used for each of these purge pin spacing configurations. Data resulting from each of the tests were used to obtain purge gas concentration profiles, blanket purge gas equilibrium concentration values, MLI blanket purging histories, and comparison with previously predicted purge values.

2.3.1 TEST CONFIGURATION AND SET-UP. The basic test apparatus used for testing consisted of a 2.62 m (8 ft) × 0.44 m (16 in) × 0.019 m (0.75 in) purge box constructed of 0.00635 m (0.25 in) thick plexiglass sheet. The top of the box was relieved along the sides to facilitate access to the MLI and to provide free venting from the MLI edge. The box contained a total of 80 purge sampling probes. Forty-one were inserted through the top of the box and 38 through the bottom. The test apparatus set-up is shown in Figure 18 through 20. Figure 21 shows a typical installation of a sampling probe.

Helium purge gas was injected by means of purge pins (Figure 22) from calibrated helium supplies through two stages of regulation. The flow was monitored by Rotameters installed in each purge pin flow line during each run. The test apparatus was flushed between runs with filtered ambient air through the center purge pin at a rate of approximately 2.83 m^3/hr (100 ft^3/hr) until all helium was displaced.

During the portion of the test which was conducted with a simulated purge bag, the entire purge box was enclosed within a polyethylene bag with a standoff distance of approximately 5.08 cm (2.0 in) from the MLI. The bag contained a 3.18 cm (1.25 in) diameter vent hole located approximately 76.20 cm (30 in) from the bag end along the centerline. Purging measurements conducted during simulated purge bag conditions were made at the blanket end furthest from the vent hole.

The MLI test blankets consisted of 22 layers of Superfloc or 34 layers of perforated aluminized Mylar/Dacron net with fine mesh face sheets. Each blanket was configured to the purge box dimensions, thus approximating the blanket size for the 2.21 m (87 in) test tank and the blanket edge butt joints. Purge gas sampling probes were installed at the 25%, 50%, and 75% depth level in each blanket. The holes cut into the blankets for probe installation were slightly smaller in diameter than the probe pin. The resulting tight fit eliminated the need for MLI-to-probe pin adhesive.

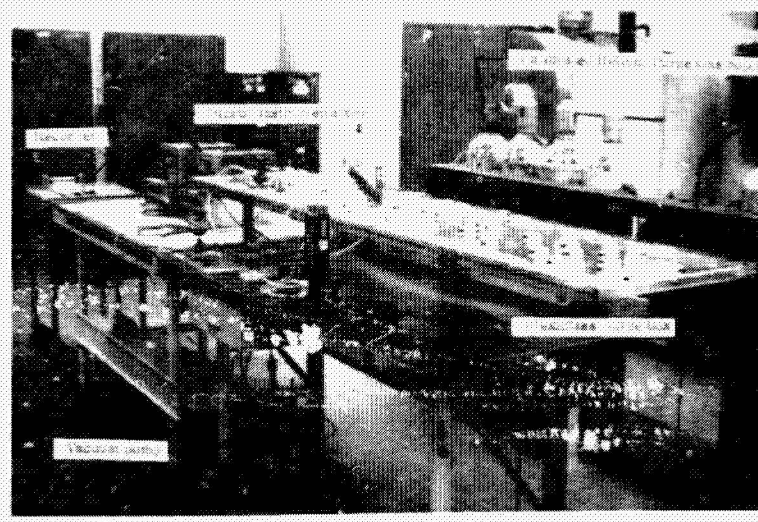

Figure 18. MLI Purge Pin Test Apparatus

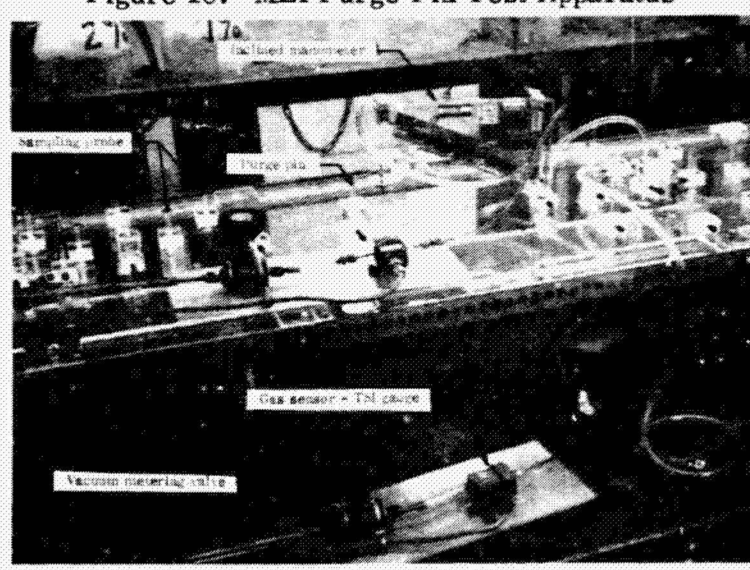

Figure 19. MLI Purge Box

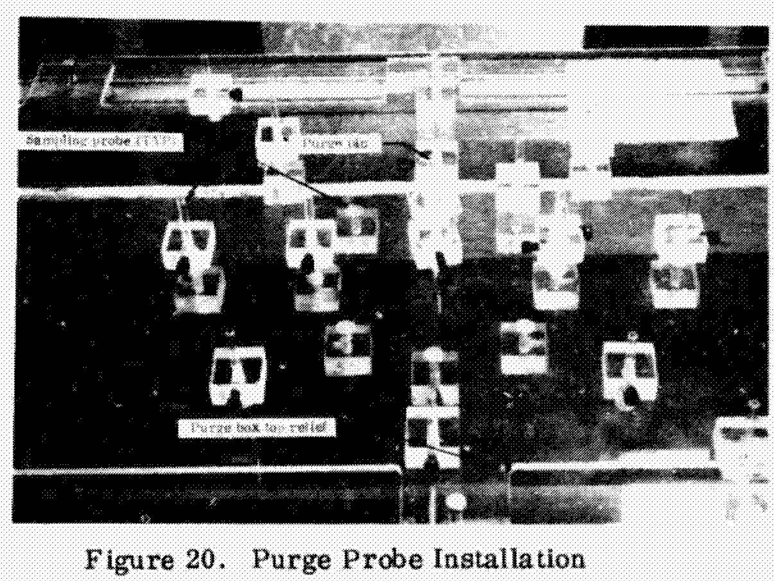

Figure 20. Purge Probe Installation

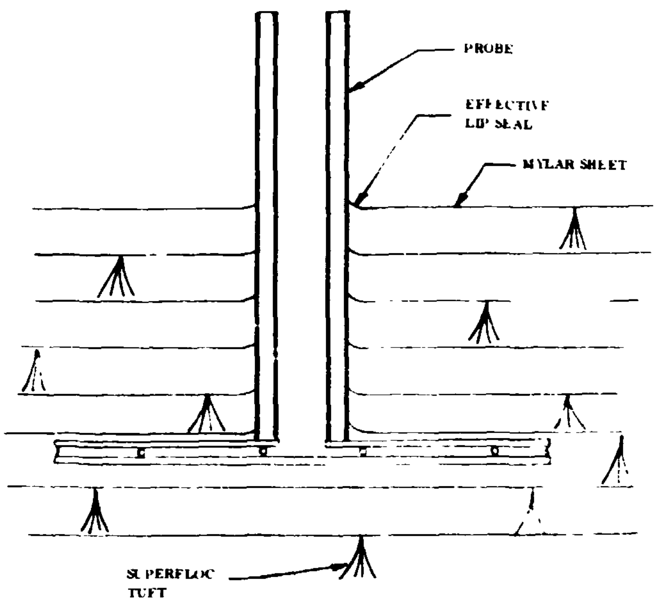

Figure 21. Purge Gas Sample Probe Typical Installation (Superfloc System Shown)

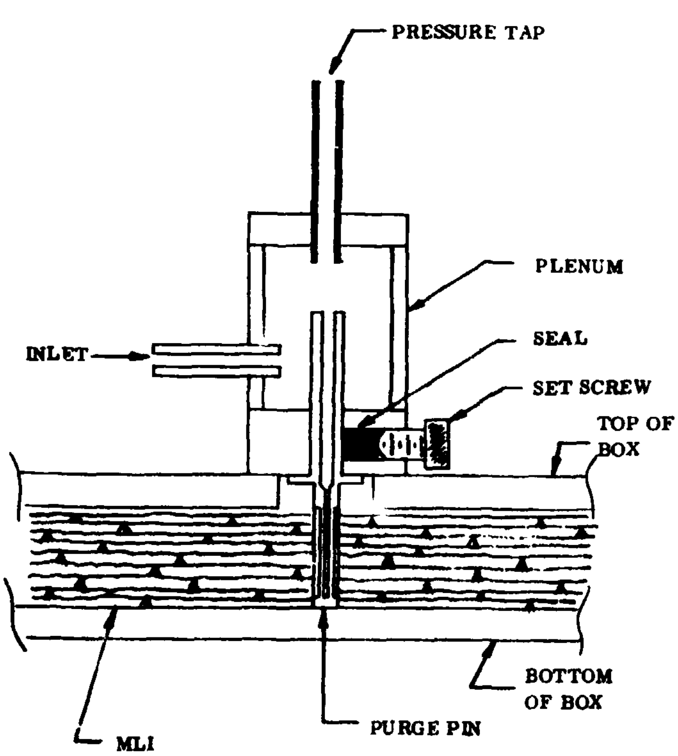

Figure 22. Purge Pin Typical Installation (Superfloc System Shown)

After purge sampling probe installation, the perforated aluminized Mylar/Dacron net blanket was stitched together on approximate 30.5 cm (12 in) centers using Dacron "I" fasteners. Materials and blanket fabrication instructions were provided by McDonnell Douglas (References 3 and 4).

2.3.2 <u>INSTRUMENTATION</u>.

2.3.2.1 <u>Pressure</u>. Differential pressures between purge pins and sampling probes were measured using a Dwyer 7.62 ± 0.025 cm (3 ± 0.01 in) water inclined manometer. A Meriam 76.2 ± 0.254 cm (30 ± 0.1 in) water manometer was used for pressures greater than 7.62 cm (3.0 in) of water.

2.3.2.2 <u>Purge Gas Concentration</u>. The GHe/air volumetric composition within the MLI blankets was obtained using two Thermo System Inc. (TSI) Model 1352-AA1 hot film anemometers (Figure 23). The output from these sensors results from the cooling effect of the helium gas flow over the sensing element.

This cooling effect is dependent upon gas composition and velocity. Thus, the sensors may be calibrated for use as flow meters by maintaining a constant gas composition, or as binary composition meters by maintaining a constant flow. Generally, the condition necessary for use as a composition meter is that the flow be a single valved function of composition.

During testing, the flow was determined by maintaining a constant pressure differential across a series

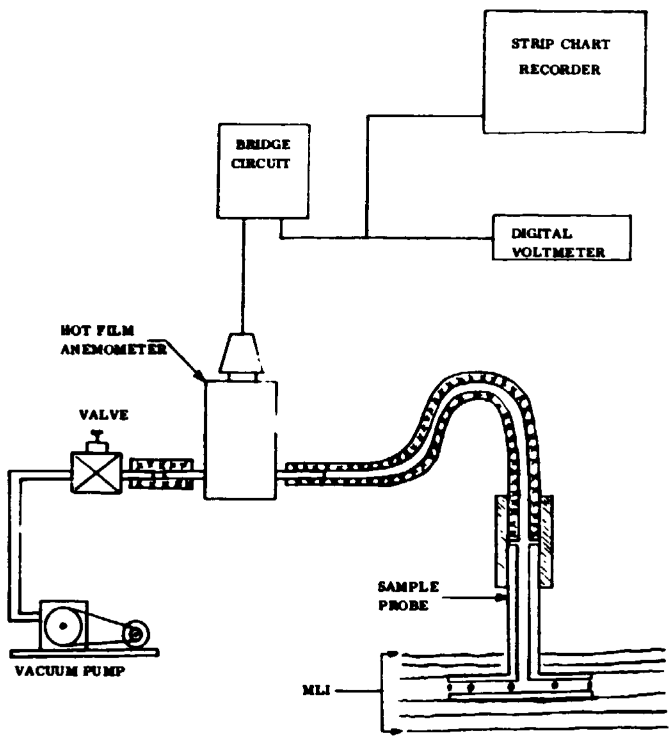

Figure 23. Typical Purge Gas Sampling Probe Measurement Configuration

orifice. Thus, sensor output changes occurred as a result of changes in gas composition. For a binary mixture of helium and air, the sensor output increases for both an increasing helium concentration and an increasing volumetric flow. Since an increase in helium concentration results in an increasing volumetric flow, the effects are additive yielding a larger output than if the flow were constant. Calibration of the system was thus possible, and was conducted using calibrated gas concentration supplies. The final eight point physical calibrations were made using prepared GHe/air mixtures of 100%, 99%, 98%, 95%, 90%, 80%, and 40% GHe. These calibration mixtures were made by filling storage bottles to the desired partial pressure of air ≈ 0.138 MN/m^2 (≈20 psid) for 99% GHe to ≈ 8.27 MN/m^2 (≈ 1200 psid) for 40% GHe) and then bringing the total pressure to 13.8 MN/m^2 (2000 psig) with U.S. Bureau of Mines Grade A Helium. After filling, the storage bottles were laid horizontally and turned occasionally for three days to insure good mixing. The actual volumetric GHe percentage (± 0.05%) was then determined using a Beckman Model GC-2A gas chromatograph. When in use, the systems were repeatedly checked in 100% GHe.

The sensor outputs were displayed on both Cimron Model 7500A/6900A digital voltmeters and on a Sanborn Model 7702A two channel recorder. The total system accuracies in the 80% to 100% GHe range were determined to be better than ± 0.1% of the full scale reading using the digital voltmeters and ± 0.2% of full scale using the strip chart recorder. Below 80% GHe, the accuracy slowly degraded to ± 1% full scale in air.

2.3.3 <u>TEST PROCEDURE</u>. All MLI blanket pressures were measured relative to atmospheric pressure (gage pressure). Purge pin inlet pressures were measured both with pickup and supply taps as shown in Figure 22. All pressure measurements were made after achieving equilibrium gas concentration during each run.

Purge gas concentration tests were one of two basic types.

2.3.3.1 <u>Uprun</u>. Starting with air at normal room conditions in the MLI blanket, a flow of GHe purge gas (50, 100, or 200 MLI blanket volumes/hr) was initiated through a specific purge pin configuration (1, 3, or 5 pins). The GHe purge gas concentration history was recorded with two sampling probes during each run. Multiple runs were required to sample all probes. The number and location of purge probes sampled was unique for each of the three purge pin configurations. These runs were conducted without a simulated purge bag enclosing the MLI blanket. For maximum accuracy at the higher GHe concentrations, the strip chart recorder was adjusted to record 80% to 100% GHe with the 0% to 80% range suppressed below scale.

2.3.3.2 Downrun. Starting with a minimum of 99.8% GHe in the MLI blanket, the GHe inflow was reduced in discrete steps. The GHe concentration in the blanket was allowed to achieve equilibrium concentration. The flow was reduced until the percent GHe at the two probes being sampled fell below 90%. These tests were conducted with simulated purge bag enclosure.

2.3.4 PURGE PIN TEST RESULTS. Results from the purge gas concentration tests are presented in Figure 24 through 29. Figures 24 and 25 show selected purge gas distribution profiles surrounding a single MLI purge pin. The profile results demonstrate that the radial flow distribution around a purge pin is uniform for both the Superfloc and aluminized Mylar/Dacron net MLI blanket systems.

Figures 26 and 27 present the MLI blanket centerline purge gas distributions at selected times without a simulated purge bag. As noted, the aluminized Mylar/Dacron net MLI generally purges more rapidly than the Superfloc in the region adjacent to a purge pin, but less rapidly than Superfloc at distances removed from a purge pin (eg at the end of the blanket). This is probably due to the helium diffusing through the perforations rather than flowing along the sheets as with Superfloc. Further, neither insulation purged to less than 1% residual condensables at the edges or ends of the blankets. This results from diffusion of air back into the blankets from the GHe/air boundaries. Figures 28 and 29 show the blanket equilibrium purge gas concentration which results at the ends and distant edge of each blanket for each purge pin configuration with a simulated purge bag. The enclosing purge bag intercepts the infinite air boundary, thus permitting MLI purging to less than 1% condensables. However, the aluminized Mylar/Dacron net MLI required a minimum of twice the purge gas volumetric flow rate as the Superfloc to achieve 1% residual condensable gas concentration in the MLI blanket.

A significant improvement (decreased flow) in purge system flow rate was achieved when, at a constant flow rate, the configuration was changed from one purge pin to three. Increasing the number of pins from three to five did not significantly increase the performance further for either MLI system. It is concluded, therefore, that a three pin per blanket configuration will be used on the full scale Convair Aerospace test system.

Complete purging of the test blankets to less than 1% condensables in the recommended three pin configuration with a nominal 100 vol/hr flow rate occurs in approximately 5 minutes for Superfloc and 12 minutes for the aluminized Mylar/Dacron netting MLI. Based upon the subject test results, it is concluded that the full scale test tank MLI will

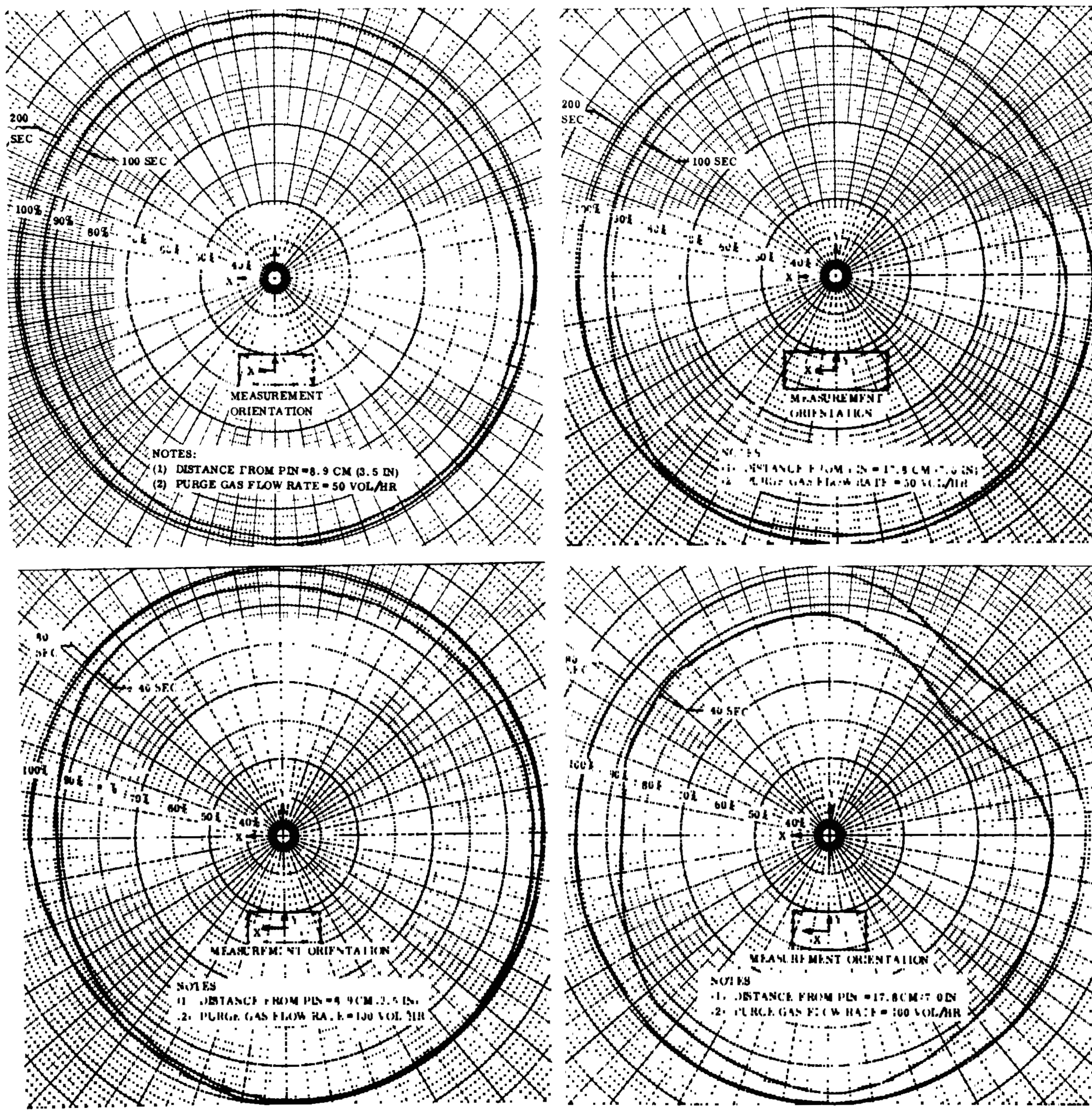

NOTES: (1) One Purge Pin
(2) Blanket Midlayer Measurement

Figure 24. Purge Gas Distribution Profile Superfloc MLI

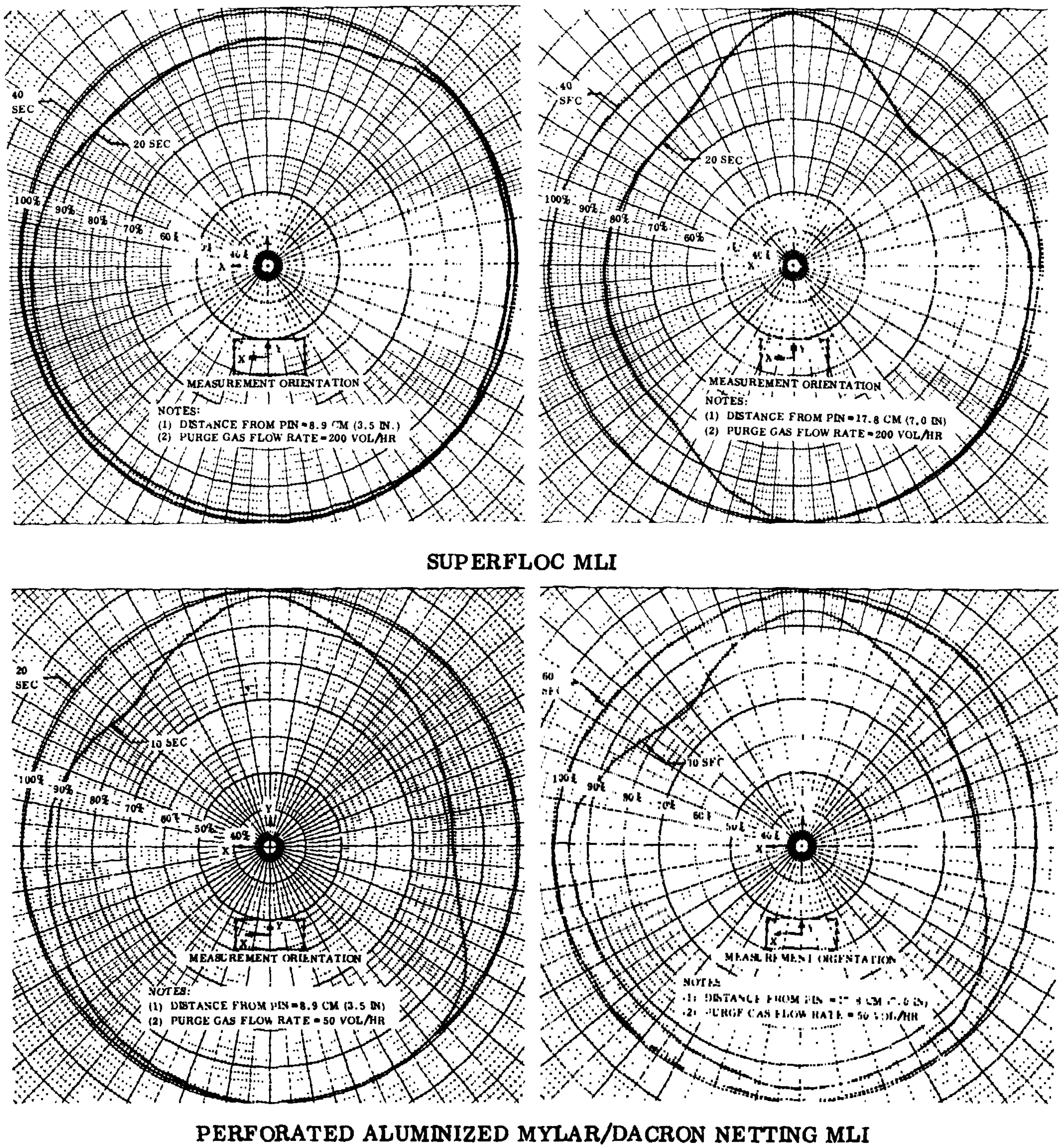

NOTES: (1) One Purge Pin Configuration
(2) Blanket Midlayer Measurement

Figure 25. Purge Gas Distribution Profile - Superfloc and Perforated Aluminized Mylar/Dacron Netting MLI

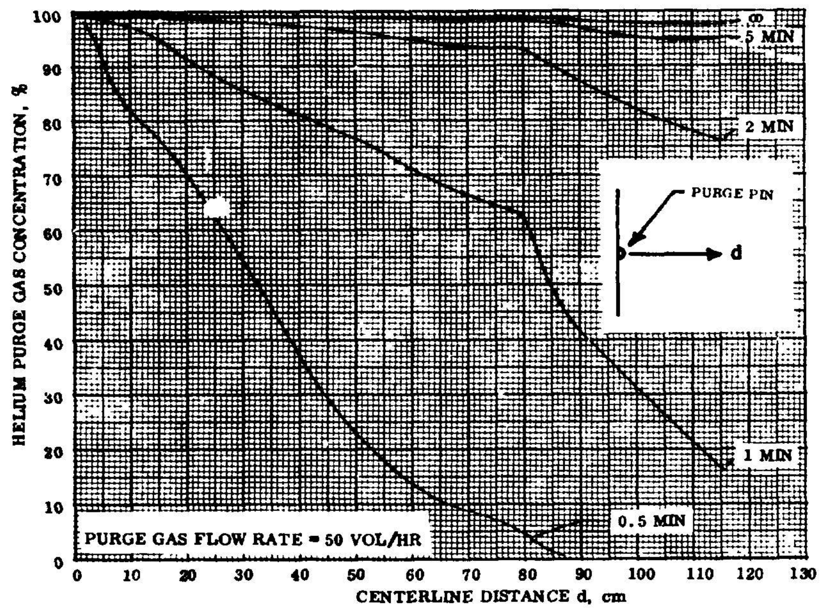

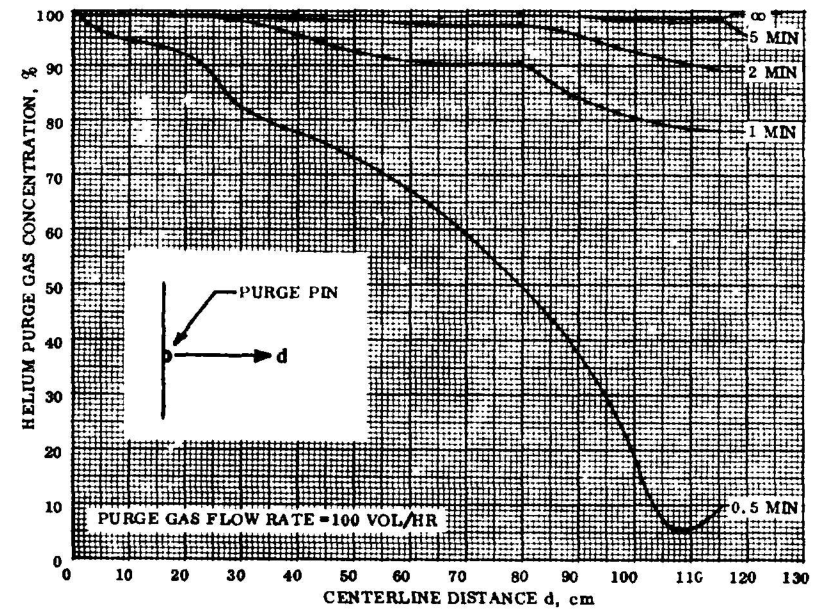

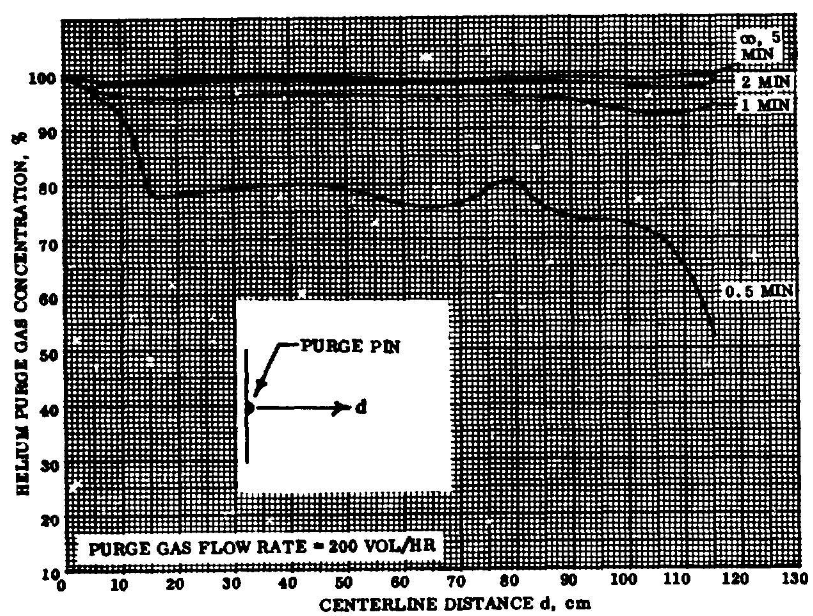

NOTE: No Simulated Purge Bag

Figure 26. Superfloc MLI Blanket Centerline Purge Gas Distribution

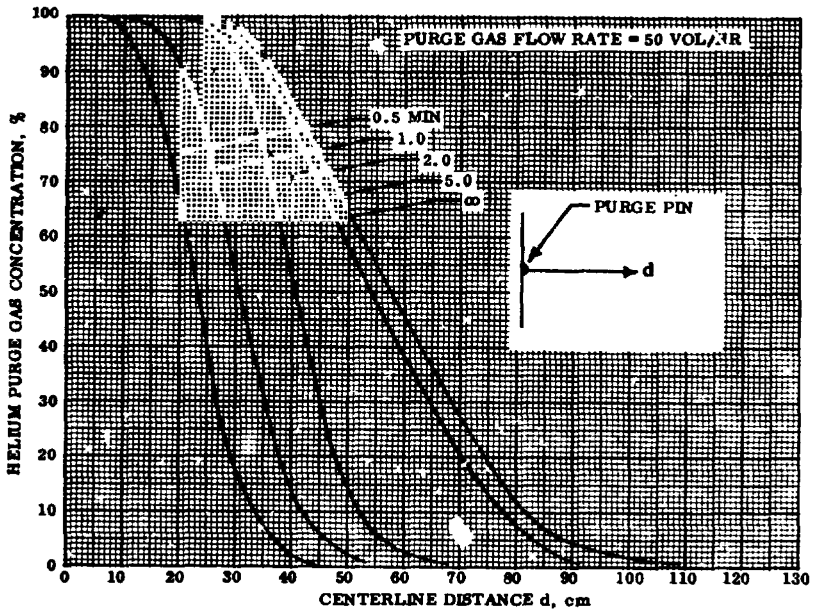

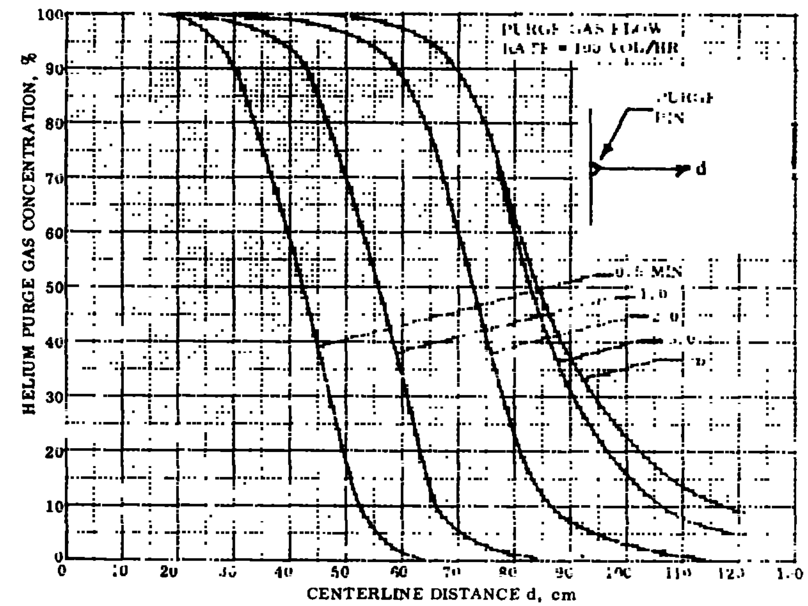

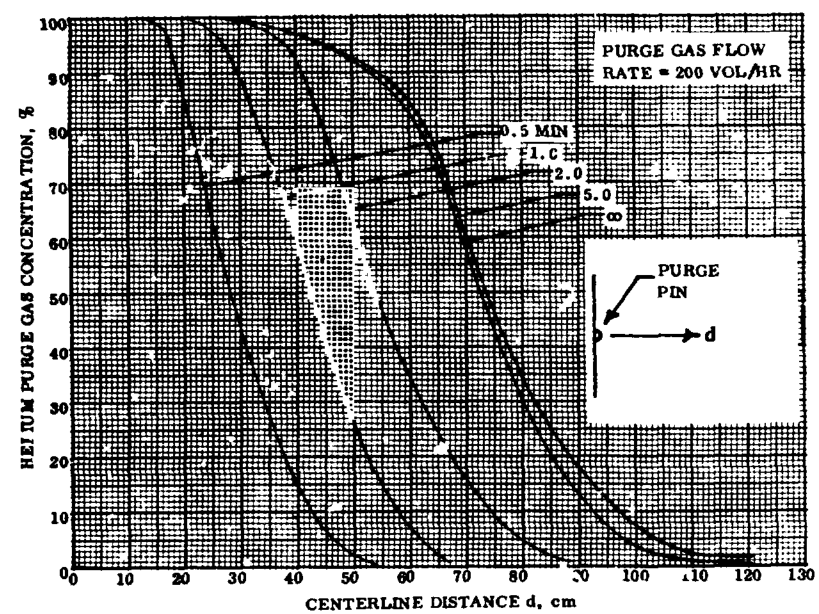

NOTE: No Simulated Purge Bag

Figure 27. Perforated Aluminized Mylar/Dacron Netting MLI Blanket Centerline Purge Gas Distribution

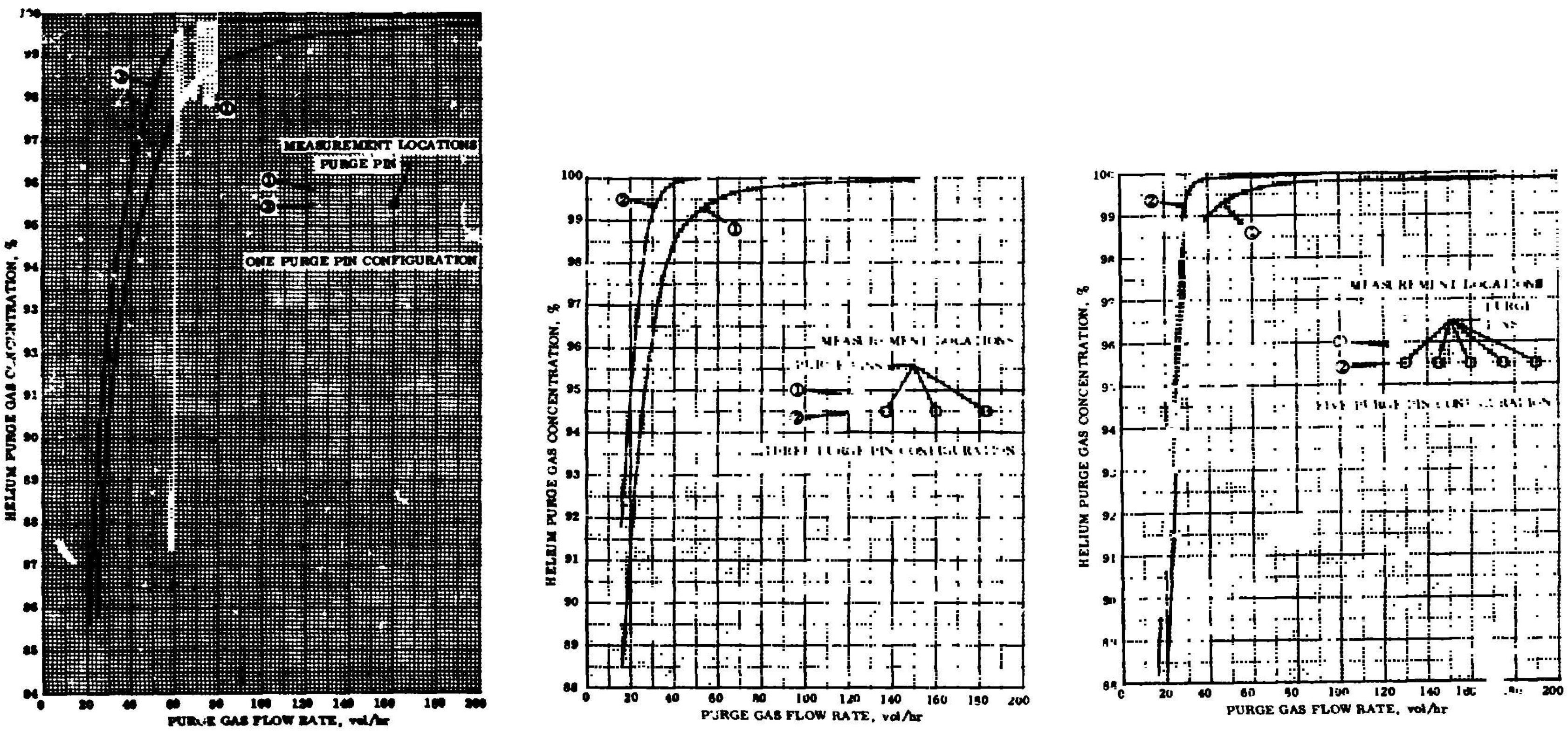

NOTES: (1) Helium Purge Gas
(2) With Simulated Purge Bag

Figure 28. Superfloc Blanket Edge and End Equilibrium Purge Gas Concentrations

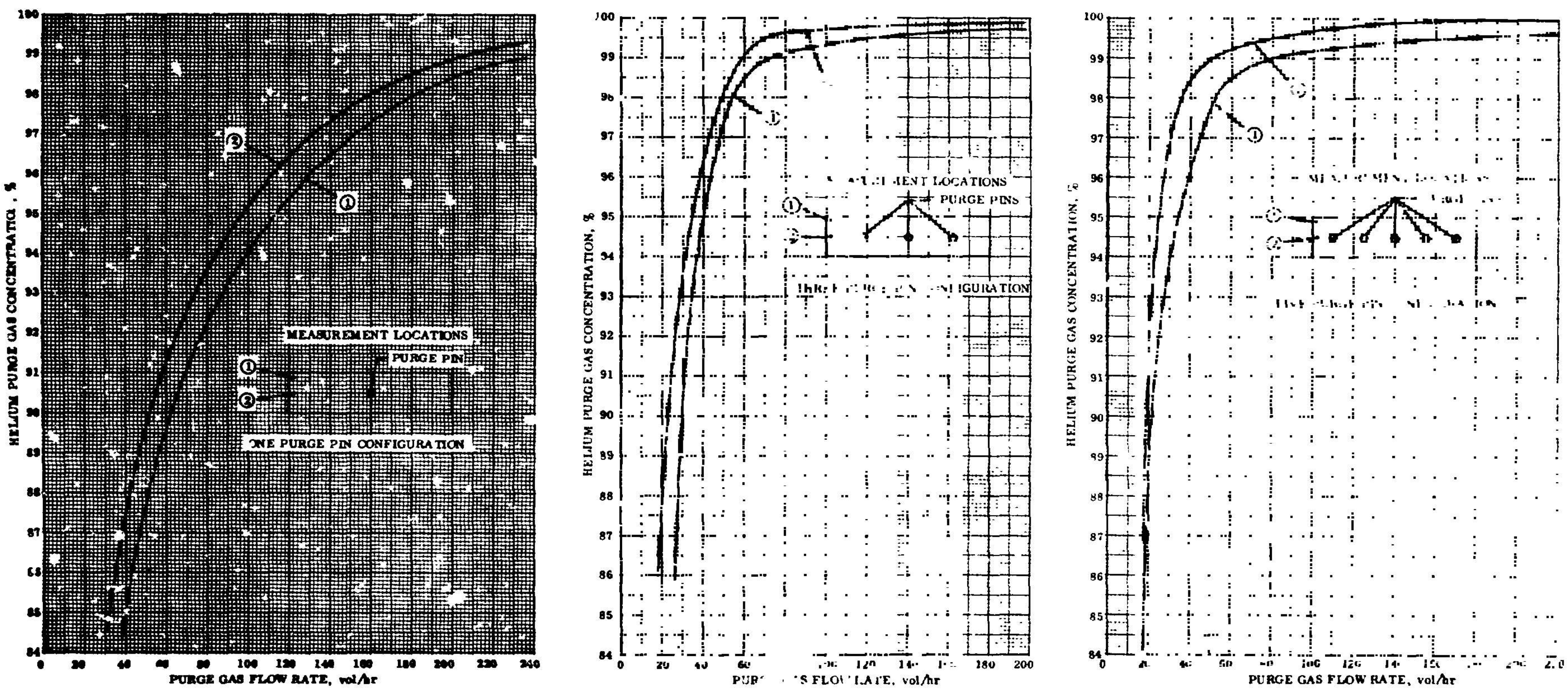

NOTES: (1) Heli... Purge Gas

(2) With Simulated Purge Bag

Figure 29. Perforated Aluminized Mylar/Dacron Netting MLI Edge and End Equilibrium Purge Gas Concentration

require approximately 5 minutes duration purge for a 100 vol/hr nominal purge rate, and that the exact duration will be configuration dependent.

Figure 30 presents a comparison of test data in the region of a purge pin with predicted purging history of Reference 2. As noted, good agreement was obtained between predicted values and test data.

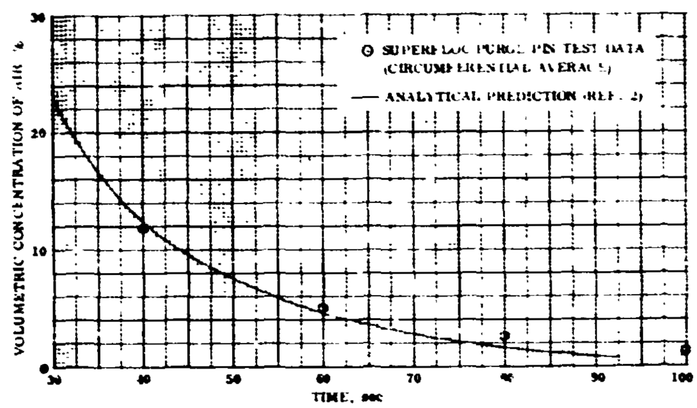

Figure 30. Comparison of Superfloc Purge Pin Test Data With Analytical Predictions

All pressure drop measurements obtained throughout the MLI test blankets indicated pressure differentials less than the tolerance of the pressure sensors. Thus, pressure effects were ignored.

3

PURGE SYSTEM DESIGN (TASK 4)

The purge system design task includes both the development of purge system detailed designs and the performance analysis of the test article design. A significant effort during the performance of the task was the definition of the fluid loop concept and hardware to be procured for use with the full scale test article experimental evaluation.

3.1 FLUID LOOP HARDWARE DEFINITION STUDY

3.1.1 TEST SYSTEM CONFIGURATION. The basic purge and repressurization system for the test program is schematically described in Figure 31. Component functional requirements, ie, size, power, response, leakage, etc, have been established, and vendor parts selected for the test article to meet these requirements.

The component selection process generally consisted of reviewing vendor data obtained from the data search. From these data and from vendor contacts, as many candidates as possible were selected which appear capable of meeting the overall requirements. A request for quote was then prepared and transmitted to each prospective vendor, along with a description of the minimum requirements. Where several candidates were involved, final selection depended upon availability, cost, design features, and qualification status.

3.1.2 SUBSYSTEM REQUIREMENTS. Major subsystem functions were described in Reference 2. For the test system, the major subsystem functions will be provided as described below.

3.1.2.1 Gas Storage and Feed Subsystems. These subsystems for the test system will be part of the test facility, external to the test enclosure. No flight hardware will be procured for this function. As a minimum the test setup will include the the items shown in Figure 31. Facility gas storage bottles will provide the source of helium and nitrogen required for purging, pressurization and repressurization of the purge bag.

A manually adjustable regulator (Item 1) will allow the inlet pressure to the supply flow control valve 7, to be adjusted. This permits the supply flow rate to be conveniently set at different levels. A flow meter (Item 5) will be installed in the feed line for flow measurement. A pressure gauge (Item 6) will be provided for measurement of the feed line pressure.

A relief valve (Item 4) will limit the pressure in the feed line to prevent an excess flow rate to the purge bag. This safety feature will protect against bag rupture from excess supply flow caused by erroneous regulator setup or regulator failure.

Item	Description
1	Pressure Regulator - Manually Adjustable
2	Manual Shutoff Valve
3	Manual Shutoff Valve
4	Relief Valve
5	Flow Meter
6	Pressure Gauge
7	Supply Flow Control Shutoff Valve - Solenoid Operated
8	Gauge Pressure Switch - Supply Control
9	Distribution Manifold Tube
10	Bleed Flow Control Shutoff Valve
11	Orifice - Bleed Flow
12	Vent Valve - Motor Operated Butterfly
13	Orifice Plate - Vent Flow
14	Relief Valve - Secondary
15	Gauge Pressure Switch - Primary Relief Control
16	Gauge Pressure Switch - Gas Feed

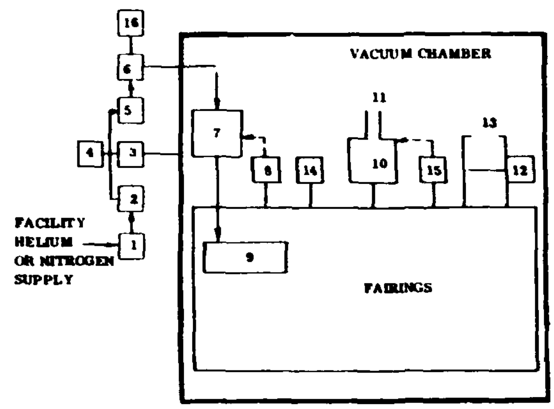

Figure 31. Purge and Repressurization System Schematic

Manual shutoff valves (Items 2 and 3) will allow the feed line to be vented to vacuum chamber pressure. This will prevent gas leakage through the supply flow control valve from entering the purge bag during flight simulation tests.

3.1.2.2 Gas Supply Flow Control Subsystem. This subsystem will consist of a normally closed, solenoid piloted, poppet type shutoff valve (Item 7) controlled by a differential pressure switch (Item 8) or direct signal. Valve 7 is opened by direct command for purging operations. In the pressure control mode, purge bag gauge pressure will cause pressure switch 8 to close on decreasing pressure at 3.44 kN/m^2 (0.5 psig) minimum and generate a signal to open valve 7. Switch 8 opens on increasing pressure at 10.33 kN/m^2 (1.5 psig) maximum to release the opening signal to valve 7. This sequence will repeat several times during an entry repressurization cycle. At ground level, valve 7 will open occasionally to replenish pressure lost due to gas leakage from the purge bag.

The pressure switch controlled supply flow control subsystem was selected because it is readily available. The data search failed to locate available qualified pressure controller operated flow control valves which meet the design criteria required for this application. Such a system is feasible, however.

The supply flow control valve has a flow area equivalent to a sharp edge orifice of 0.605 cm (0.238 in) diameter (C_o = 0.6). Port size is for 0.95 cm (3/8 in) tubing. Maximum feed line gauge pressure will be 1.38 MN/m^2 (200 psig).

3.1.2.3 Gas Distribution Subsystem. This subsystem receives gas from the supply flow control subsystem and distributes it throughout the MLI. The gas distribution approach is to route a manifold tube through each of three purge fairing plenums under the MLI. The manifold tube will have an orifice outlet in each plenum. The purge gas is conducted from the plenums into the layers of MLI through purge pins.

Examination indicates that the existing manifold tube 0.635 cm (1/4 in) diameter on the 2.2 m (87 in) test tank is adequate for the purge distribution system.

3.1.2.4 Bleed Flow Control Subsystem. This subsystem maintains the bag pressure within allowable limits during controlled operations. The normally closed bleed flow control valve (Item 10) is opened to allow purge bag gas to vent during purging. The bleed flow control subsystem will also sense excessive purge bag pressure and act to open the bleed flow control valve until excess pressure is relieved. This action is required to prevent bag rupture during go-around ascent, ferry mission ascent, or internal leakage failure of the supply flow control valve.

The minimum flow capacity of the bleed flow control valve is dictated by the maximum flow required at the minimum absolute pressure of the purge bag. The worst case would be failure of the supply flow control valve to close during deorbital maneuvers. Analysis has shown that an effective sharp edge orifice sized for this condition, will maintain an acceptable purge bag pressure during ground purging operations.

The bleed orifice (Item 11) required is of 2.34 cm (0.921 in) diameter for a 0.0063 Kg/sec (50 lb/hr) maximum helium flow capability. The effective throat diameter of the bleed flow control valve is 4.11 cm (1.62 in).

3.1.2.5 Vent Subsystem. This subsystem consists of an electrically operated 15.24 cm (6 in) butterfly valve (Item 12) which will be opened during vacuum chamber evacuations simulating ascent. The large size valve is compatible with experimentation with various vent area sizes up to 15.24 cm (6 in) in diameter.

3.1.3 FAIL SAFE FEATURES. The purge bag will be protected against collapse and rupture by incorporating the following fail safe features.

A secondary excess pressure relief valve (Item 14) will act as a back-up for failure of the bleed flow control subsystem during test. A pressure operated mechanical valve will be used so that it is active at all times. The relief valve will have a minimum crack pressure slightly above bleed flow control subsystem full flow pressure. Maximum full flow pressure will not exceed a safe limit of purge bag pressure.

3.1.4 SYSTEM DESIGN PARAMETERS. Table 5 summarizes the preliminary design parameters being used to design the purge and repressurization system. All other system parameters and requirements are in the system requirements document found in Reference 2.

3.1.5 SYSTEM PERFORMANCE CRITERIA. The criteria used to define the system performance requirements are described below.

Purge bag pressure control function levels shown in Table 6 were selected to allow each pressure control function to operate within the purge bag pressure parameters without interference. Under normal conditions of pressurization and repressurization, the

Table 5. Design Parameters for the Purge and Repressurization System

Parameter Description	Value	Units	Remarks
Helium Flow Capability	.0063 max	kg/sec	Factor of 2.5 × calculated estimate of max repressurization flow rate. Same flow rate is used for purge and repress.
	50 max	lb/hr	
Temperature of He Gas Supply	280 to 288	K	1. Normal facility gas temp. range. 2. Typical of flight gas supply temp. range.
	45 to 70	F	
Purge Enclosure Ult. Gauge Press.	25.8 min	kN/m^2	Based on tensile tests of bag material.
	8.42 min	lb/in^2	
Purge Enclosure Free Gas Volume	2.42	m^3	Calculated.
	85.5	ft^3	
Nitrogen Purge Gas Temperature	394 max	K	Preconditioning Purge
	250 max	F	
Purge Enclosure Operating Gauge Press. Range @ 200°K to 450°K (-100°F to +350°F)	0.21 min 24.13 max	kN/m^2	Minimum limit is arbitrary. Maximum limit pressure is based on ultimate gage pressure where $P_{oper} = P_{Ult}/2.5$
	0.03 min 3.50 max	lb/in^2	
Purge Enclosure Buckling Gauge Pressure	-46.8	N/m^2	Calculated.
	-6.79×10^{-3}	lb/in^2	
Allowable Tot. Sys. Leakage to Test Chamber	.252 max	mg/sec	Calculated.
	2.0×10^{-3} max	lb/hr	
Propellant Tank Temp During Purg'g	Ambient	-	
Purge Distribution 1. Fwd Fairing 2. Mid Fairing 3. Aft Fairing	4.2 max	mg/sec	Flow will be nearly equally divided to each fairing.
	33.3 max	lb/hr	
Helium Supply Pressure (Absolute)	1482 max	kN/m^2	Supply flow control valve inlet pressure based upon a practical residual level for a flight gas storage container.
	215 max	lb/in^2	
Ambient Pressure Change Rate for Go Around and Ferry Mission	-0.34 max	kN/m^2 sec	Based on an assumed moderate rate of climb to 26,000 ft maximum.
	-0.05 max	lb/in^2 sec	

Table 6. Purge Bag Design Pressure Levels

Purge Bag Gauge Pressure kN/m²	(psig)	Value	Pressure Control Event
24.13	(3.50)	max	Secondary relief valve at max flow on increasing pressure.
18.62	(2.70)	min	Secondary relief valve cracks on increasing pressure.
17.23	(2.50)	max	Bleed valve max full flow pressure.
15.86	(2.30)	max	Bleed pressure switch closes on increasing pressure.
13.80	(2.00)	max	Supply flow control limit of overshoot.
10.33	(1.50)	max	Supply pressure switch opens on increasing pressure.
8.96	(1.30)	min	Bleed pressure switch opens on decreasing pressure.
4.48	(0.65)	min	Bleed flow control valve closes on decreasing pressure.
3.44	(0.50)	min	Supply pressure switch closes on decreasing pressure.
1.38	(0.20)	min	Supply flow control valve is open on decreasing pressure.
0.21	(0.03)	min	Bag pressure lower limit during purge.

supply flow control subsystem will maintain purge bag gauge pressure between the arbitrarily established limits of 13.8 kN/m^2 (2.00 psig) max to 1.38 kN/m^2 (0.2 psig) min. The other control function is provided to prevent bag rupture or collapse.

The supply flow control subsystem worst case response requirements are defined as follows:

a. The closing or shutoff response of the supply flow control subsystem shall prevent purge bag pressure from exceeding 13.8 kN/m^2 (2.0 psig) when charging the bag at maximum flow with the LH_2 tank at room temperature. Calculated maximum rate of pressure increase is 1.84 kN/m^2 sec (0.375 psi/sec).

b. The opening response of the supply flow control subsystem shall prevent purge bag pressure from decreasing below 1.38 kN/m^2 (0.2 psig) for a maximum rate of ambient pressure increase of 0.69 kN/m^2 sec (0.1 psi/sec) (estimated from descent pressure curve of requirements document, Reference 2).

Figure 32 shows system response requirements for a pressure switch controlled solenoid shutoff valve system. This type of system could tolerate as much as a 0.267 sec closing response and a 3.0 sec opening response. Actual response of this type of system is on the order of 0.08 to 0.12 sec.

The bleed flow control subsystem worst case response requirements for a pressure switch controlled electrically operated bleed valve are defined as follows:

a. The opening response of the bleed valve control subsystem shall prevent purge bag pressure from increasing above 17.23 kN/m^2 (2.50 psig) when charging the bag at maximum flow with the LH_2 tank at room temperature. The maximum calculated rate of pressure increase is 1.84 kN/m^2 sec (0.375 psi/sec).

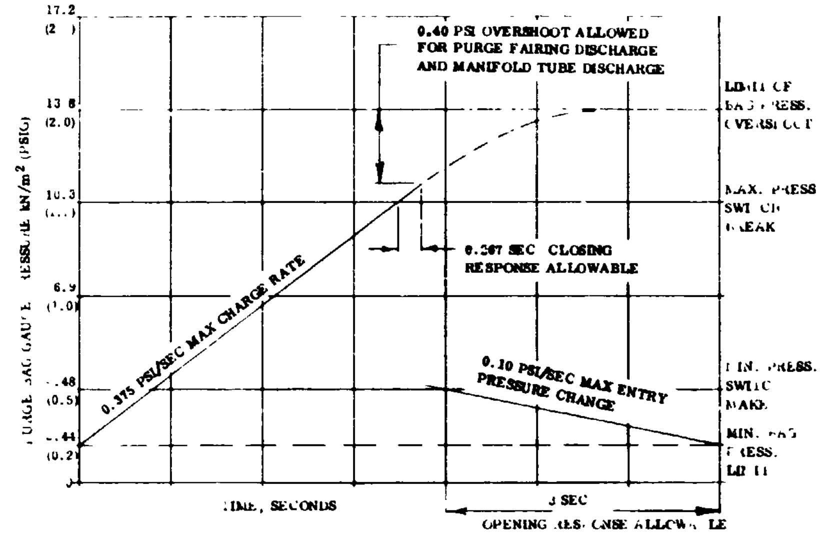

Figure 32. Supply Flow Control Valve Response Requirements

b. The bleed flow control valve shall close under the worst condition of bag pressure decay, prior to the time the pressure reaches a level which will cause the supply flow control valve to open. The worst case pressure decay rate would be a sea level blowdown of the purge bag through the open bleed valve. The minimum pressure is assumed to be 4.48 kN/m^2 (0.65 psig).

Figure 33 shows system response requirements for a pressure switch controlled, electrically operated shutoff valve system. This type of system would require a 1.00 second opening and closing response. This response rate is a consequence of sizing the supply and bleed system for 0.0063 kg/sec (50 lb/hr) maximum flow. A smaller flow capability would result in increased response time.

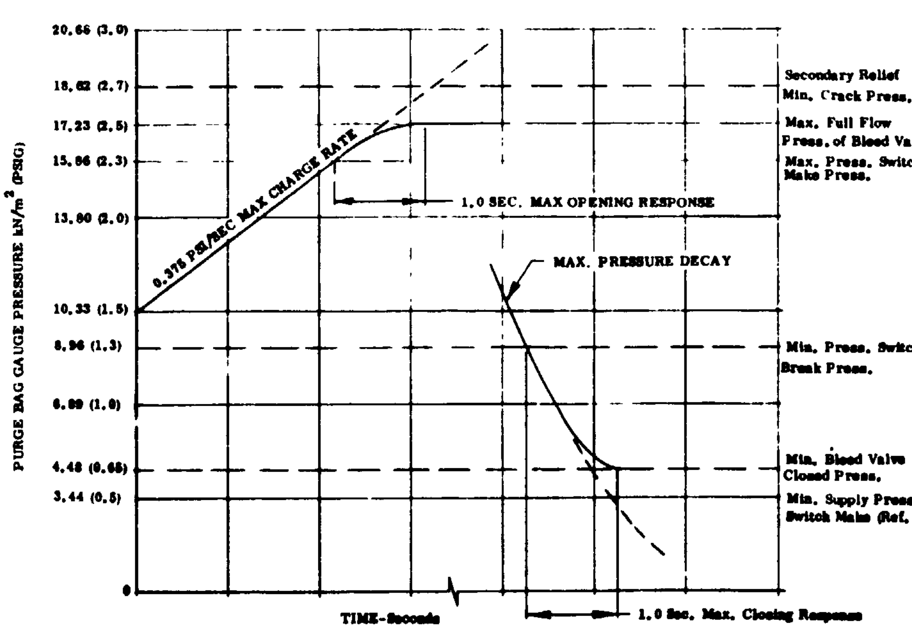

Figure 33. Bleed Flow Control System Response Requirements

3.2 ANALYTICAL STUDIES

Analyses were conducted in order to establish the test tank purge system flow rate requirements or tank system overall thermal performance. The analyses conducted include a purge and repressurization gas flow rate analysis, a parametric MLI gold thickness analysis, a purge plenum venting and repressurization analysis, and a system thermal analysis. The analyses were conducted either parametrically or for worst case parameter conditions.

3.2.1 PURGE AND REPRESSURIZATION GAS FLOW RATE ANALYSIS. Sizing of the purge and repressurization system fluid loop hardware necessitates that helium mass flow rates be established for the required flow conditions. Three flow conditions requiring flow rate definition were established: (1) system repressurization during re-entry, (2) purge gas make up during tank chilldown, and (3) system purging prior to cryogen tanking. The purge and repressurization system is designed for a single helium gas mass flow rate that will accommodate all of the above flow conditions. Thus, only a single gas distribution system is required.

3.2.1.1 Analytical Approach. Each of the flow conditions defined above has been analyzed to determine the transient helium gas flow rate required to maintain a positive pressure in the purge bag. Purge bag negative pressure differentials may result in bag collapse or nitrogen or air in-flow into the system which cannot be tolerated during cryogenic operation. Thus, the predicted flow rates obtained are the minimum rates necessary for proper system operation.

A transient analysis has been conducted to determine the total helium purge or repressurization mass requirement for the 2.2 m (87 in) diameter test tank for each of the three flow conditions above. The mass flow rates were determined as the time rate of change (slope) of the transient total gas mass curves.

System pressure during the tank chilldown and purging portion of the analysis was assumed to be one atmosphere and utilized a purge bag external radiative environmental temperature of 316 K (570R). During the re-entry analysis, the system pressure was as indicated in the first quarterly report (Ref. 2, Figure A5). The corresponding external radiative temperature was allowed to increase linearly from 200 K (360 R) to 450 K (810 R) in 900 seconds, maintain 450 K (810 R) to 1100 seconds, and decay to 397 K (715 R) at 1300 seconds. This temperature history follows the general temperature increase suggested in Reference 2.

Purge gas make up during tank chilldown was analyzed for three separate tank chilldown rates; 5 minutes, 10 minutes, and 20 minutes. These chilldown rates represent values that might be used on typical cryogenic tanks.

Mass flow rates during MLI purging were obtained from the analytical results presented in the second quarterly progress report (Ref. 1) and converted here to mass flow units.

3.2.1.2 Repressurization Model Description. A typical repressurization model of the gas filled MLI is presented in Figure 34. The model consists of a section of test tank skin covered with 44 layers of Superfloc MLI, enclosed within a purge bag which has a standoff distance of 2.54 cm (1.0 in). The mode of heat transfer between each MLI layer and between the MLI and purge bag was gaseous conduction and thermal radiation.

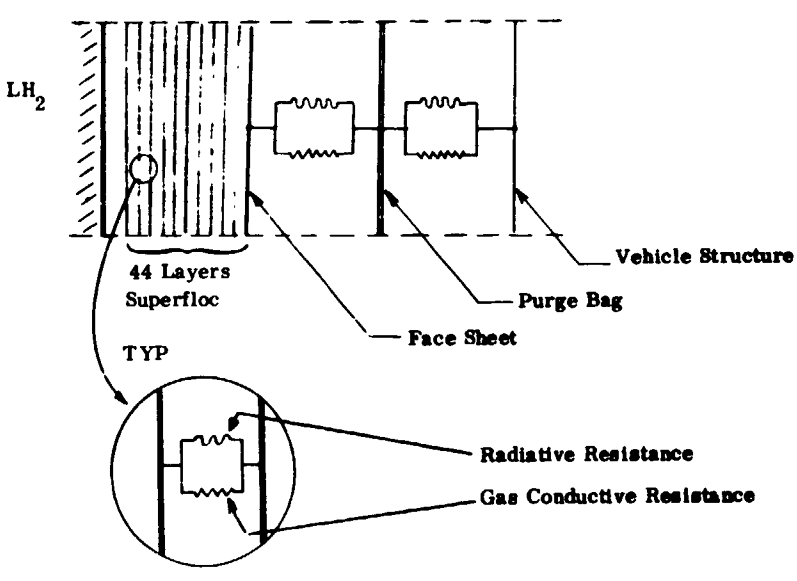

Figure 34. Repressurization Model (Reentry Condition Shown)

The model was segmented into 47 thermal nodes and contained 92 thermal resistances between nodes. A transient thermal solution to the network of nodes, resistances, and associated boundary conditions, was provided by means of a modification of the numerical procedure of the Convair Aerospace thermal analyzer computer program (Reference 5). The program is a versatile heat conduction code which accommodates a broad variety of boundary conditions and includes convenient simulation of free and/or forced convection, and radiative heat exchange. A modification to the program, which is as yet unpublished, provides an option in which conduction linkages are adjusted to accommodate varying interlayer pressures (if required). A simplified solution of the average interlayer pressure is obtained by means of a solution based upon the momentum relationships of Reference 6. The continuum regime value of gaseous thermal conductivity is accordingly reduced based upon the Corrucini relationship which predicts the effect upon thermal conductivity due to gas rarification.

3.2.1.3 Analytical Results. Results of an analysis are presented in Figures 35 through 38. Figure 35 shows the total repressurization helium gas mass flow rate during re-entry for the test tank configuration. As shown in Figure 35, the peak repressurization flow rate of 9.0 kg/hr (19.9 lbs/hr) occur after approximately 1140 seconds of re-entry flight (ie, time from 121,920 m (400,000 ft)). The greatest effect upon repressurization gas mass flow rate is from increasing atmospheric pressure rather than chilling of the repressurization gas. Figure 36 shows the purge gas total mass flow rate requirement during tank chilldown prior to cryogen tanking. Three tank chilldown rates were considered; 5 minutes, 10 minutes, and 20 minutes. A linear tank chilldown from 316K (570R) to 22K (40R) in the time specified was used in the analysis. The peak purge gas mass flow rate occurs for the shorter chilldown time as expected. The greatest value obtained was 3.42 kg/hr (7.55 lbs/hr) for the 5 minute

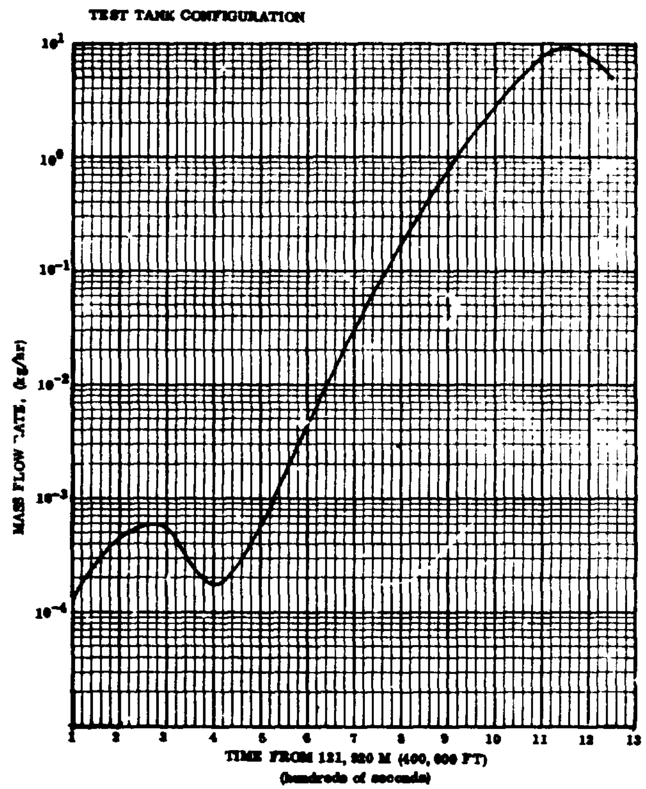

Figure 35. Minimum Total Repressurization Gas Flow Rate During Re-entry

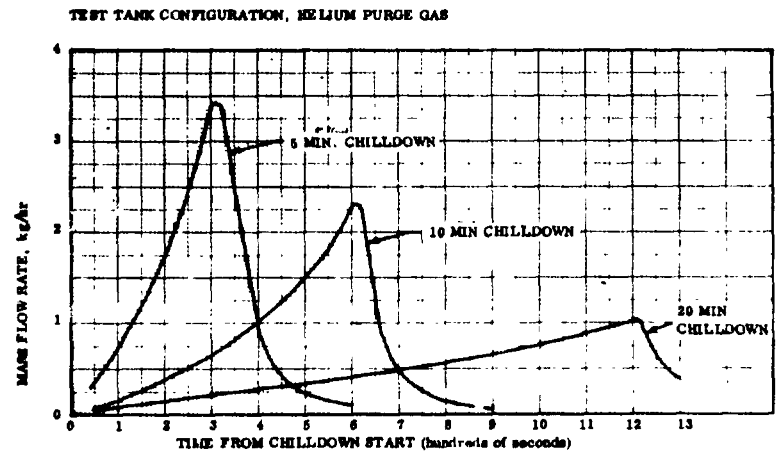

Figure 36. Minimum Total Gas Flow Rate During Tank Childown

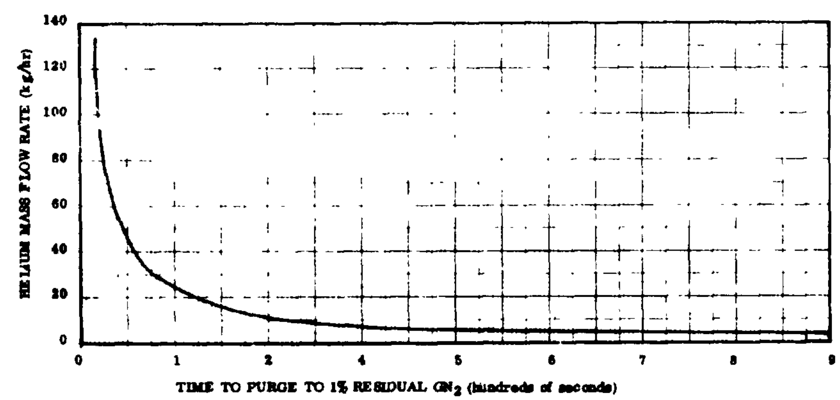

Figure 37. Total Purge Gas Flow Rate Versus Time to Purge to 1% Residual GN_2

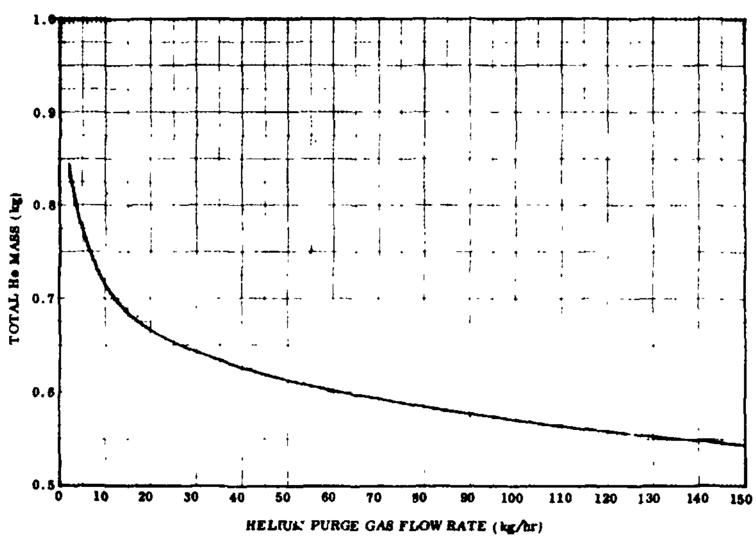

Figure 38. Total He Mass Required for Purging to 1% GN_2

tank childown time. Childown times shorter than 5 minutes duration were not considered as they were deemed impractical. Figures 37 and 38 present the helium mass flow rate requirement during pretanking purging. Figures 37 and 38 were determined in mass flow rate units from the purging analysis information presented in the Second Quarterly Progress Report (Reference 1).

As shown in Figure 37, any mass flow rate in excess of 7 kg/hr (15.5 lbs/hr) results in MLI purging within 300 seconds. Figure 38 presents the total helium ma*ʳ*. required to purge the MLI to 1% residual nitrogen. As indicated in Figure 38, only approximately 0.2 kg (0.44 lbs) of helium could be saved by increasing the purge gas flow rate as high as 100 kg/hr (220 lbs/hr). This gas savings has been deemed insignificant which eliminates purge gas total mass as an effective mass flow rate parameter. Thus, any purge gas flow rate which results in a satisfactory MLI purge time to 1% residual nitrogen is acceptable during MLI purging prior to tanking. Seven kg/hr (15.5 lbs/hr) has been selected as the minimum permissible flow rate for this purpose.

3.2.1.4 Gas Flow Analysis. The following conclusions and recommendations are presented as a result of the purge and repressurization system helium mass flow rate requirements analysis.

1. The repressurization gas mass flow rate during re-entry must be sufficient to provide at least 9 kg/hr (19.9 lbs/hr).

2. During tank childown, the purge system must provide a helium mass flow rate of 3.42 kg/hr (7.55 lbs/hr) for a tank childown duration of 5 minutes.

3. Purge gas mass flow rates of at least 7 kg/hr (15.5 lbs/hr) will provide MLI purging to 1% residual nitrogen within 300 seconds.

4. The flow rate requirement for repressurization satisfies each of the mass flow requirements of 1 through 3 above. Thus, 9 kg/hr (19.9 lbs/hr) has been adopted as the minimum required purge and repressurization gas mass flow rate.

5. For the Convair Aerospace test tank configuration, a mass flow rate requirement of 22.65 kg/hr (50 lbs/hr) has been adopted for hardware sizing. This value provides a large flow rate safety factor and will permit variable flow rate testing.

3.2.2 PARAMETRIC STUDY OF MLI GOLD THICKNESS. An analysis had been previously reported (Reference 1) in which the minimum gold total thickness requirement for the Superfloc goldized MLI was established, (800Å). A subsequent analysis has been completed to determine the sensitivity of the gold thickness requirement due to MLI average temperature, layer transmittance, and fractional total black body radiant energy maximum wavelength variances. The previous analysis uses an MLI average temperature of 222K (400R) a layer transmittance of 0.005 (0.5%), and a 95% total black body radiant energy maximum wavelength. The current analysis includes MLI average temperatures of 211K (380R) and 233K (420R), layer transmittances from 0.005 to 0.02, and a 90% total black body radiant energy maximum wavelength.

The current calculations use analytical techniques identical with those of the previous analysis. The techniques consist of repeatedly solving Lambert's absorption equation and Maxwell's electromagnetic equations for gold layer thickness using different initial parameters. The gold thicknesses computed are the minimum values which will limit the layer transmittance to the initially desired value, at the specific MLI average temperature and fractional black body energy value. Although the results are determined from two different theories in different spectral regions, coincidence was established at the longer wavelengths.

Results are presented in Figures 39 and 40. Figure 39 provides a summary of the analysis. Shown is the minimum required gold total thickness as a function of the three variables (MLI average temperature, layer transmittance, and fractional total blackbody energy maximum wavelength). Figure 40 presents the minimum required gold thickness as a function of wavelength and transmittance. The wavelength parameter in Figure 40 combines the effects of temperature and fractional total black body energy wavelength. The analysis shows that minor changes in the MLI average temperature and fractional total black body energy wavelength results in only minor changes in the gold thickness requirement. Further, large relative changes in transmittance (eg, 100%) results in minimum required gold thickness changes of only approximately 15%. Thus, the minimum gold thickness requirement is not extremely sensitivie to any of the parameters investigated and the 800 Å total gold thickness requirement per layer of MLI appears to be applicable over a moderately wide range of boundary conditions.

3.2.3 PURGE PLENUM VENTING AND REPRESSURIZATION. The 2.21 m (87 in) diameter test tank is designed such that the MLI system purge and repressurization gas is injected equally into the plena formed by the forward, aft and mid fairings on the tank. The MLI purge pins are mounted through the fairings and subsequently provide gas injection into the MLI as the plena become pressurized. Structural analyses have indicated that the existing fairings require stiffening in order to withstand plenum pressurization in excess of approximately 5.2 Torr (0.1 psid).

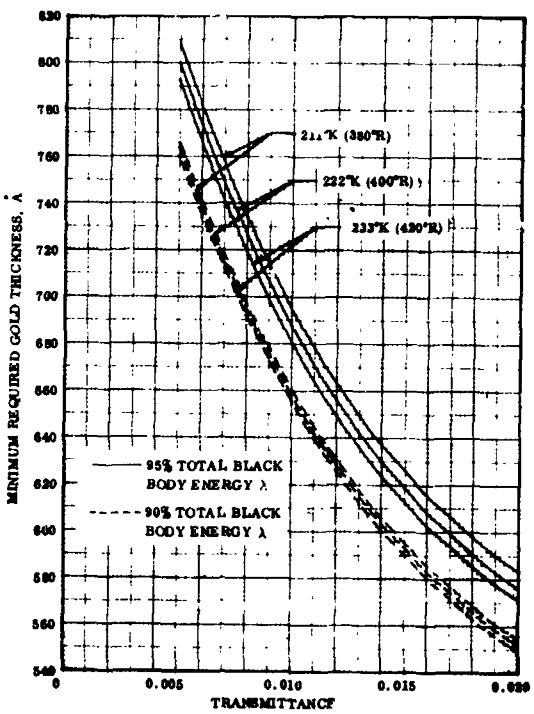

Figure 39. Predicted Total Gold Thickness Versus Transmittance

This limited plenum pres ure vessel capability was deemed inadequate to withstand repressurization loads. Subsequent redesign of the fairings have increased the maximum allowable plenum pressure differential capability to 83 Torr (1.6 psid) and 516 Torr (10 psid) for the forward/aft and mid fairings, respectively. Because of the plenum repressurization structural requirements an ascent plenum venting and repressurization analysis were required to insure the plenum maximum allowable pressure differentials are not exceeded and to establish the maximum repressurization gas flow rates. In addition, the test tank system includes a repressurization flow termination pressure sensor internal to the purge bag but external to the plena. As the pressure in the purge bag increases during repressurization to the normal operating pressure of 77 Torr (1.5 psid), the inlet

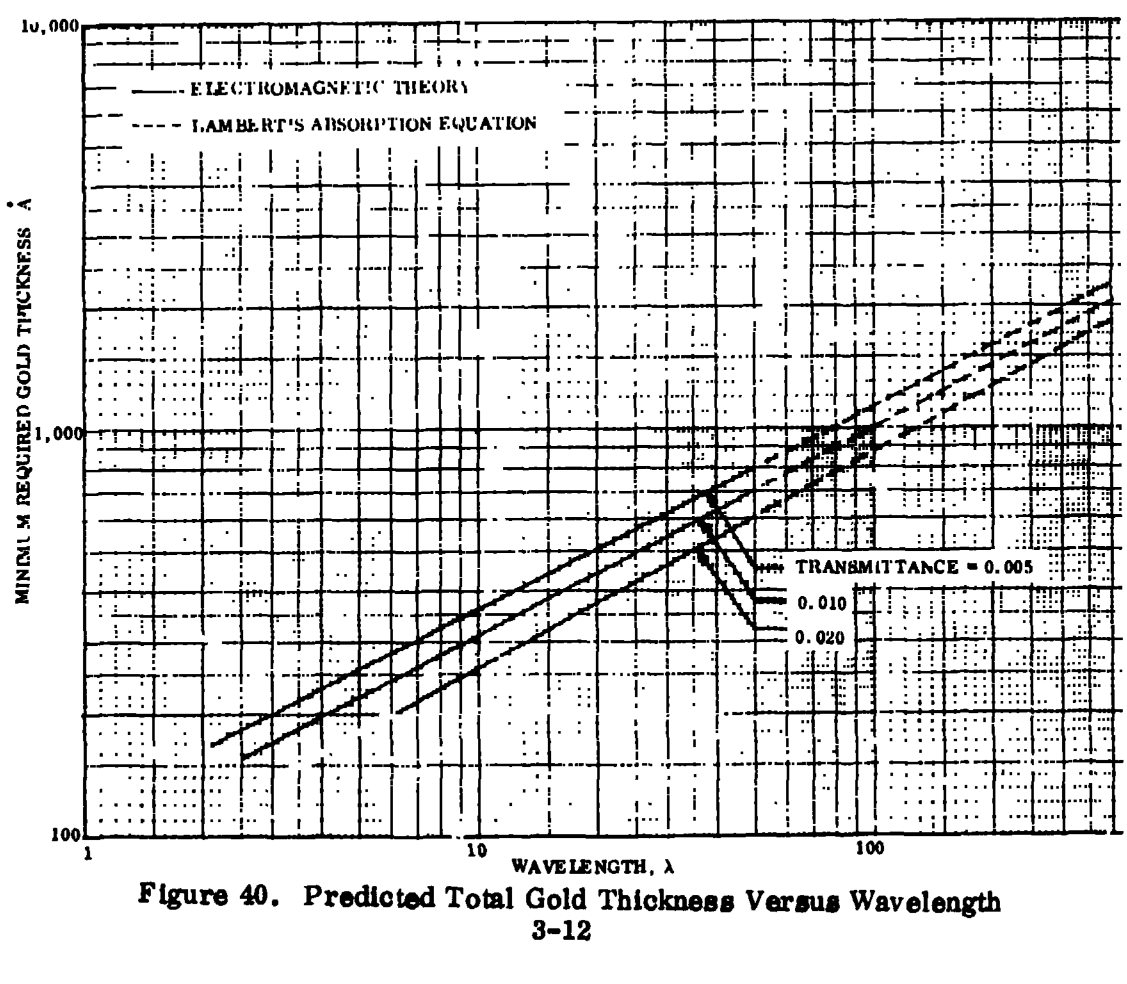

Figure 40. Predicted Total Gold Thickness Versus Wavelength

flow to the plena is terminated. The gas within the plena vent down into the purge bag until plena/purge bag pressure equilization is achieved. The purge bag pressure in excess of the flow termination pressure is defined as the purge bag pressure overshoot. An analysis has thus been conducted in which the pressure differential across the plena and the magnitude of the purge bag pressure overshoot have been established during plenum ascent venting and plenum re-entry repressurization.

3.2.3.1 Plenum Venting and Repressurization Analytical Techniques. Plenum or plenum/purge bag combination pressure changes were computed by the techniques presented in Reference 2. An expression describing the time rate of change of pressure was derived from the non-steady energy equation. The expression depends upon plenum vent or repressurization gas net flow rates. With flow into and out from the plenum in pressure-volume units (flow rates, Q, in micron-cc-sec^{-1})

$$\frac{dP}{dt} = \frac{\gamma}{V} (Q_{in} - Q_{out}) \qquad (1)$$

where

P = plenum pressure
γ = the ratio of specific heats
V = plenum volume
Q_{in} = flow into the plenum
Q_{out} = flow out from the plenum

Gas flow through the plenum purge pin orifice is given by

$$Q_{continuum} = C_v A \sqrt{P \Delta P}$$

or

$$Q_{free\ molecular} = C_m A (P - P_o)$$

where

C_v = a numerical constant = 54800 cm/sec
C_m = a numerical constant = 25700 cm/sec
A = purge pin orifice flow area
P = pressure in the plenum
$\Delta P = \begin{cases} P - P_o & \text{non-choked flow} \\ 0.5133\, P & \text{choked flow} \end{cases}$
P_o = pressure outside plenum (ambient pressure per Ref. 2, or pressure in purge bag)

The constants C_m and C_v contain factors for unit conversion and 0.6 as the flow discharge coefficient.

To compute transition and slip-flow through the purge pin orifice a linear interpolation is performed on the Knudsen number (Kn) within the range $0.01 < Kn < 1.0$ at $Kn = 1.0$, $Q = Q_{molecular}$ and at $Kn = 0.01$, $Q = Q_{viscous}$. At intermediate values of Kn the linear interpolation results in a Q which is weighted between $Q_{molecular}$ and $Q_{continuum}$ by the Knudsen number.

Integration of Equation 1 was accomplished by Euler's method. The program for integrating Equation 1 was written for venting studies and was coupled to the CABRÓN code described in Reference 2, as a subroutine.

For the venting analysis, the time dependent ascent ambient pressure (Po), from Reference 2, was programmed in table form, and was evaluated by linear interpolation at the current computational time.

For the repressurization analysis, the pressure in both the plenum and purge bag were determined using Equation 1. The Q_{out} from the plenum was updated as Q_{in} for the purge bag. The boundary pressure for the plenum was the purge bag pressure at the previous time step. The repressurization analysis was conducted parametrically with the repressurization gas flow rate as the independent variable.

The block diagrams of Figures 41 and 42 illustrate the computational steps for the plenum venting and repressurization analyses, respectively.

3.2.3.2 Plenum Venting and Repressurization Analytical Models. During venting, the purge bag 15.24 cm (6.0 in) diameter vent valve is open to ambient. In the venting configuration, the resulting purge bag pressure is equal to the ambient pressure (see Reference 2). Thus, the venting model consists of a single plenum, venting to ambient pressure through purge pins which are simulated by a sharp edge orifice of equivalent flow area.

During repressurization, the helium gas is introduced into the plenum. Subsequent venting of the plenum into the purge bag through the purge pins occurs as the plenum pressure increases. The resulting rise in purge bag pressure establishes the boundary pressure for the plenum. The repressurization model thus simulates two plena in tandem, separated by an equivalent flow area sharp edge orifice. The repressurization gas is introduced equally into the forward, aft, and mid fairings.

The analytical models for plenum venting and repressurization are shown in Figure 43.

3.2.3.3 Analytical Results. Results from the venting analysis are presented in Figure 44. The predicted maximum pressure differential across a plenum during ascent venting is 5.2 Torr (0.1 psid). This value is well below the maximum allowable and is thus satisfactory.

Repressurization and purge bag pressure overshoot analytical results are presented in Figures 45 through 47. Figure 45 shows typical repressurization plena pressure

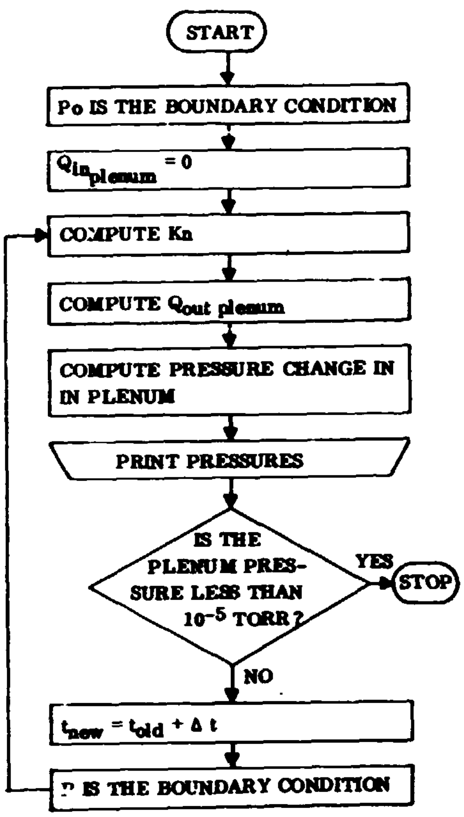

Figure 41. Computational Block Diagram for Plenum Venting Analysis

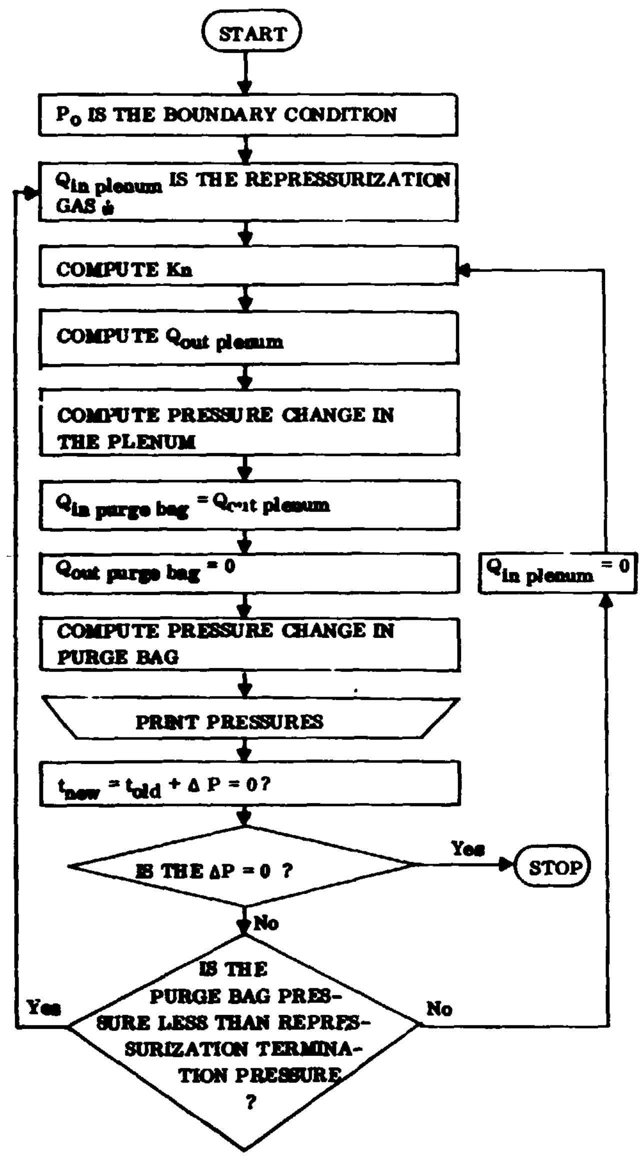

Figure 42. Computational Block Diagram for Plenum Repressurization Analysis

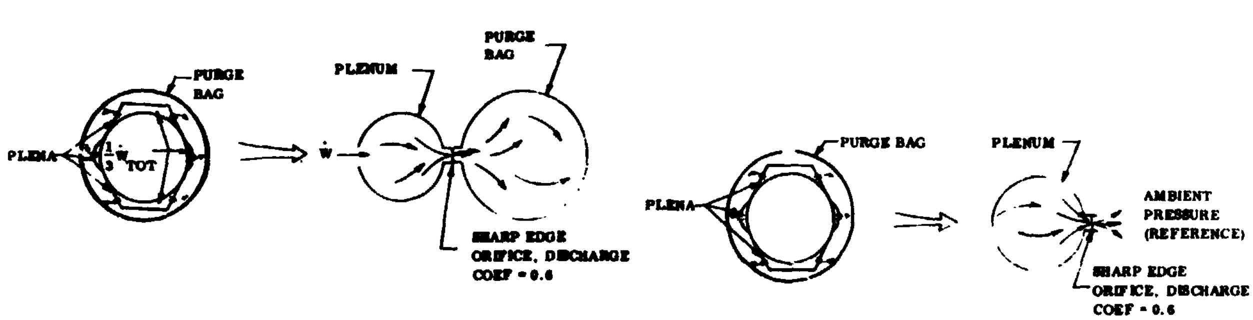

Figure 43. Plenum Venting and Repressurization Models

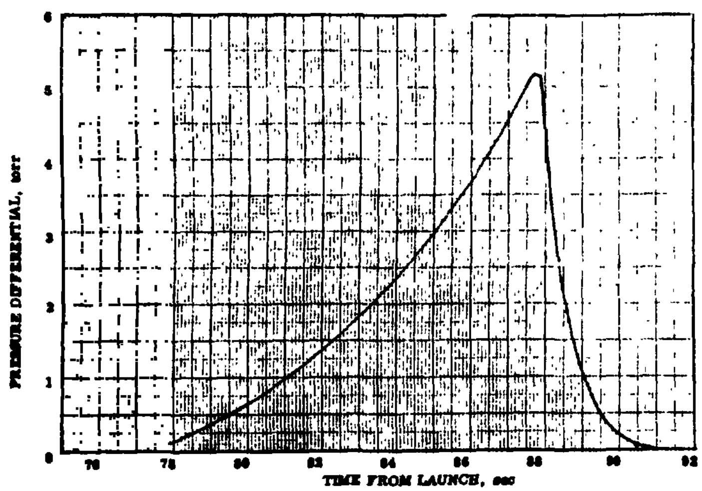

Figure 44. Forward/Aft Fairing Pressure Differential History During Launch Vent Down Transient

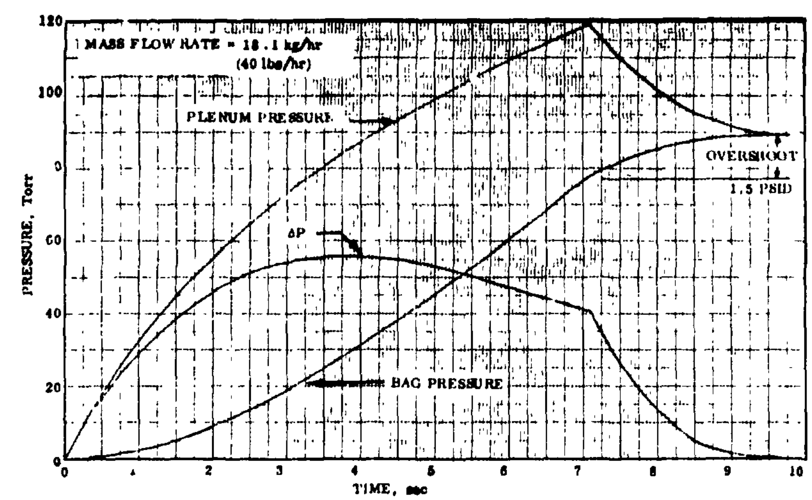

Figure 45. Forward/Aft Fairing Typical Pressure History During Repressurization

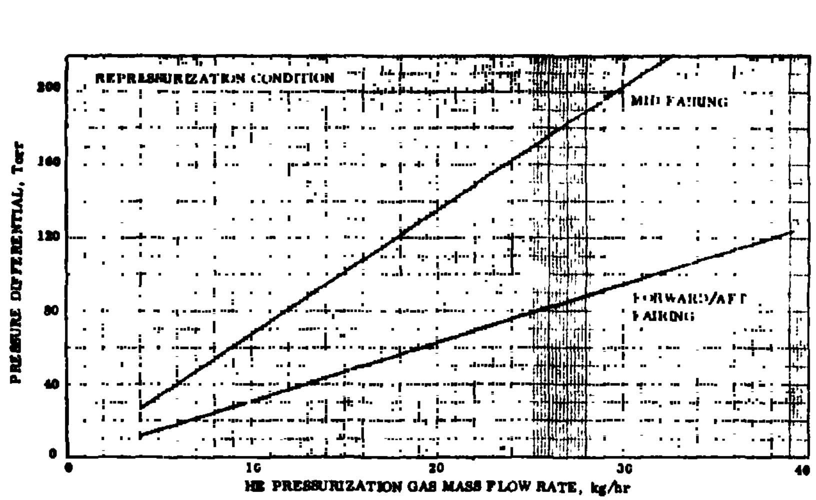

Figure 46. Fairing Maximum Pressure Differential Versus He Pressurization Gas Mass Flow Rate

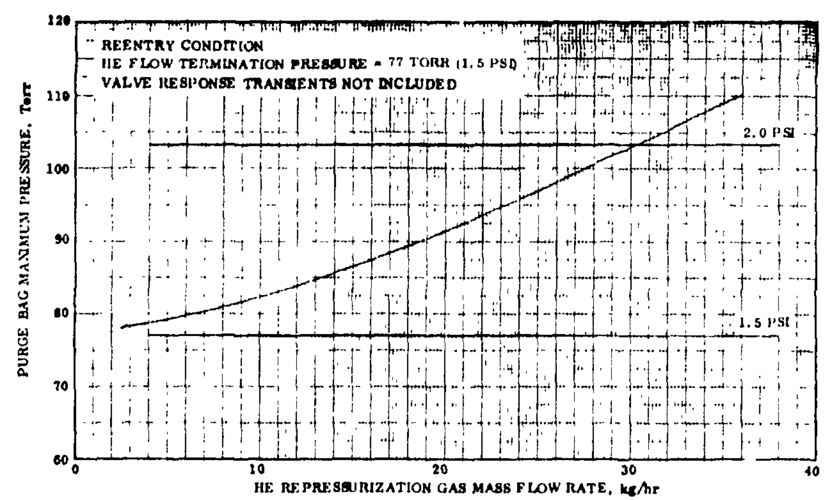

Figure 47. Fairing Maximum Pressure Differential Versus He Repressurization Gas Flow Rate

histories as well as the resulting pressure differential history. Figure 46 provides the maximum plenum pressure differential versus repressurization gas flow rate. For a maximum allowable forward/aft plenum pressure differential of 83 Torr (1.6 psid), Figure 46 indicates a maximum allowable repressurization gas flow rate of 26 kg/hr (57 lbs/hr). Further, from Figure 46, the maximum allowable repressurization gas flow rate for the mid fairing (maximum allowable pressure differential of 516 Torr (10 psid)) far exceeds that for the forward/aft fairings. Thus, the 26 kg/hr (57 lbs/hr) establishes the maximum allowable repressurization gas flow rate. Figure 47 shows the purge bag overshoot pressure versus repressurization gas flow rate of 26 kg/hr (57 lbs/hr), the purge bag overshoot maximum pressure differential is 98 Torr (1.9 psid). Normal purge bag operating pressure is 77 to 103 Torr (1.5 to 2.0 psid), thus, no purge bag overpressurization is expected.

3.2.3.4 Conclusions and Recommendations. The following conclusions and recommendations are presented as a result of the Convair Aerospace test tank configuration plenum venting and repressurization analytical predictions:

1. Plenum maximum pressure differential during venting is 5.2 Torr (0.1 psid). This value is well below the maximum allowable and is therefore acceptable.

2. Forward/aft plenum maximum allowable repressurization gas flow rate is 26 kg/hr (57 lbs/hr). This value is much less than the maximum allowable for the mid fairing plenum and thus establishes the maximum allowable for the test tank system.

3. Purge bag pressure overshoot resulting from the maximum allowed repressurization gas flow rate is within the purge bag normal operation range.

4. The maximum repressurization gas flow rate for the Convair Aerospace test configuration will be limited to 22.7 kg/hr (50 lbs/hr). This reduced flow rate results in an approximate 12% safety margin for hardware sizing and plenum pressurization limits.

3.2.4 LARGE SCALE SYSTEM THERMAL ANALYSIS. A complete thermal analysis was conducted for simulated space thermal equilibrium conditions for the 2.21/1.89 m (87.6/74.5 in) diameter cryogenic storage tank and associated structure. The basic tank/insulation system consists of an oblate spheroid tank, low conductive fiberglass support struts, 44 layers (two blankets) of double goldized Kapton Superfloc MLI, an MLI purge system, and an enclosing shroud. Forward, aft, and mid section fiberglass fairings are fitted to the tank in order to facilitate Superfloc blanket manufacture, installation and support. The basic tank/insulation system configuration is presented in Figure 48.

The analysis was conducted in order to establish the system overall thermal performance and to investigate the effects upon thermal performance resulting from degraded

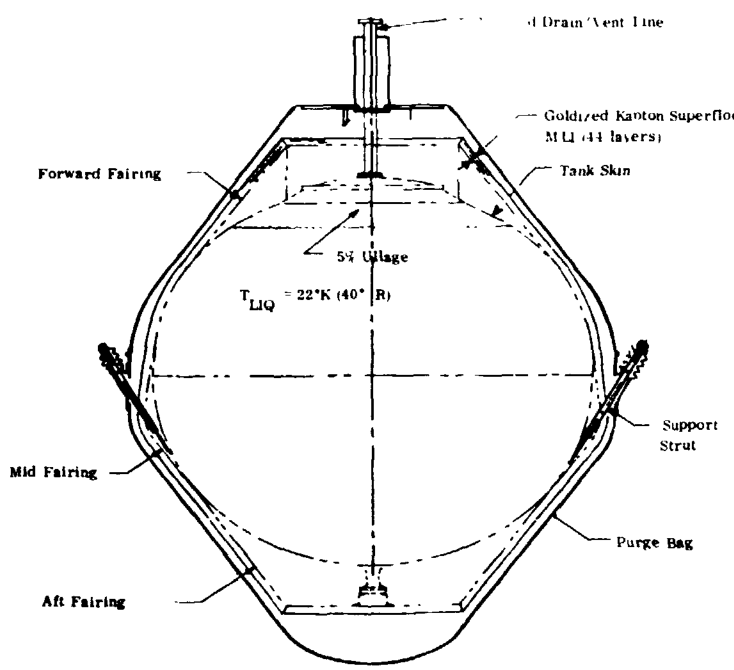

Figure 48. Convair Aerospace 2.21/1.89 m (87.6/74.5 in) Purge and Repressurization System Test Tank

MLI thermal radiation properties (emittance) and/or MLI interstitial gas pressure.

Portions of the thermal modeling and model basic computations were obtained from Reference 7 and were used in the subject analysis as required.

The thermal analysis of the purge and repressurization system test tank and associated structure was conducted using an improved version of the Reference 5 Convair Thermal Analyzer Computer Code. A thermal model composed of 231 separate thermal nodes and 688 thermal resistances was generated for solution by the above code. The thermal analysis was conducted parametrically in which the MLI emittance and interstitial pressure were independent variables. The Superfloc flat sheet emittance range was 0.010 to 0.030, while the interstitial pressure range was 1×10^{-4} to 1×10^{-6} Torr. Specified values for emittance and interstitial pressure are 0.020 and 1×10^{-5} Torr, respectively.

The system total heat leak results from six separate but interacting component contributions as indicated below.

Component	Component Heat Transfer Mode
1. MLI Layers	Solid Conduction, Radiation
2. MLI Blanket Seam Joints	Radiation
3. Purge, Support, and Twin Pins	Solid Conduction
4. Residual Gas	Conduction
5. Penetrations	Solid Conduction, Radiation
6. Support Struts	Conduction, Radiation

Each component section was thermally modeled and included in the overall computer model as discussed in the following sections.

3.2.4.1 Multilayer Insulation (MLI) Layers. Two MLI blankets were analyzed for the test tank. Each blanket consists of two face sheets and 22 Superfloc shields. However, the total number of shields considered in the analysis was 45, since some face sheets and shields are in direct thermal contact (ie, no separating tufts). The total MLI blanket was divided into 19 regions along the surface of the tank and/or fairings. Each region was segmented into five thermal nodes in depth representing the 1st, 12th, 23rd, 34th, and 45th shields. MLI inner and outer surface nodes as well as purge bag and fairing boundary nodes are shown in Figure 49.

Heat transfer through the MLI layers results from two components, interlayer radiation and solid conduction along the Dacron tufts.

The thermal radiation energy passing through n parallel surfaces is given by

$$Q_{rad} = \frac{\mathfrak{F} A \sigma (T_h^4 - T_c^4)}{n-1}$$

The radiation interchange factor for multiple shields is

$$\mathfrak{F} = \frac{1}{(1/\epsilon_1 + 1/\epsilon_2 - 1)\ (n-1)}$$

in which ϵ_2 and ϵ_1 are the emittances of the goldized Kapton shields with and without flocked tufts, respectively. Reference 8 suggests an expression for the determination of ϵ_2 from ϵ_1, based upon the ratio of tuft area to the Kapton total area, ie,

$$\epsilon_2 = \frac{A_t}{A_{tot}} \epsilon_t + \frac{(A_{tot} - A_t)}{A_{tot}} \epsilon_1$$

Since the analysis was conducted parametrically with ϵ_1 as an independent variable, ϵ_1 was considered to be independent of the shield temperature. The resulting $\mathfrak{F}$ over the range of ϵ_1 considered in the analysis (0.01 to 0.03) for 12 goldized Kapton shields is shown in Figure 50.

Solid thermal conduction through Superfloc results from intershield contact through the Dacron tufts. Conduction through Superfloc is obtained from the classical conduction equation

$$Q_{cond} = \frac{KA}{\ell} (T_h - T_c)$$

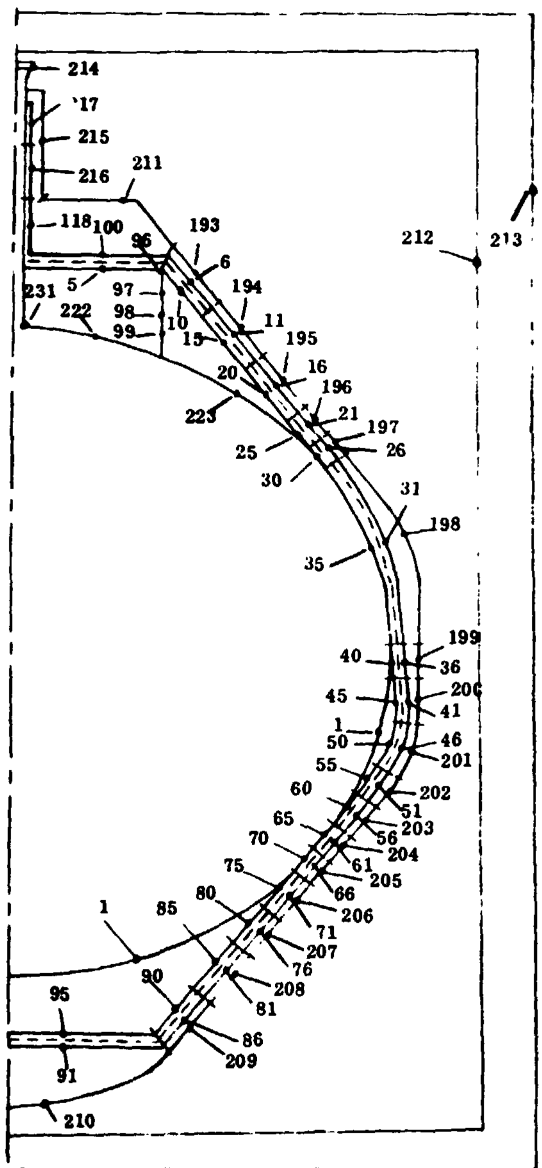

Figure 49. Thermal Model Nodal Schematic of Tank and Insulation Configuration

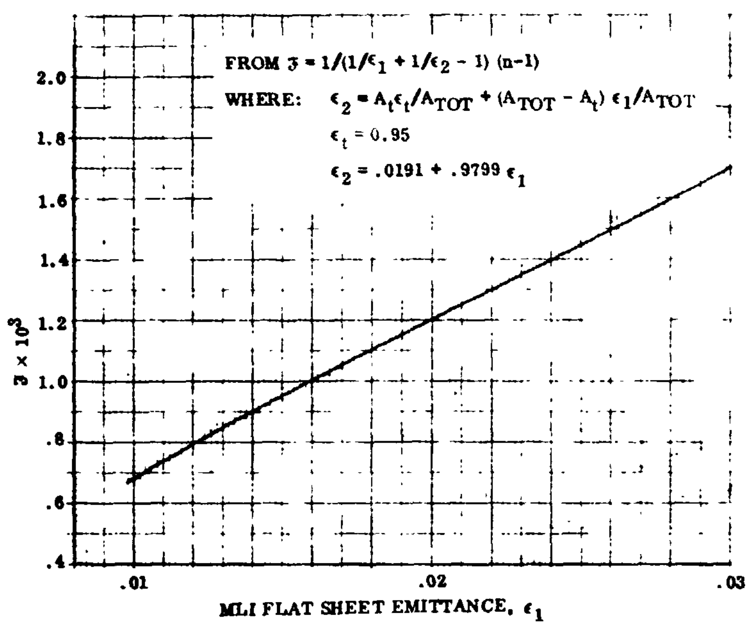

Figure 50. MLI $\mathcal{E}$ for 12 Double Goldized Superfloc Shields

in which K is the MLI effective thermal conductivity due to the Dacron tufts. The effective K has been established by combined analytical and experimental analysis in Reference 9 and is shown in Table 7. Also presented in Table 7 are the Superfloc shield characteristics employed in the analysis.

Radiation interchange factors between the fairing internal surfaces and tank skin were obtained from Reference 7. An emittance of 0.85 was used for the fiberglass fairings. The emittance of the iridite aluminum tank surface was based upon test data obtained from the Convair Space Sciences Laboratory, and by estimating the effects of degradation. A value of 0.03 (at 22K (40R)) was used.

Table 7. Superfloc MLI Parameters

Parameter	Value		
Tuft Spacing	0.95 cm	(3/8 in)	
Tuft Spacing Density	11023 tufts/m^2 MLI	(1024 tufts/ft^2 MLI)	
Tuft Diameter	0.15 cm	(0.060 in)	
Number of Dacron Needles Contacting Adjacent Shield	20 Needles per Tuft		
Needle Length	0.10 cm	(0.040 in)	
Needle Diameter	0.0018 cm	(0.000691 in)	
Emittance of Tuft Area	0.95		
Effective Tuft Thermal Conductivity (Reference 9)	T, K (R)	K, $\frac{\text{watts}}{\text{m-K}}$	$\left(\frac{\text{Btu}}{\text{hr-ft-R}}\right)$
	0 (0)	1.395×10^{-6}	$(.807\times10^{-6})$
	111.1 (200)	1.528×10^{-6}	$(.884\times10^{-6})$
	222.2 (400)	1.685×10^{-6}	$(.975\times10^{-6})$
	333.3 (600)	1.814×10^{-6}	(1.05×10^{-6})

3.2.4.2 MLI Blanket Seam Joints. Blanket seam heat transfer analysis was based upon the techniques of Reference 10. A design seam width of 0.0016 m (0.0625 in) together with a seam depth of 0.0019 m (0.75 in) (depth of one blanket) was used. The equation describing the seam radiation heat transfer rate is

$$Q_s = \ell_s \delta_s f \sigma (T_h^4 - T_c^4)$$

in which f = dimensionless function of the butted joint width to depth ratio (f = 0.0182 for the subject analysis, see Reference 10).

The Thermal Analyzer Code uses the following equation for computing radiation heat transfer

$$Q = \mathcal{F}_{ij} A_i \sigma (T_j^4 - T_i^4)$$

Radiation heat transfer correspondence thus exists when

$$\mathcal{F}_{ij} A_i = \ell_s \delta_s f = 0.001138 \ell_s$$

3.2.4.3 Purge, Support and Twin Pins. Heat transfer through the MLI due to purge, support, and twin pins, along with their associated grommets, occurs by solid conduction. The support pins are constructed of unidirectional fiberglass while the grommets, seam pins, and purge pins are manufactured from polyphenylene oxide (PPO). Temperature dependent conductive resistance parameters (ℓ/A) were computed for each pin and/or pin-grommet as required by the Convair Thermal Analyzer Code. Characteristic dimensions and resistance parameters of the pins and grommets are summarized in Table 8. The full scale design contains 49 support pins, 98 grommets, 536 seam pins with grommets, and 39 purge pins. The thermal conductivity for the fiberglass and PPO as used in the analysis were extracted from Reference 9 and are presented in Figure 51.

Table 8. Pin and Grommet Characteristics

Item	Length, cm (in)	Inside Dia, cm (in)	Outside Dia, cm (in)	Material
Support Pins	3.81 (1.5)	-	.320 (.125)	Fiberglass
Support Pin Grommet	1.91 (0.75)	.325 (.128)	.457 (.180)	PPO
Seam Pins	1.91 (0.75)	-	.210 (.0825)	PPO
Seam Pin Grommet	1.91 (0.75)	.226 (.089)	.358 (.141)	PPO
Purge Pin	3.81 (1.5)	.330 (.130) (slotted)	.508 (.200)	PPO

3.2.4.4 Residual Gas Conduction. Heat transfer through MLI results, in part, from residual gaseous conduction. For the subject analysis, residual gaseous conduction was computed using the techniques suggested by Corruccini (Reference 11) which provides for the modification of the thermal conductivity of the residual gas resulting from reduced pressures. For gaseous conduction $Q = (K_{EF} A/\ell)(T_h - T_c)$. From Reference 11

$$Q = \frac{KA}{\ell + 2g} (T_h - T_c)$$

where

$$g = \left(\frac{K}{P}\right)\left(\frac{2-\alpha}{\alpha}\right)\left(\frac{\gamma-1}{\gamma+1}\right)\sqrt{\frac{2\pi MT}{R}}$$

For Correspondence $K_{EF}/\ell = K/(\ell + 2g)$ or $K_{EF} = \ell K/(\ell + 2g)$

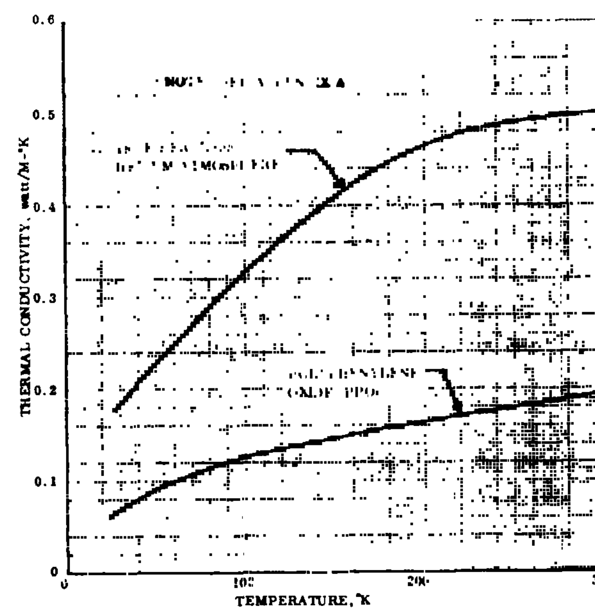

Figure 51. Thermal Conductivity of Fiberglass and Polyphenylene Oxide (PPO)

Thus, the effective gaseous thermal conductivity (K_{EF}) at low pressure as used in the analysis is defined by modifying K by the product of $\ell/(\ell+2g)$. The Thermal Analyzer Code was modified to include the above K_{EF} as a function of pressure, and thermal resistance parameters (ℓ/A) were included in the thermal model.

All resistance types which contribute to the heat transfer rate through the MLI layers and the typical MLI region thermal model are presented in Figure 52.

3.2.4.5 Penetrations. Three penetration lines (fill/drain, vent, and instrumentation) extend from the tank door to vacuum chamber facilities, thus resulting in potential heat leak paths. Superfloc MLI encloses each of the cylindrical lines. The outer MLI surface temperature for the penetrations external to the purge bag was constrained to the vacuum chamber wall temperature (292K (525R)) while the inner surface temperature was computed by an energy balance. The thermal resistance through the penetration MLI was expressed by a variable radiation resistance. The conduction resistance was considered as part of the radiation resistance. The surface area of the outer layer was used. $\mathcal{F}$ is tabulated in Tables 7, 8 and 9 of Appendix A, and includes the effects of the area ratio between the inner and outer layer surface as well as the average temperature between the two layers.

The fill/drain and vent line thermal model nodal schematic is presented in Figure 53. Hydrogen gas due to boil-off flows between the fill/drain line and the vent line, thus resulting in convective heat transfer. Heat transfer coefficient generating routines within the Thermal Analyzer Program were used to compute the convective heat

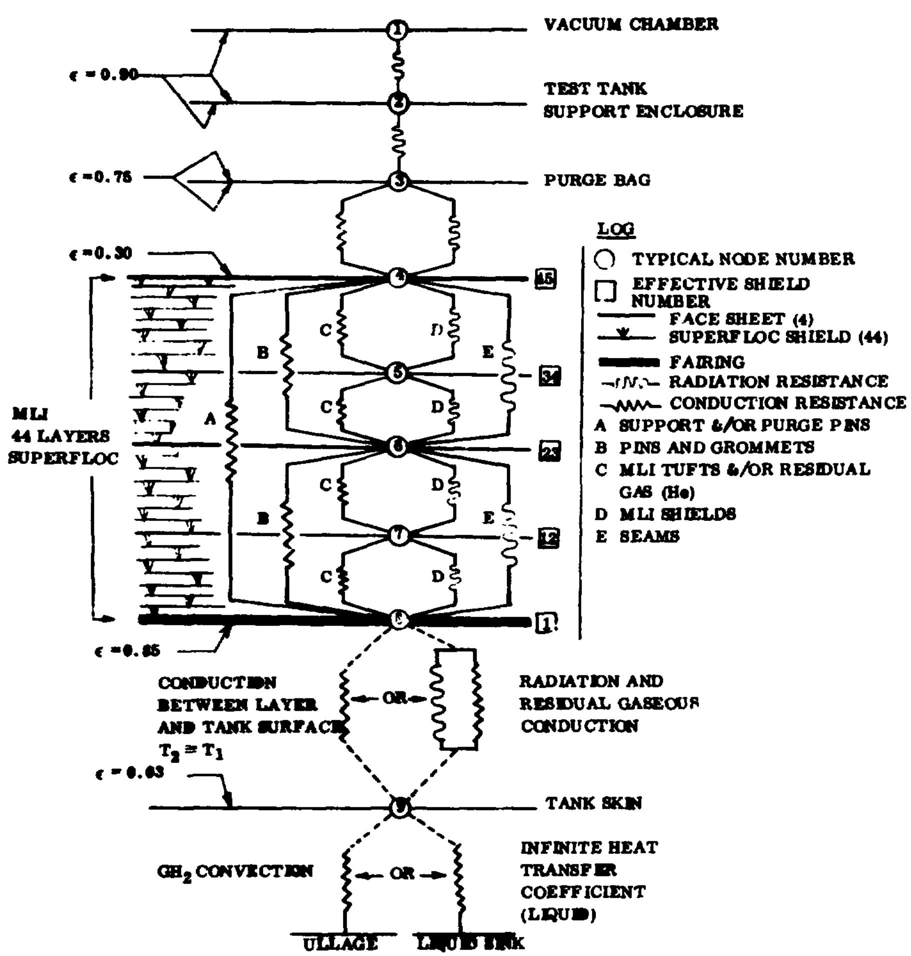

Figure 52. Convair Aerospace Test Tank Thermal Model Thermal Equilibrium Conditions

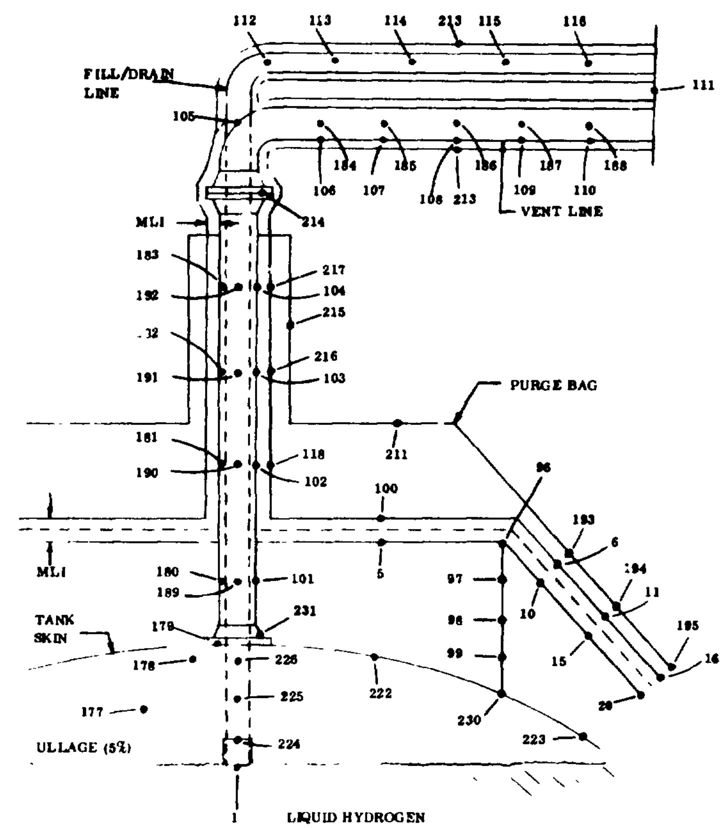

Figure 53. Thermal Model Nodal Schematic of Fill/Drain and Vent Lines and Tank Forward Region

transfer rates. Conduction heat transfer was considered along each of the lines from the test facility heat source to the tank. For the fill/drain line, solid conduction occurred along an aluminum line from the test facility to the junction of the fill/drain line with the fiberglass line internal to the tank then along the fiberglass line to the liquid. For the vent line, conduction occurred along an aluminum line from the test facility to the flange (node 214) just external to the purge bag, then along a stainless steel line from the flange to the tank forward door.

The instrumentation line thermal model nodal schematic is presented in Figure 54. The thermal model provides for chromel/constantan thermocouple and copper liquid level sensor wires. The chromel/constantan wires are 36 gauge. The length of the entire instrumentation line was 3 m (118 in). The instrumentation line was considered connected to an LH_2 temperature test facility guard heat exchanger. The line was composed of the wires contained within a .0254 m (1.0 in) O.D. tube from the exchanger to the passthrough connector on the purge bag forward plate. From the connector, the wire bundle separated as indicated in Figure 54. The effective thermal conductivity of the bundle from the heat exchanger to the passthrough connector was computed from a cross-sectional weighted average basis. The resulting weighted average thermal conductivity is shown in Table 10 of Appendix A. Conductive heat transfer was considered from the passthrough connector to the tank forward door (copper wires),and from the passthrough connector to insulation layer nodes (chromel/constantan wires), as shown in Figure 54. For the copper wires after penetration of the MLI, the bundle was considered wrapped with goldized tape. The emittance was estimated as 0.072 which accounts for the degradation due to wrapping the line. Further, after penetration of the MLI, one half of the bundle surface area radiated to the fairing while half radiated to the tank skin.

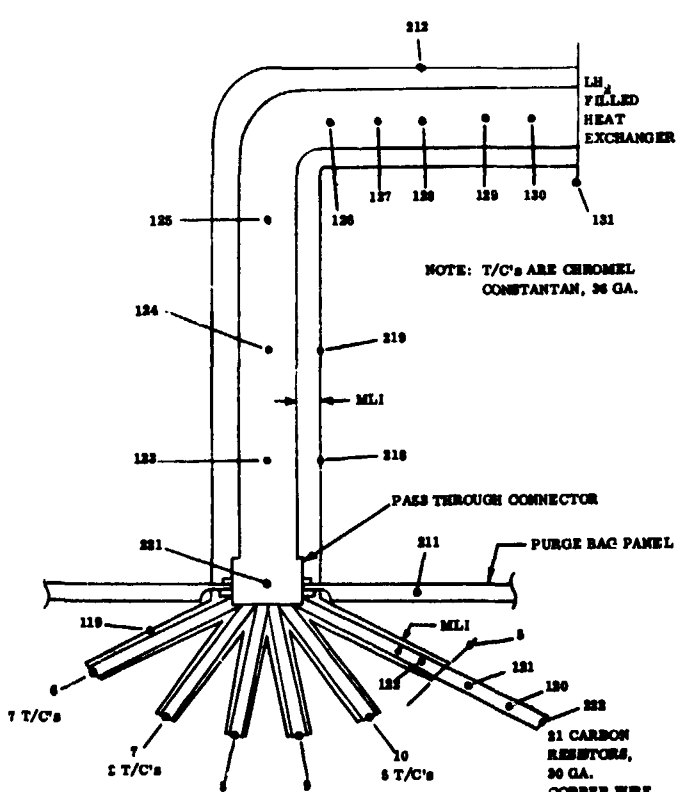

Figure 54. Thermal Model Nodal Schematic of Instrumentation Line and Boundary Nodes

3.2.4.6 Support Struts. Six struts are used to support the test tank inside the support enclosure. The struts are primarily hollow fiberglass tubes with fittings at each end. MLI (2 layers) encloses the portion of the struts between the tank MLI and the support enclosure. A total of 90 radiation shield disks are located inside the fiberglass tube section at the region of tank MLI penetration. The support strut thermal model schematic is shown in Figure 55. The

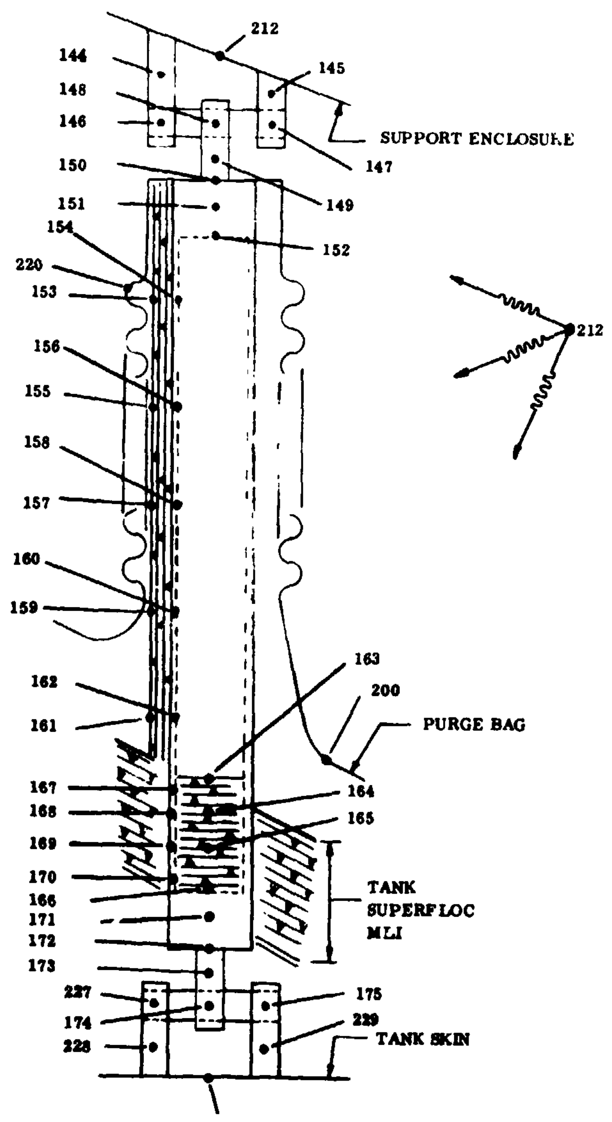

Figure 55. Thermal Model Nodal Schematic of Support Strut

The modes of heat transfer employed in the model include; (1) conduction from the shroud wall through the strut to the tank skin, (2) radiation from the purge bag boot, (3) radiation and conduction through the two layers of MLI to the strut, (4) radiation tunneling down the hollow strut, and (5) radiation and conduction through the 90 internal radiation shields. Appropriate radiation and conduction terms for one strut were computed and included as input to the Thermal Analyzer Program. The temperature dependent radiation and conduction heat transfer terms for the strut internal MLI disks are presented in Figure 13, Reference 7. The computer model yields the heat transferred to the tank by one strut and is thus multiplied by six to obtain the strut total heat leak contribution.

3.2.4.7 Results and Conclusions. Results fromthe analysis are presented in Figures 56 through 63. Figures 56 through 59 show the parametric analysis heat transfer rate results versus emittance and interstitial pressure. Results are presented as heat rates and as the ratio of the thermal model heat rate to specified parameter heat rate. As noted, for the specified parameter heat rate ($\epsilon = 0.02$, $P = 1\times10^{-5}$ Torr), the system predicted heat leak is 9.25 watts (31.5 Btu/hr). Further, the heat rate is not extremely sensitive to MLI emittance within the range of emittances examined, but is sensitive to interstitial pressures in excess of 1×10^{-5} Torr.

Figure 58 presents the breakdown of the predicted total heat leak (for specified parameters) into components. As noted, the single major heat leak contribution results from radiation/conduction through the MLI sheets. The seam radiation and pin conduction represent the largest heat leak to the system (55%), while the penetrations, residual gaseous conduction and support struts each result in relatively minor heat leaks. Figure 58 also shows for comparison test results obtained from an identical installation of a double-aluminized-Mylar Superfloc system as reported in Reference 12.

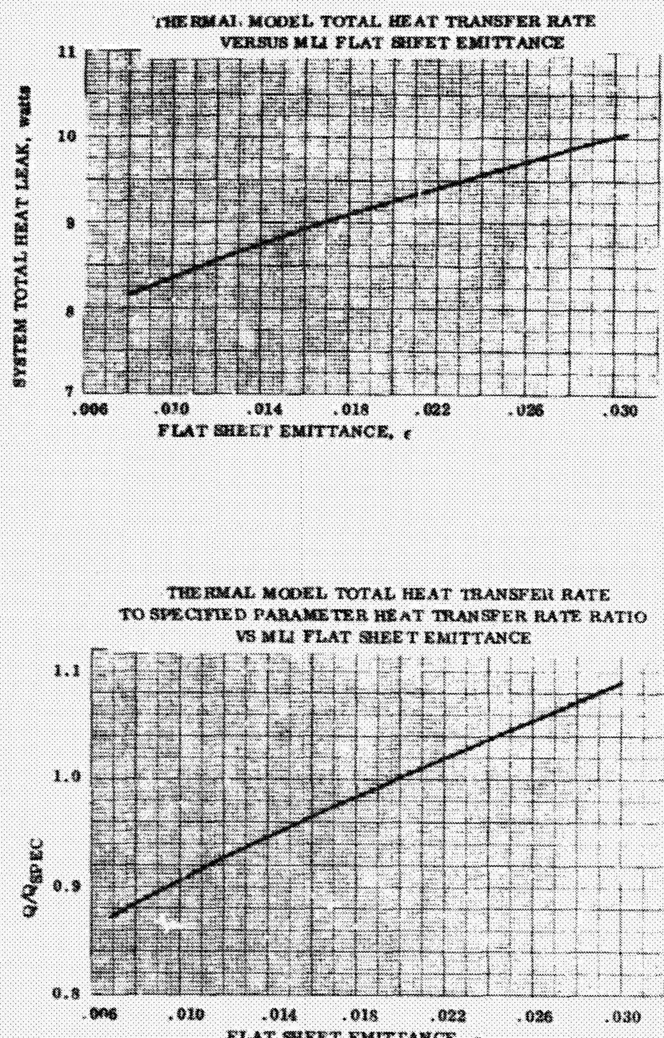

Figure 56. System Total Heat Leak Versus MLI Emittance Parameter

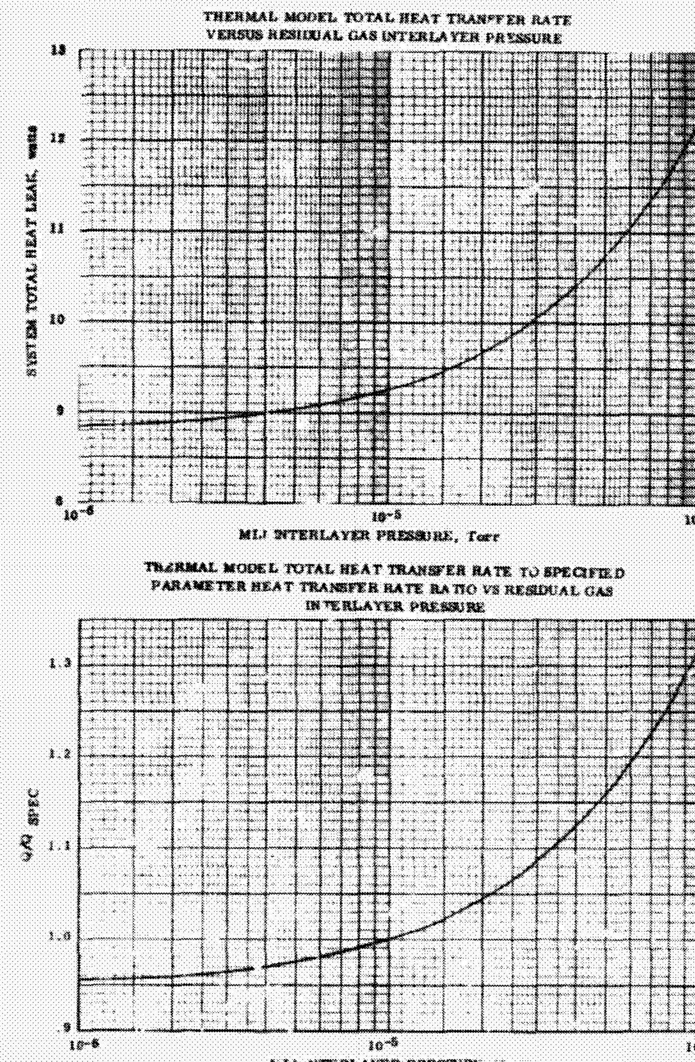

NOTES: (1) MLI Flat Sheet Emittance = 0.02
(2) External Boundary Temp = 292K (525R)
(3) Interlayer Gas = Helium

Figure 57. Thermal Model Total Heat Transfer Rate Vs Residual Gas Interlayer Pressure

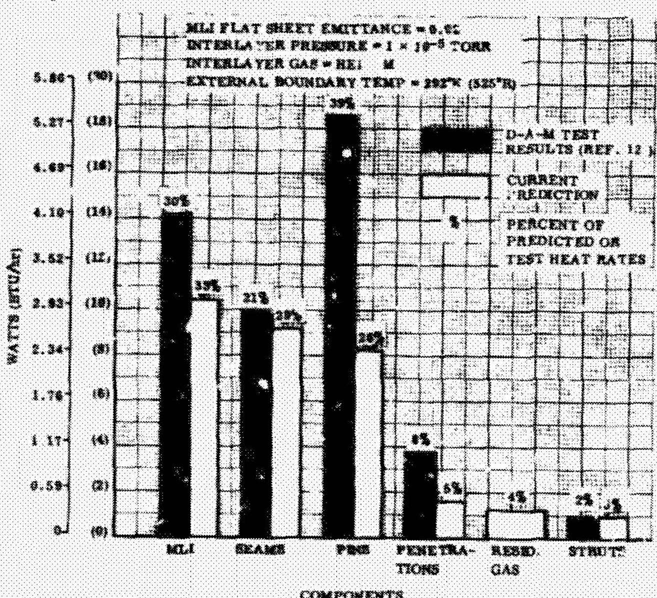

Figure 58. Specified Parameter System Heat Transfer Rate Breakdown

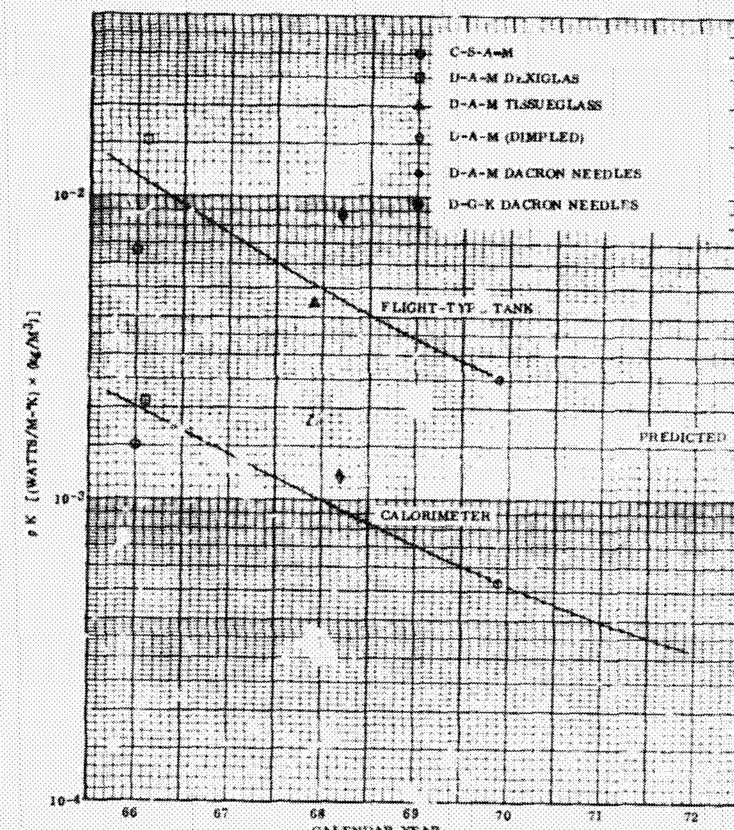

Figure 59. MLI Thermal Performance History

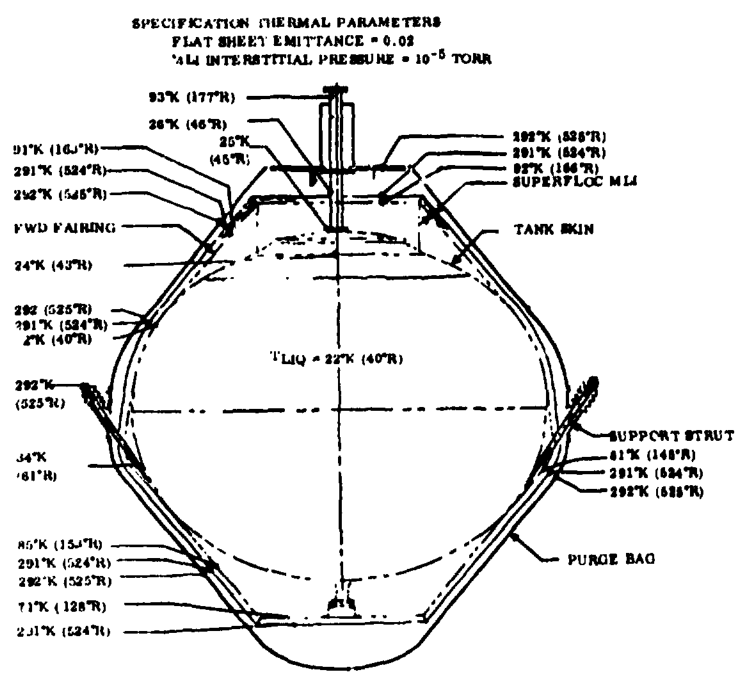

Figure 60. Thermal Analysis Temperature Distribution

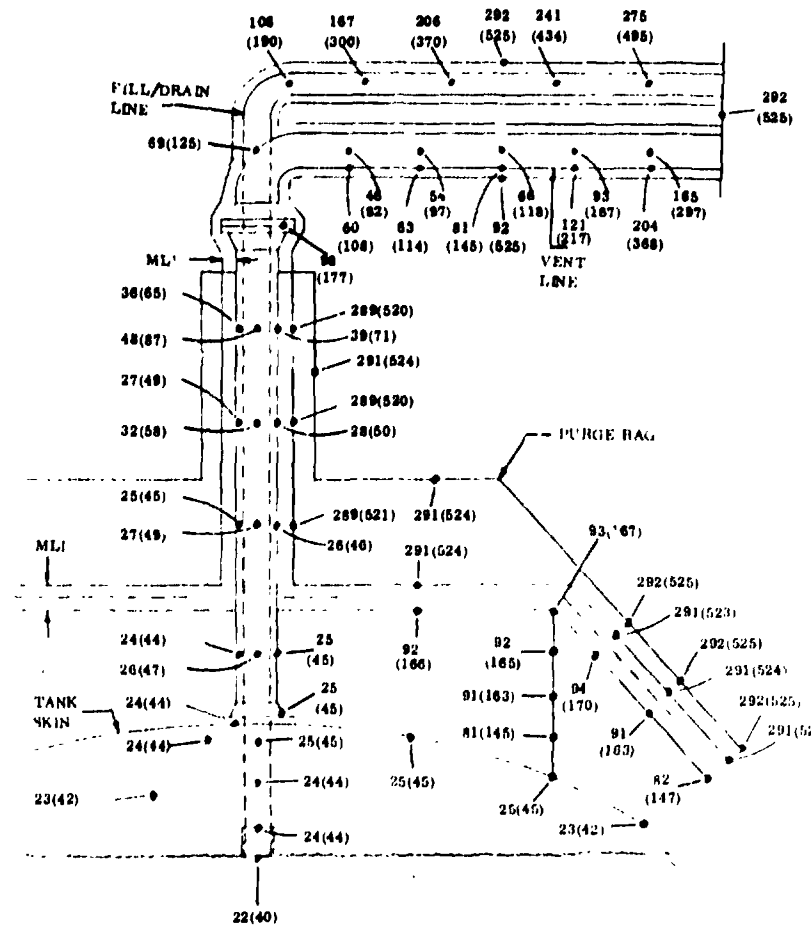

Figure 61. Thermal Analysis Fill/Drain, Vent and Forward Fairing Temperature Distribution, K (R)

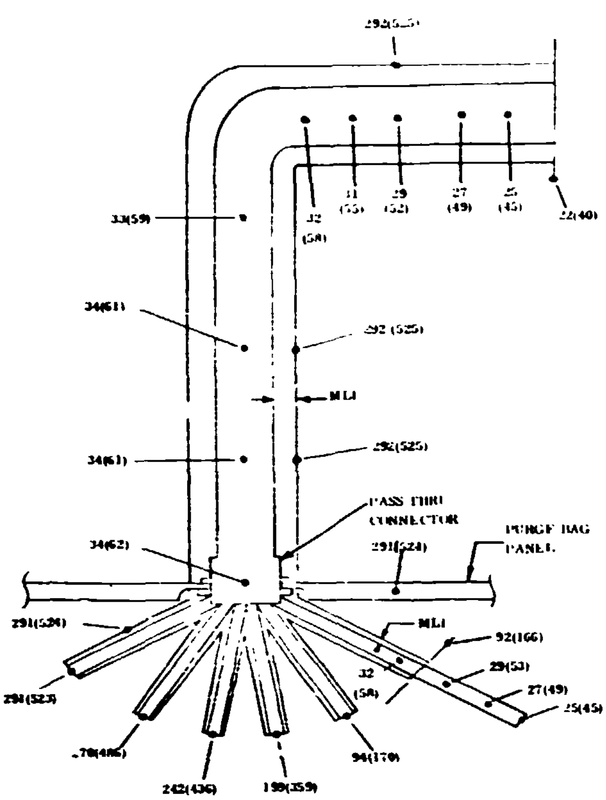

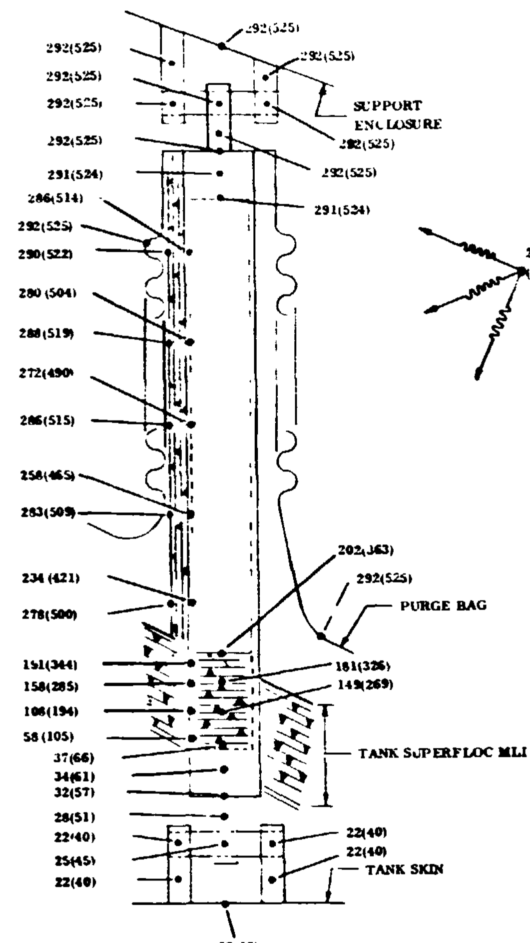

Figure 62. Thermal Analysis Instrumentation Line Temp Distribution, K (R)

Figure 63. Thermal Analysis Support Strut Temp Distribution, K (R)

The predicted ρK value for the current test tank installed goldized Kapton Superfloc system is 1.65 mw-Kg/m^4-K (5.97×10^{-5} Btu-lb/hr-ft^4 F). Figure 59 (Ref. 13) presents a chronological comparison of existing MLI system ρK values for as-installed and calorimeter test configurations. As indicated, an improvement of approximately 30% in ρK is expected for the current goldized Kapton (DGK) system.

Figure 60 through 63 present the resulting analytical temperature mapping of the entire test tank/MLI system for the specified parameters condition. The temperature locations presented follow closely the figures shown in Section 2.

3.3 DETAILED DESIGN

Detailed design of the large scale test article for the MLI purge/repressurization system has been completed. Twenty drawings were completed describing the manufacturing and assembly of the MLI system, purge bag, pressurization system and handling fixture. These documents include complete bill of materials, process specifications, assembly procedures, cleaning, inspections, and leak checking.

The test article design is built around an existing Convair Aerospace 2.21 m (87 in) diameter cryogenic storage tank. The tank is to be insulated with 44 layers of goldized Kapton Superfloc MLI and an epoxy/fiberglass laminate purge bag installed. Purge and repressurization fluid loop hardware will be mounted to forward end of the bag as an integral part of the total test system. Temperature, pressure and flow instrumentation will be integrated into the system when fabricated to evaluate system performance when subjected to simulated life cycle testing. The instrumentation drawings and specifications showing general arrangements, coordinates of all instrumented points, electrical plug assignments, manufacturing details of instrumentation components, and assembly will be reported in the next phase report covering fabrication and large tank testing.

Additional design activities included the rework of the present tank fairings to meet the new requirements. Designs were also completed for rework of the present co-axial fill/drain/vent line assembly to satisfy the thermal requirements of purge/repressurization system. A complete weight analysis was made for the large scale test article showing comparisons between using fiberglass fabric and DuPont's new high-modulus fiber PRD-49.

3.3.1 TEST TANK. An existing reworked fairing system, the insulation lay-up, and the purge bag are mounted on a previously developed tank. The tank (Figure 64) is a 2.21/1.89 m (87.6/74.5 in) diameter oblate spheroid fabricated from 2219-T62 aluminum alloy and is equipped with a .61 m (24 in) diameter access door with ten 37 pin electrical pass through fittings. The tank assembly also includes a co-axial vent, fill, and drain tube assembly which penetrates the access door. An instrumentation tree mounted inside the tank is equipped with liquid level sensors. Tank surface area and capacity are 14.12 sq m (152 ft^2) and 4.95 cubic m (175 ft^3) respectively.

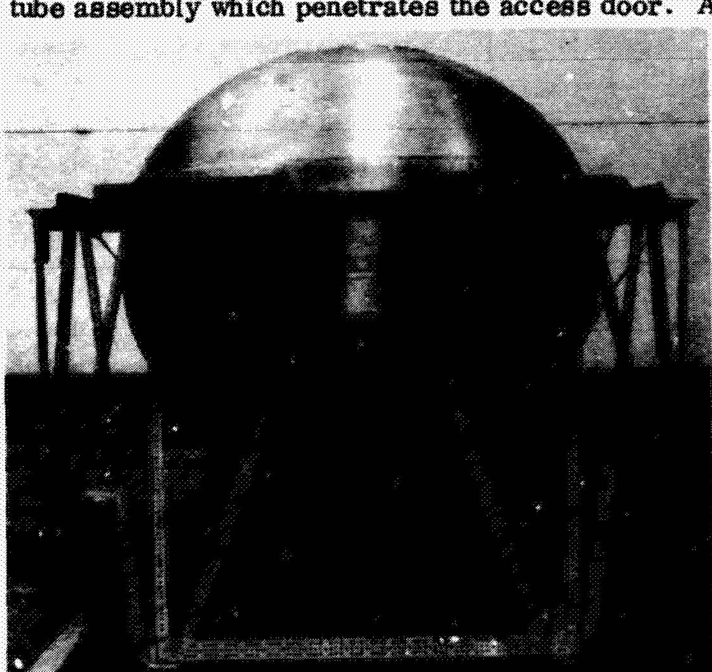

Figure 64. Convair Aerospace 2.21/1.89 m (87.6/74.5 in) Dia Oblate Spheroid Tank in Support Fixture

3.3.2 TEST TANK SUPPORT SYSTEM. The test tank is supported with three pairs of existing struts arranged in a "V" pattern. The centerlines of a typical pair of struts converge at a tangent point on the tank bulkhead. Fittings welded to the tank wall provide attachments for the struts.

A strut consists of an epoxy/fiberglass tube (incorporating titanium spools on each end) and two CRES spherical ball fittings.

Superfloc MLI discs are stacked inside the tubular section at one end to intercept radiation exchange between the hot and cold fittings.

3.3.3 TEST TANK FILL/DRAIN/VENT LINE. The present fill/drain/vent line on the test tank is a 6061 aluminum alloy co-axial assembly consisting of a 6.35 cm (2.5 in) O.D. outer tube and a 3.80 cm (1.5 in) O.D. inner tube. The heat transfer characteristics of this assembly are improved by inserting a steel section in the outer tube and a fiberglass section in the inner tube. For the outer tube, the steel section is a 304L CRES tube flanged at both ends and located adjacent to the tank interface. Two hubs added to this CRES tube section provide support for the fairing and purge bag assemblies. The section for the inner fill/drain tube is an epoxy/fiberglass tube extending from the ullage space to the aft end of the tank. This fiberglass tube is connected to the aluminum alloy section by bonding and riveting.

3.3.4 PURGE DISTRIBUTION SYSTEM. The purge distribution system is basically a tube assembly (equipped with orifices), three plenum cavities, and 43 PPO purge pins. A general arrangement is shown in Figure 65. The tube assembly is located inboard of the fairings, is supported from the test tank wall, and routes from the pressurization system to the aft area of the test tank.

The three cavities formed between the fairings and the tank wall serve as plenum chambers for the purge gas. Each plenum is supplied with gas through the orifices on the tube assembly. The purge pins mounted in the fairings engage with holes in the MLI blankets. A typical purge gas flow therefore starts at the pressurization system, through the tube assembly and into the plenums. From the plenums, the gas flows through slots in the purge pins which results in gas distribution between the MLI layers. The total purge volume between tank wall and bag is 2.42 m^3 (85.5 ft^3).

The existing epoxy/fiberglass fairing structure on the test tank is insufficient for the pressure differential loads imposed by the new purge system. Designs for reworking this structure were therefore created. The rework is basically the addition of stiffeners in the forward and aft flat panel sections, improved bonding and sealing between tank wall and fairings, and provisions for sealing with the tank support struts. The forward flat section (including the stiffeners) is removable for access to the tank interior.

3.3.5 MULTILAYER INSULATION (MLI) ASSEMBLY. The MLI assembly is applied over the tank fairing surfaces in gore and flat blanket sections. Two blanket layers are used. These blankets are supported from the fairings with pins and interconnected at the seams with rigid "twin pin" fasteners (see Figure 66). Individual MLI layers are applied over the vent line and the six tank support struts. The forward flat area of the assembly includes provisions for the vent, purge, and electrical penetrations.

3.3.5.1 Gore Blankets. A typical gore blanket is a preformed assembly consisting of a 22 ply double goldized Kapton Superfloc core (see Figure 67) sandwiched between two

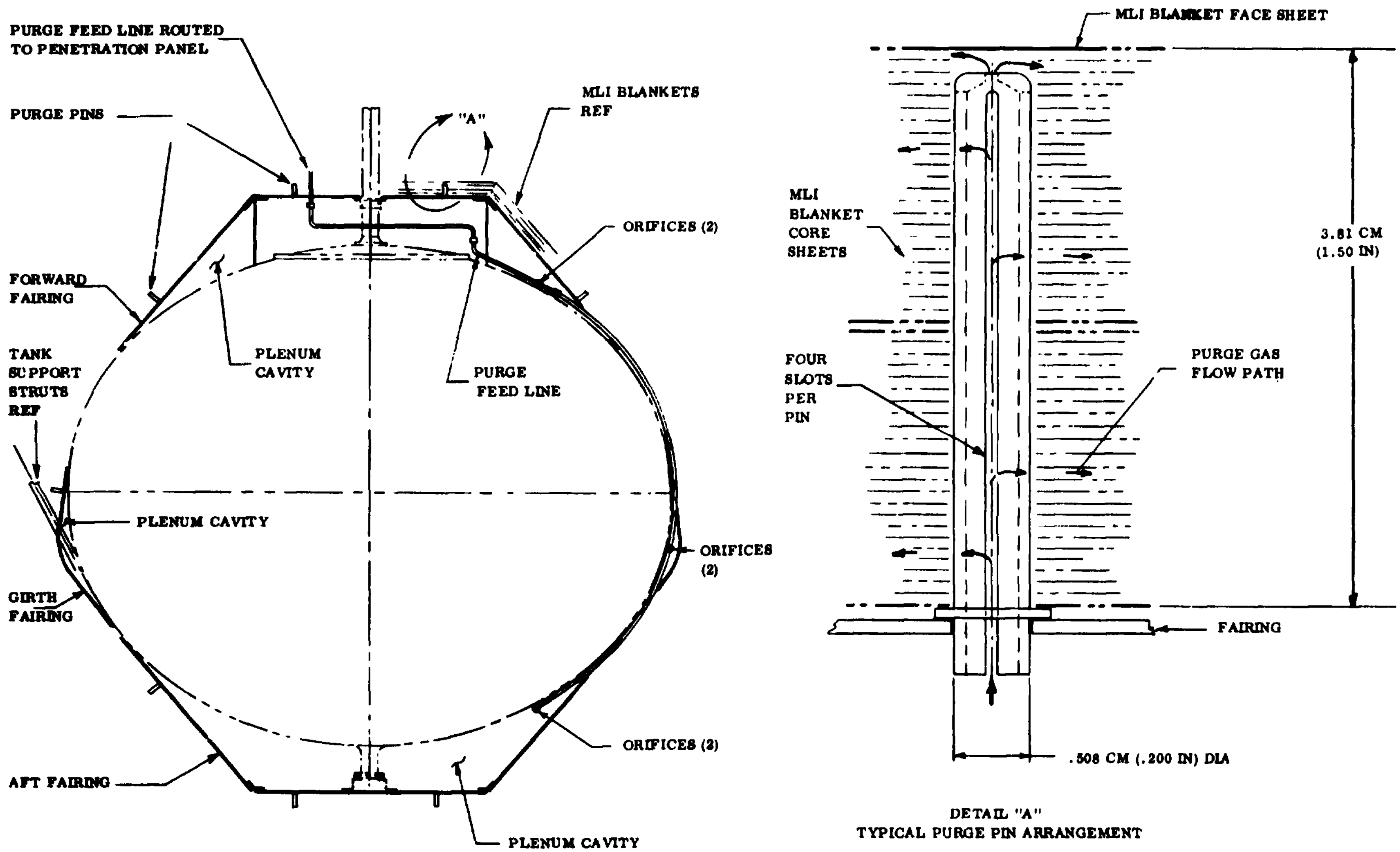

Figure 65. Purge Distribution System

FOLDOUT FRAME 1

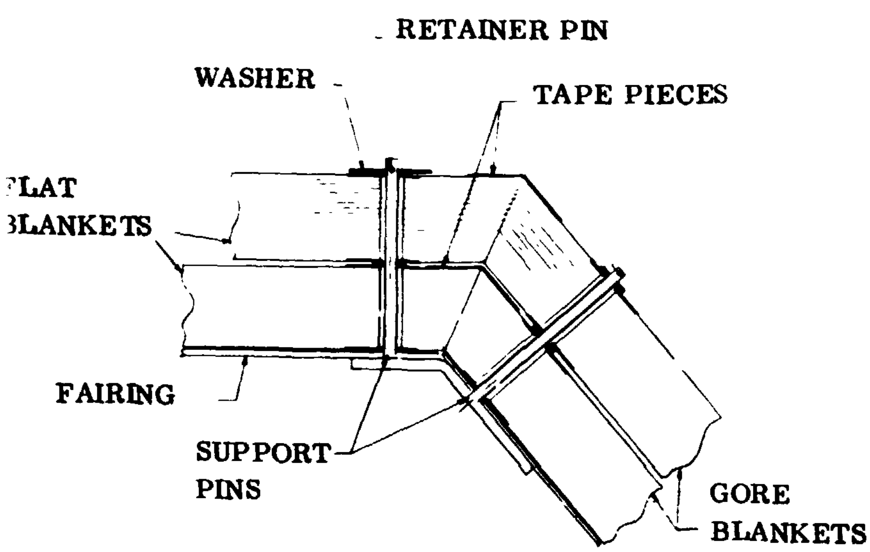

DETAIL "C"
TYPICAL BLANKET SUPPORT ARRANGEMENT

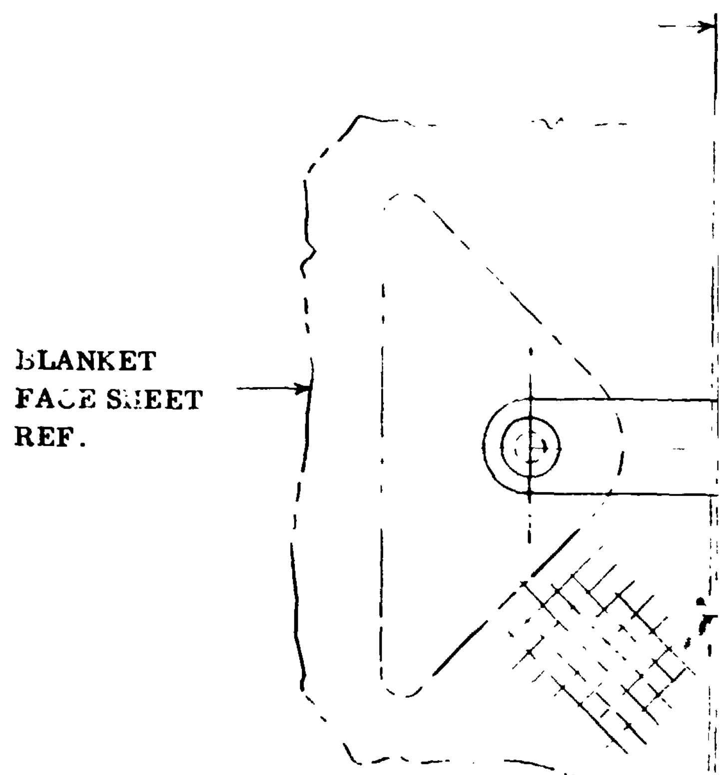

VIEW

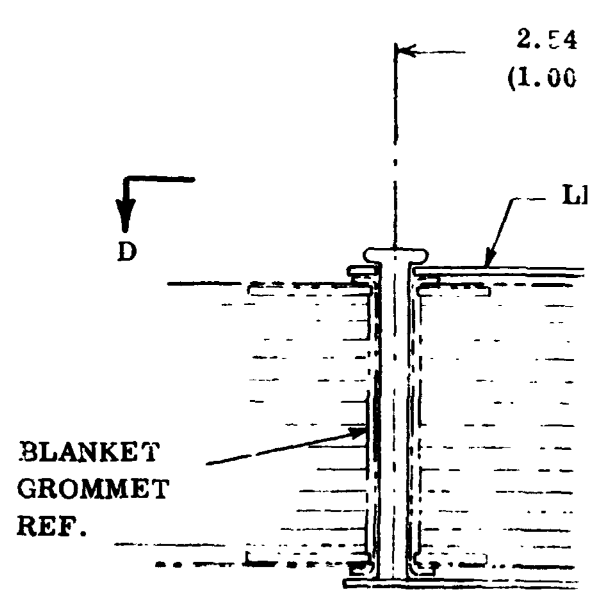

DETAIL "B'
TYPICAL TWIN PIN FASTEN

FOLDOUT FRAME 2

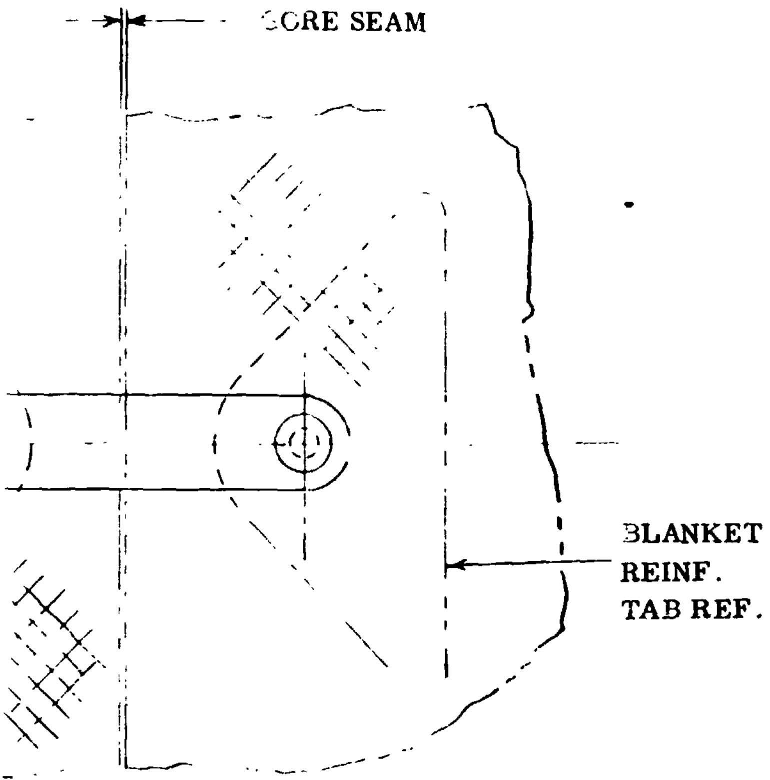

VIEW DD

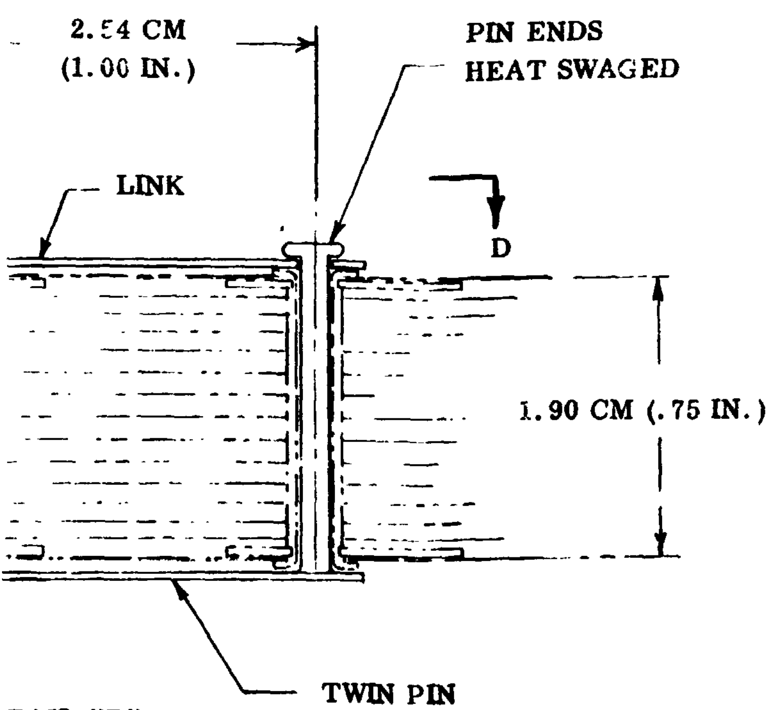

TAIL "B"
FASTENER ARRANGEMENT

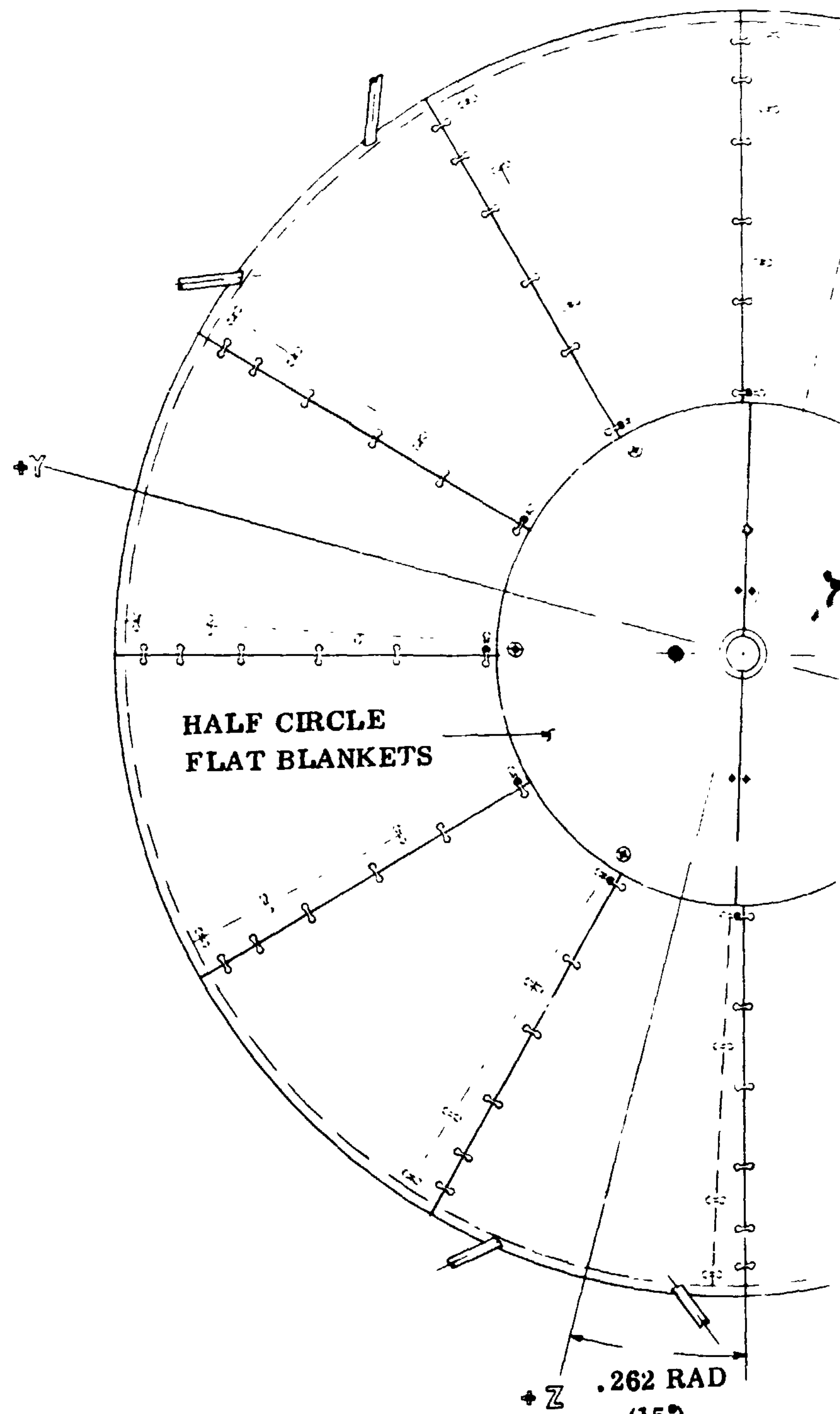

VIEW AA

FOLDOUT FRAME 3

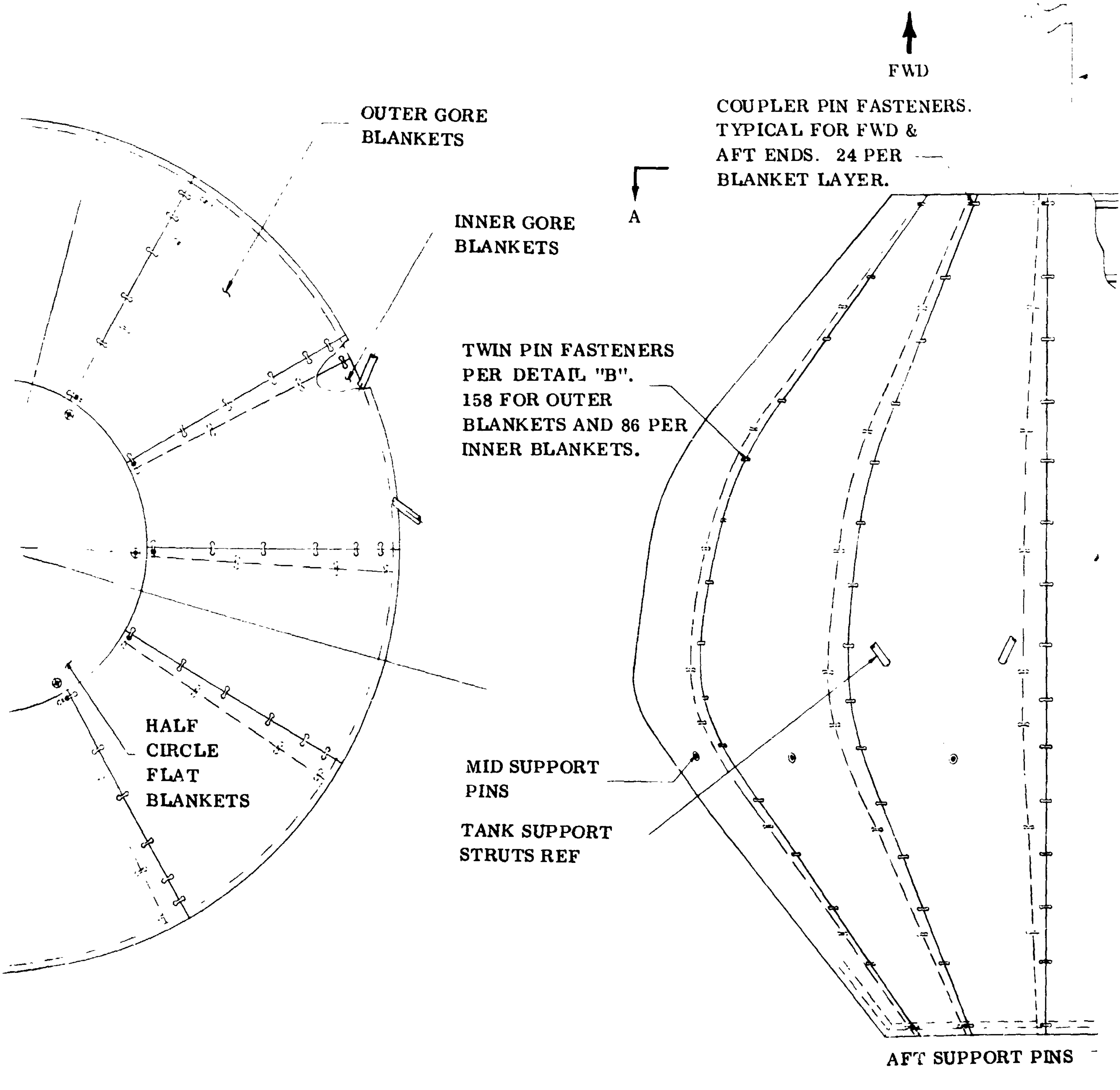

Figure 66. Insulation

FOLDOUT FRAME 4

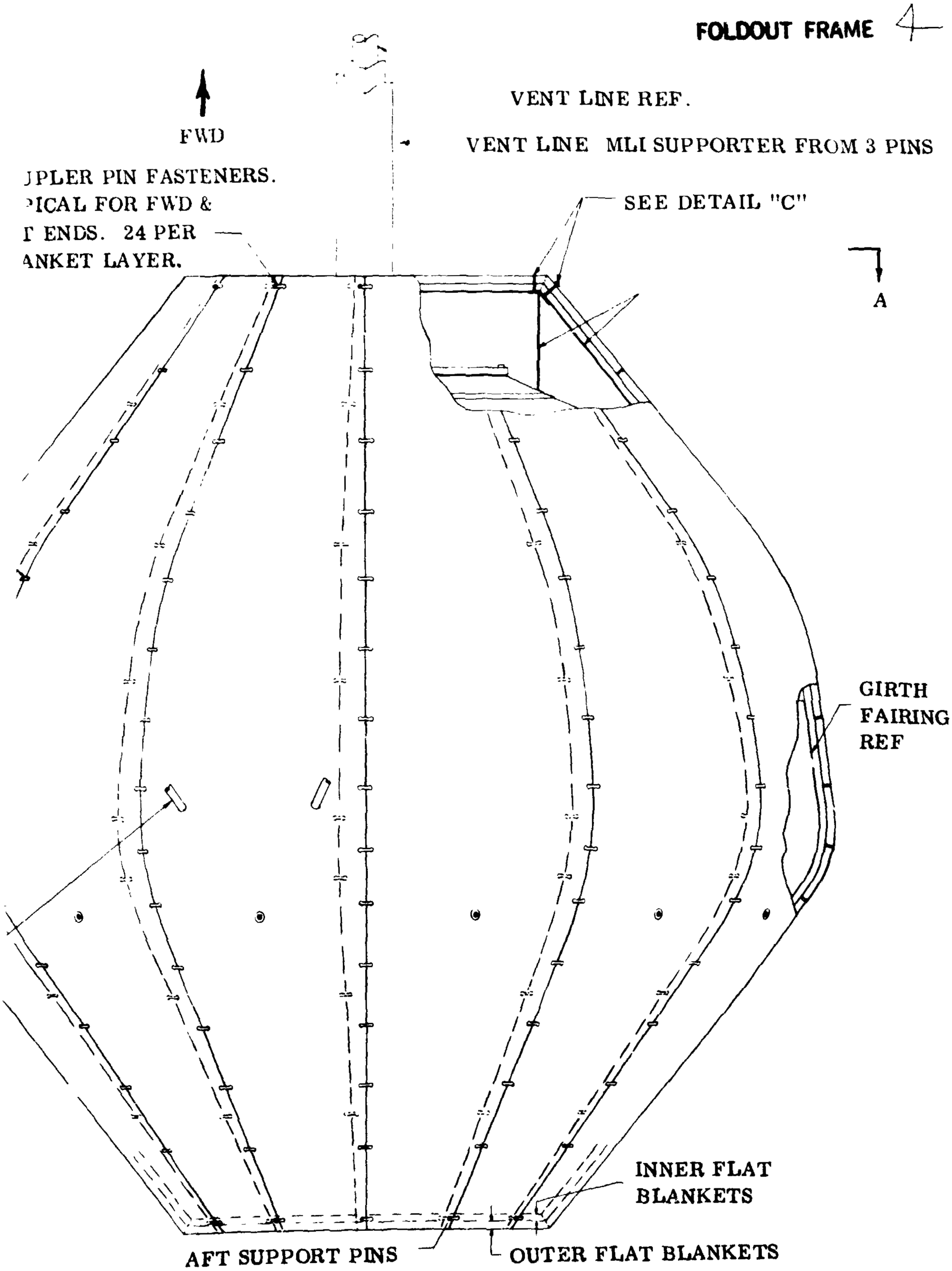

Figure 66. Insulation Assembly

FOLDOUT FRAME 1

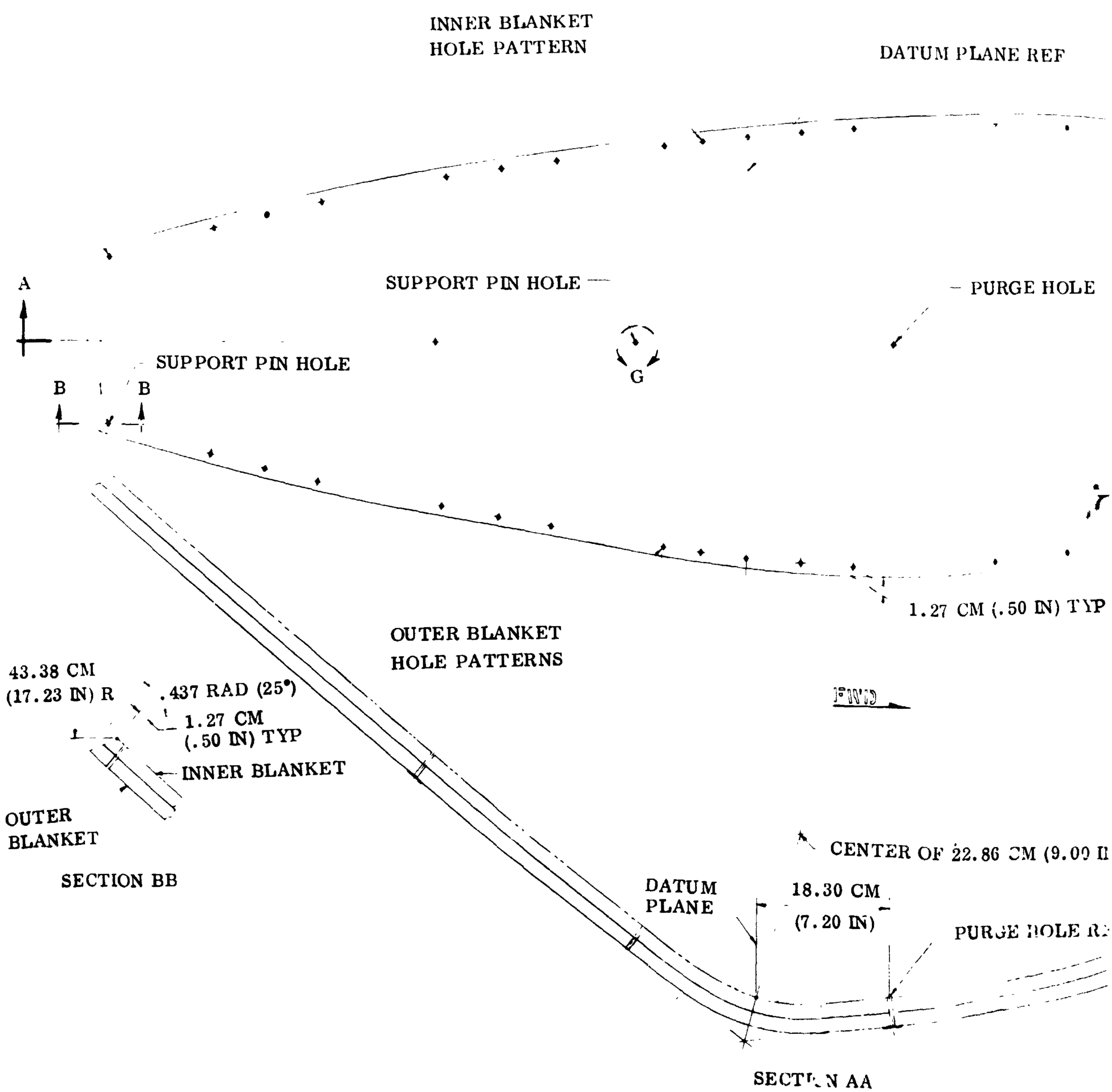

FOLDOUT FRAME 2

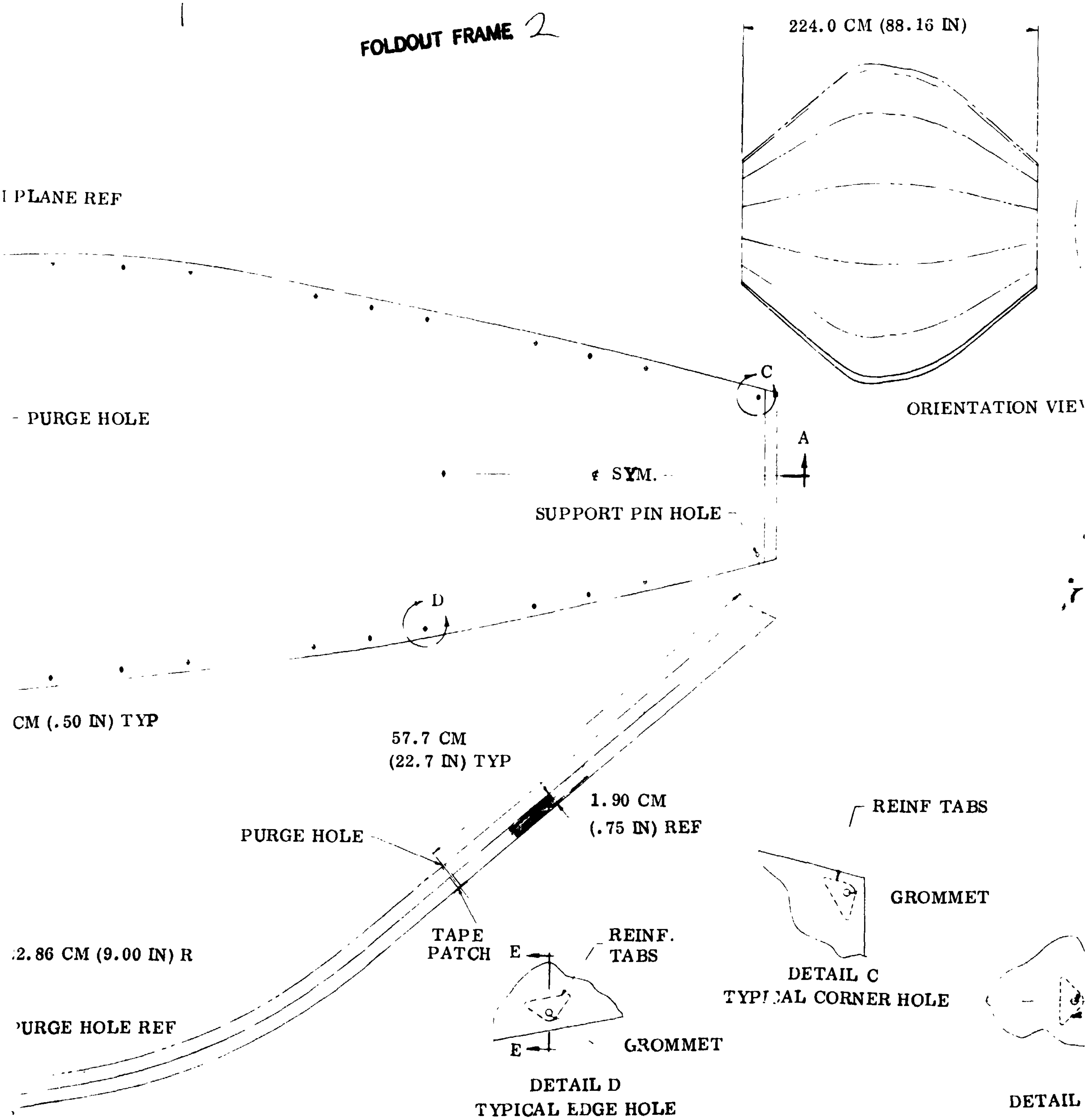

FOLDOUT FRAME 3

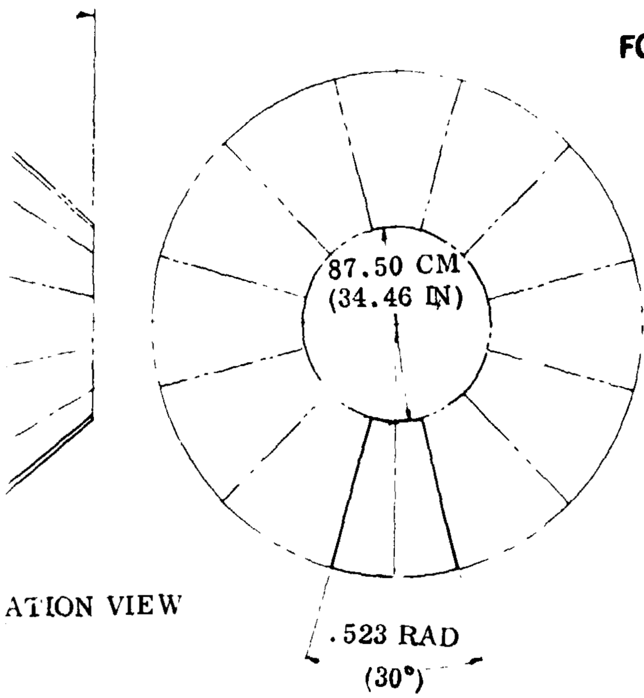

ATION VIEW

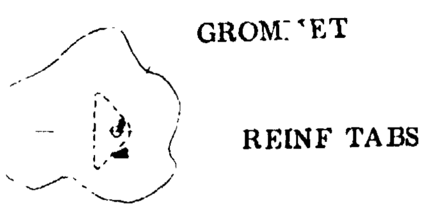

DETAIL G

FOLDOUT FRAME 4

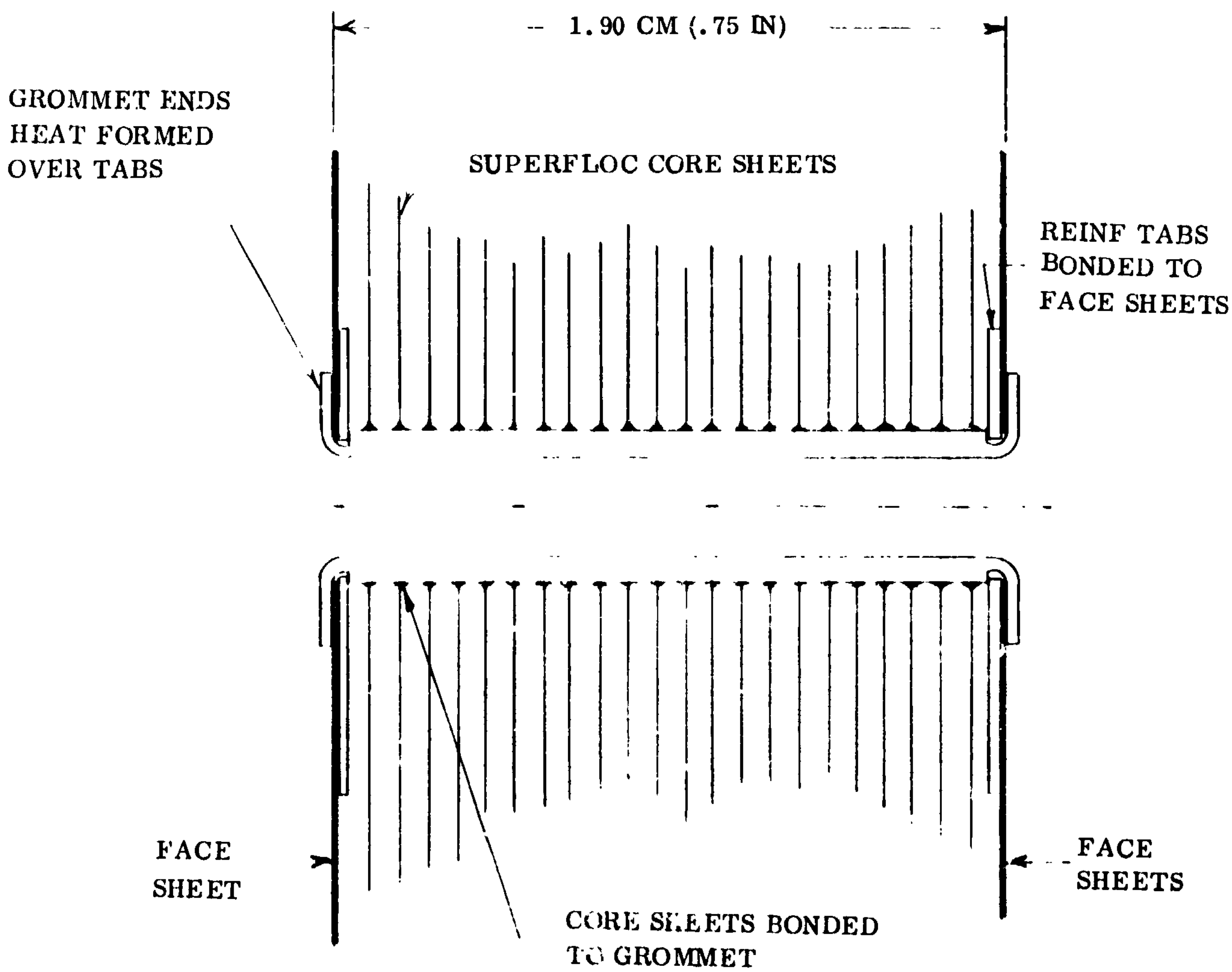

SECTION EE
TYPICAL GROMMET INSTALLATION

Figure 67. Typical Gore Blanket Construction

PRECEDING PAGE BLANK NOT FILMED

Pyre-M.L. (polyimide)/Beta glass face sheets. A single Superfloc sheet consists of 30 gauge (0.00076 cm) double Goldized Kapton film flocked on one side (see Figure 68).

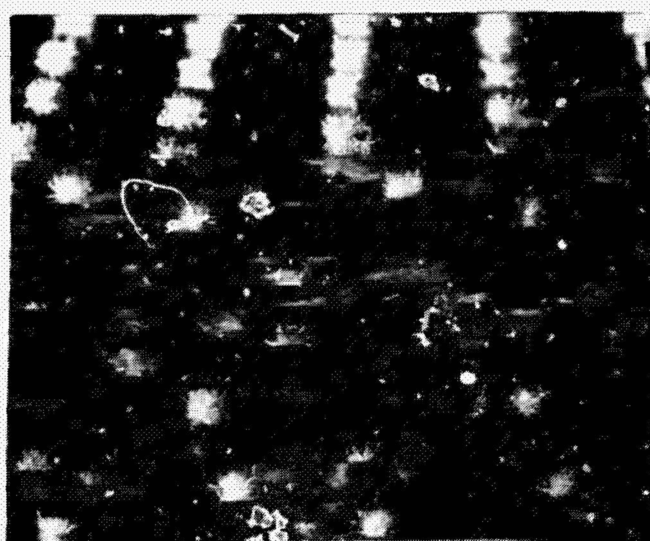

Figure 68. End View of Typical Superfloc MLI Lay-up

Average face sheet thickness is 0.0173 cm (0.007 in). The core and face sheets are interconnected at the edges with polyphenylene oxide (PPO) grommet and tab fittings. The blanket support pins and twin pins for the seams engage with these grommets at assembly. The primary load path is therefore from the grommet, to the tabs, and through the face sheets. The grommets are installed using a frozen adhesive technique which bonds the edges of the core sheet holes to the grommet. This core sheet to grommet attachment prevents core sheet tear out. The grommet ends engage with the tabs which in turn are bonded to the face sheets. A complete assembly uses twenty four 0.523 rad (30°) gore blankets (12 per layer).

3.3.5.2 Flat Blankets. Four half circle and two full circle flat blankets are used at the forward and aft ends respectively. The construction and support of these flat blankets is the same as that described for the gore blankets. The forward half circle blankets feature cut outs for the vent, purge, and electrical lines.

3.3.5.3 Twin Pin Fasteners. The twin pin fastener set consists of one PPO twin pin (which is two pins and one link integrally molded) and one separate PPO link (see Figure 66). Assembly consists of inserting the twin pin into the blanket grommets, engaging the link with the pin ends, and heat swaging the ends of the twin pin. Removal consists of cutting the swaged ends off the twin pin.

3.3.5.4 Vent Line MLI Lay-up. The MLI lay-up for the vent line consists of 30 layers of Superfloc enveloped with one Pyre-M.L./Beta glass face sheet. Each layer is applied individually using overlap seams which are staggered between layers. The seams for the Superfloc sheets are spot taped and the seam for the face sheet is continuously taped. Three PPO pins bonded to the forward end of the duct provide support for all layers.

3.3.5.5 Strut MLI Lay-up. The six support struts are wrapped (3 turns) with Superfloc and retained at the outboard ends with a tape wrap. The MLI wrap is terminated at the outboard face sheets on the gore blankets with a butt joint. This butt joint area is trimmed to fit at assembly.

3.3.5.6 Seams. Butt type seams are used between the forward half circle flat blankets and between the gore blankets. At the corner intersections (between the flat blankets and the gore blankets), mitered joints spot taped on the outboard face sheets are used. Total seam length per blanket layer is 40 m (131 ft).

Joints at the vent and purge line penetrations are corner butt types staggered between blanket layers (see Figure 69). Tape pieces applied at the inside corners serve as retainers.

After installation, holes are cut in the gore blankets for the tank support struts. These are straight through holes with centerline directions matching the struts. The resultant joint between strut and MLI layers is a close fitting butt type.

Instrumentation wires penetrate two of the foreward half circle blankets. Intersection between wire bundle and the MLI layers is similar to that for the tank support struts.

3.3.6 PURGE BAG. The purge bag assembly consists of a forward section, an aft section and a penetration panel. These three sections are interconnected at the girth and forward ends with flanged joints (see Figure 70). The assembly is supported by a fixed connection at the forward end and radially restrained at the aft region. Except for the ends, the profiles and wall construction of both bag sections are identical.

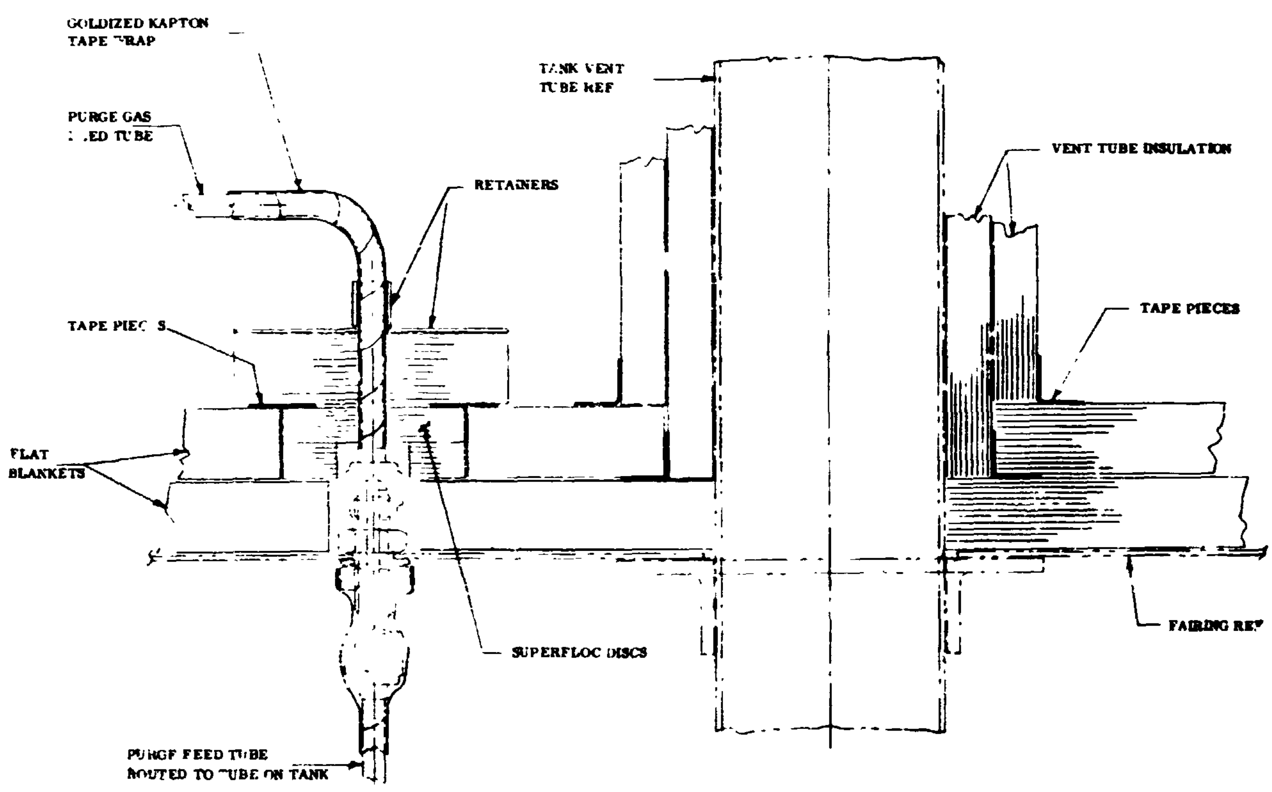

Figure 69. Insulation Arrangement at Penetrations

FOLDOUT FRAME 1

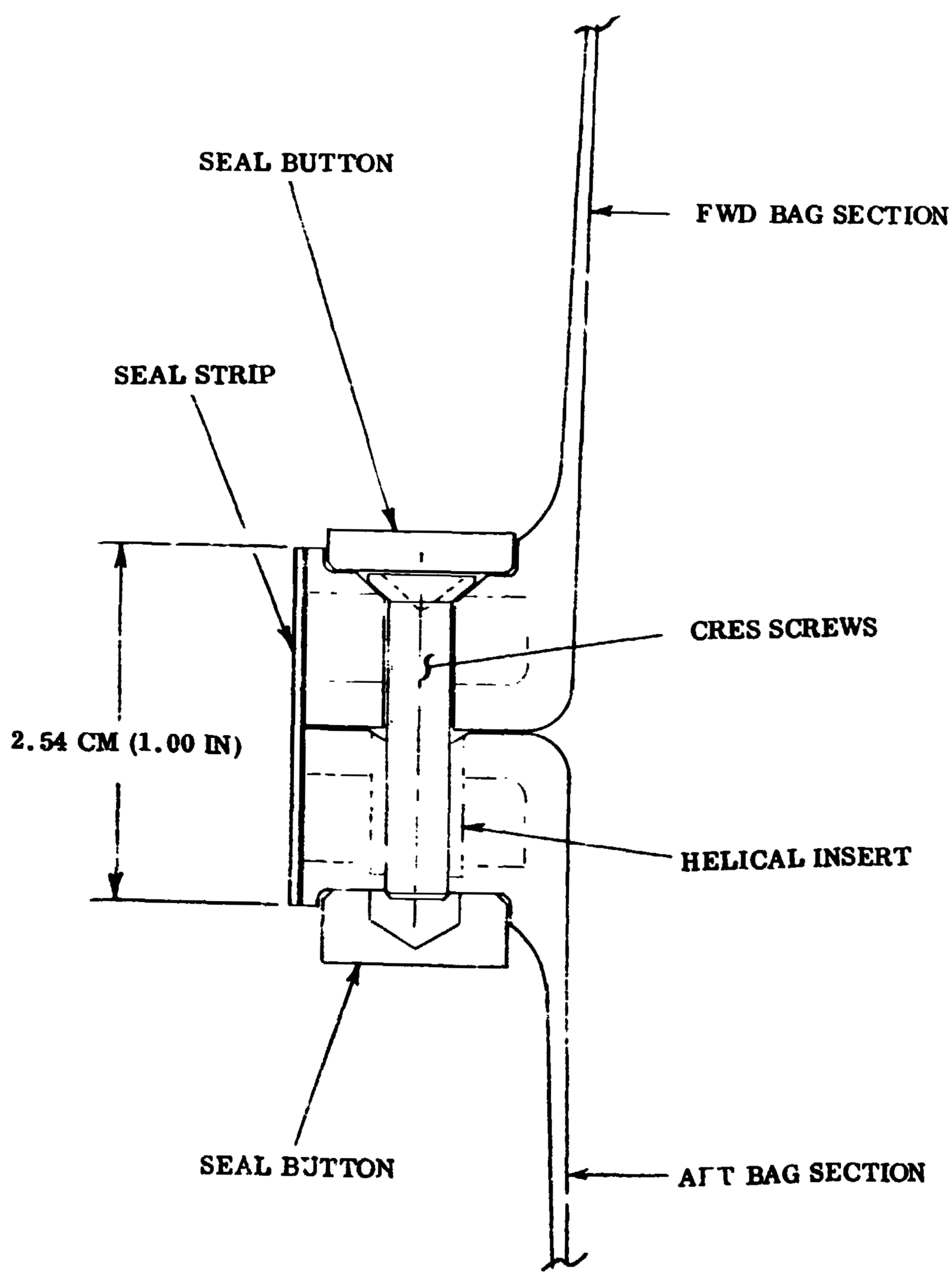

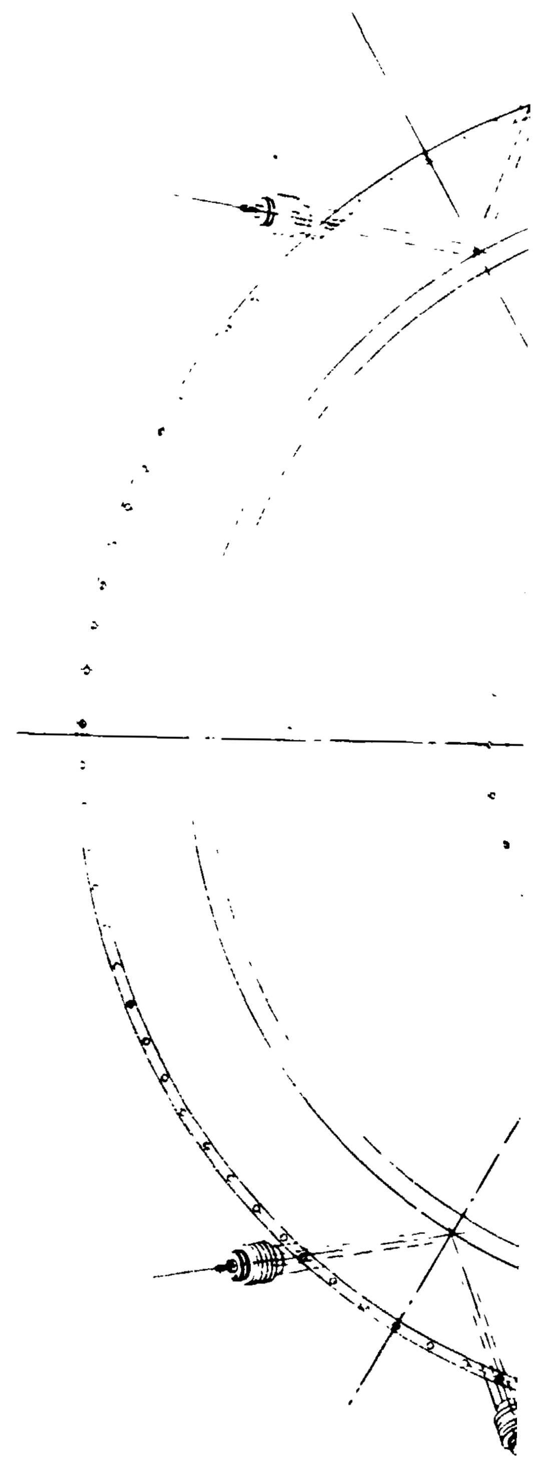

DETAIL "B"
TYPICAL FLANGED JOINT

FOLDOUT FRAME 2

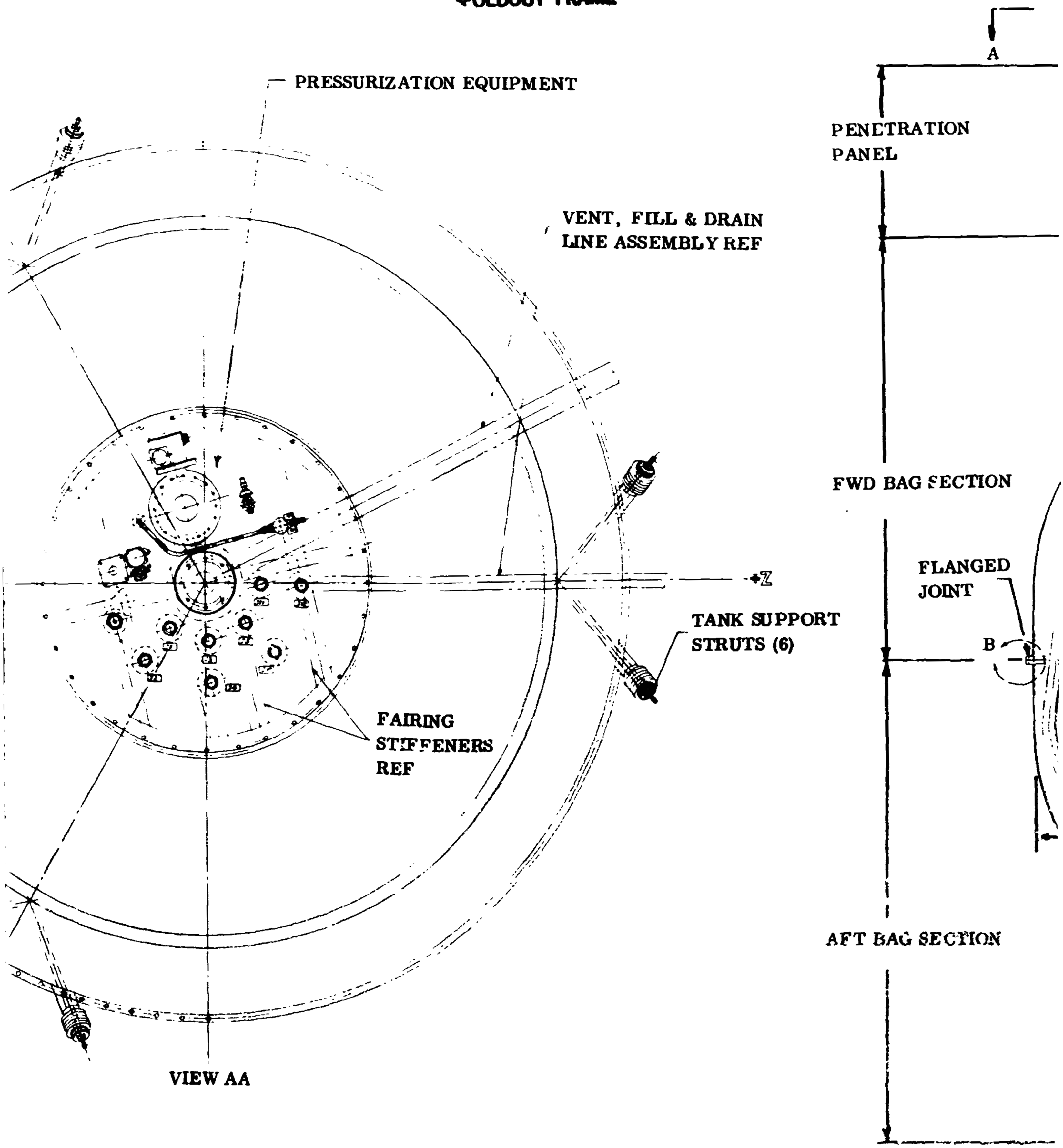

FOLDOUT FRAME 3

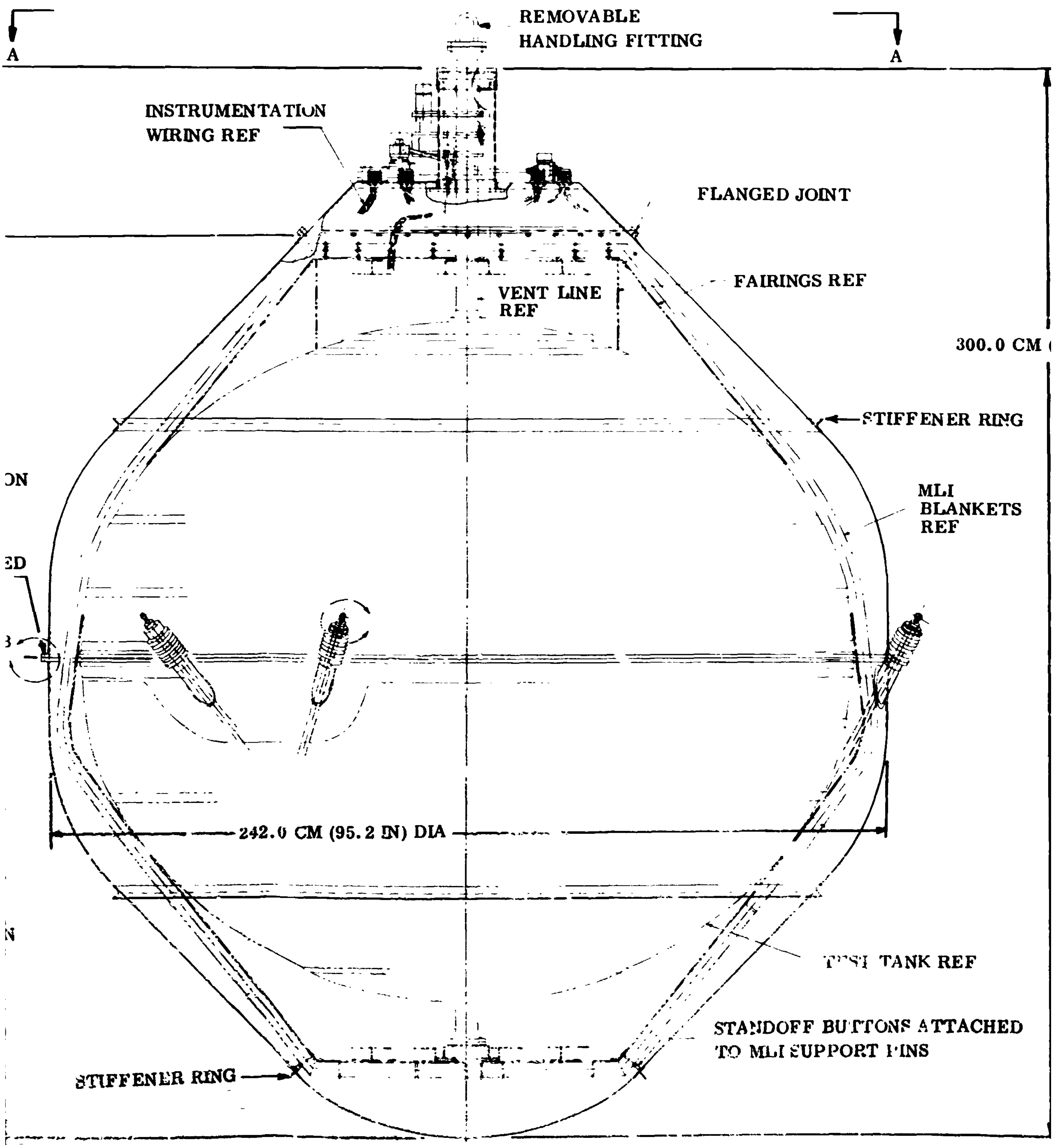

FOLDOUT FRAME 4

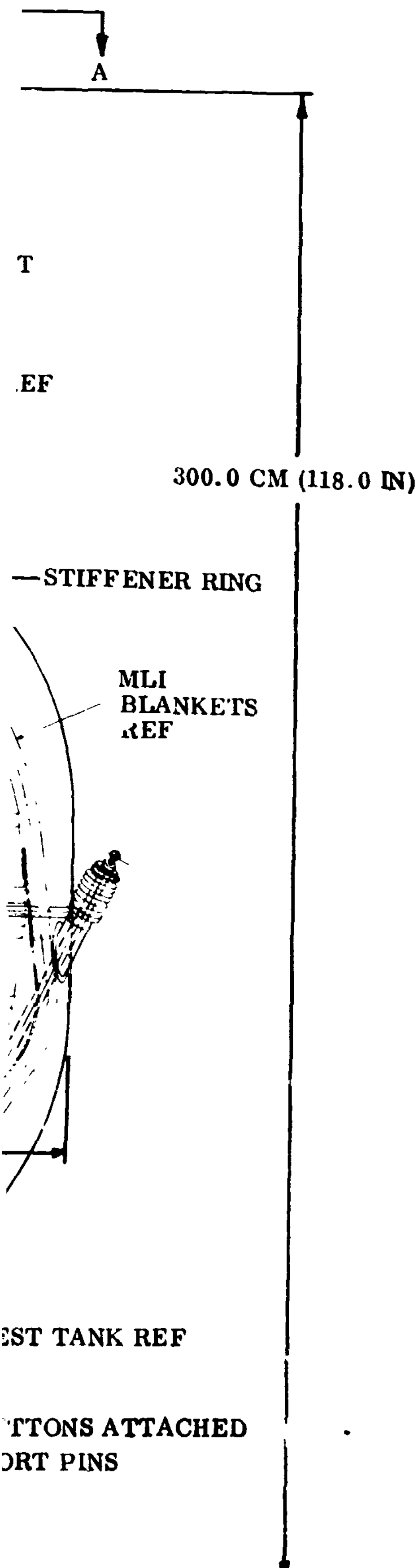

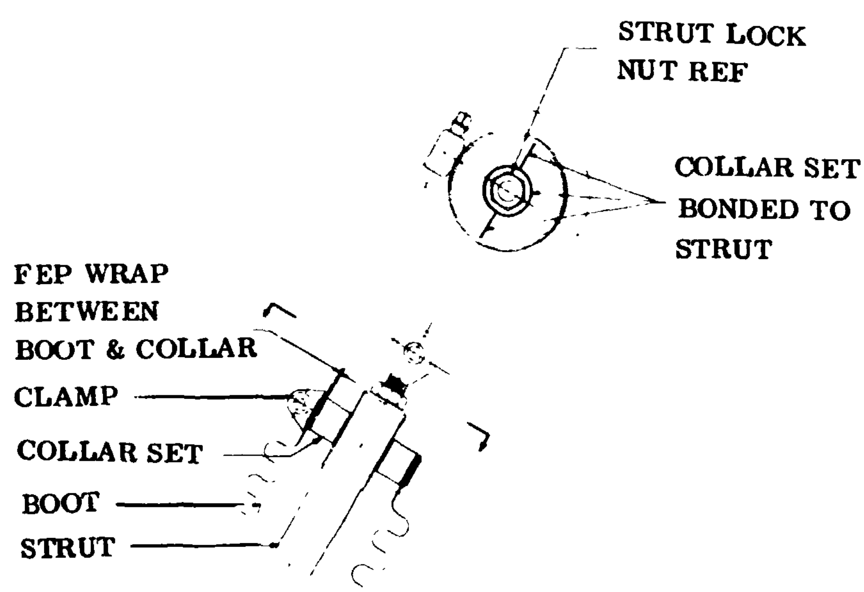

DETAIL "C"
TYPICAL BOOT TO STRUT ATTACHMENT

Figure 70. Purge Bag Assembly

PRECEDING PAGE BLANK NOT FILMED

The bag is made from a laminate consisting of two plys of epoxy/181 Style fiberglass cloth sandwiched between two FEP Teflon skins.

3.3.6.1 Forward Bag Section. The forward bag section is a single piece semi-rigid unit incorporating a flange at each end and a stiffener ring. The flange at the forward end contains helical coil inserts for fastening to the penetration panel. The aft flange contains a through hold pattern (no helical coils) with countersunk surfaces for receiving the screws and sealing accessories. The stiffener ring is located near the tangent line (between the conical and curved surfaces) and is bonded to the exterior surface of the bag.

3.3.6.2 Aft Bag Section. The aft bag section is a single piece semi-rigid assembly containing one flange, six boots for receiving the tank support struts, and two stiffener rings. The aft end is capped off with an integral spherical section and the flange contains helical coils for fastening to the mating forward bag. The six boots are convoluted FEP tubes bonded to aluminum alloy fairings. The fairings provide the transition from the bag wall profile to a tubular configuration. All fairings contain a flange section which is bonded to the inboard side of the bag wall. The two stiffener rings are located near the profile tangent lines and are bonded to the external surface of the bag wall.

3.3.6.3 Flanged Joints and Strut Seals. The flanged joints which interconnect the two bag sections and the penetration panel are sealed with a continuous pre-cured epoxy/fiberglass strip bonded to the outside diameter of the flanges (see Figure 70). Sealing for the screws is accomplished with epoxy/fiberglass buttons bonded to the countersunk surfaces on the flanges. The boots are attached to the struts through epoxy/fiberglass collars. Sealing between struts and boots is accomplished by bonding the collars to the struts and clamping the boot ends to the collars with standard CRES fittings.

3.3.6.4 Bag Support System. The bag assembly is supported at the forward end by a fixed connection between the penetration panel and a hub welded to the tank vent line. Radial restraint only is provided at the aft end by attaching stand-off buttons to the ends of the MLI support pins. These MLI support pins are bonded to the fairing structure. In actual vehicle applications, radial restraint may be accomplished by connecting the external stiffener ring to the vehicle structure with drag links.

3.3.6.5 Bag Profile. Commonality of tooling; minimum purge gas volume; structural integrity; and clearances between bag, MLI, test enclosure, and support struts are the primary factors which determined the bag profile. Except for the forward end (at the penetration panel) and the aft spherical cap section, the profiles for both bag sections are identical. The length of the cylindrical sections were fixed by the clearances required between the strut boots and the girth flanges. To avoid a hoop compression mode, the transition radius between the conical and cylindrical sections was made equal to 1/4 the diameter at the girth The diameter at the girth in turn was determined by the clearance required between bag and MLI.

3.3.6.6 Bag Wall and Penetration Panel Construction. The bag wall is a high temperature cured composite consisting of pre-impregnated epoxy/fiberglass (2 plys) sandwiched between two 0.0051 cm (0.002 in) thick FEP film layers. The purpose of the FEP films is to reduce gas permeability and moisture absorption. The two ply epoxy/fiberglass is the minimum gage due to poor tear strength of a single ply layup. Greater than two plys are used to reinforce areas at the flanges and the strut penetration zones.

The penetration panel walls are similar to the bag except one layer only of FEP film is used on the inner surface. The panel wall thicknesses exceed those for the bag due to the necessity for numerous cut outs and stiffened areas to carry structural loads.

3.3.6.7 Penetration Panel. The penetration panel contains the purge and repressurizati . fluid loop hardware, instrumentation pass through fittings and provides the primary support for the entire bag assembly (see Figure 71). The basic panel is an integral "dish type" member flanged at the base and attached to a cylindrical section located at the center. The cylindrical section in turn interfaces with a hub on the tank vent line through a sealed flange connection.

One vent valve, one bleed valve, one gas inlet valv two pressure switches, one relief valve, two valve filters, eight instrumentation pass through fittings, and one gas feed line are attached to the flat section of the panel. The locations of these components are dictated by the structural requirements for the panel and accessability. Except for the vent, bleed and inlet valves, all components are bulkhead mounted through the panel with adhesive seals. Helical coil inserts in the panel and flat gaskets provide the mounting and sealing for the three valves and two filters.

3.3.7 INSTRUMENTATION. The complete test article assembly has instrumentation for the liquid level plus temperatures at the internal and external surfaces on the fill/vent/drain line, tank wall surfaces, fairings, MLI blankets, support struts, purge bag, pressurization system, and the test enclosure structure. Included are four gages located at the aft end of the purge bag for sensing interstitial pressures. One hundred-seven points are instrumented. Carbon type sensors are used for liquid level sensing and chromel/constantan thermocouples with welded junctions are used for temperature sensing.

For the MLI blankets, temperature sensing is provided throughout the core and face sheets, the twin pin fasteners, and the primary support pins. Details of the test tank instrumentation system design will be presented in the next phase report for the study.

3.3.8 WEIGHT ANALYSIS. Weight computations were made for each component in the bag sections, penetration panel, pressurization system, MLI lay-up, purge gas distribution and the fairings. Assembly hardware such as rivets, bolts, washers, seals, retainers, MLI fasteners, etc, were also included. For those parts constructed

FOLDOUT FRAME 1

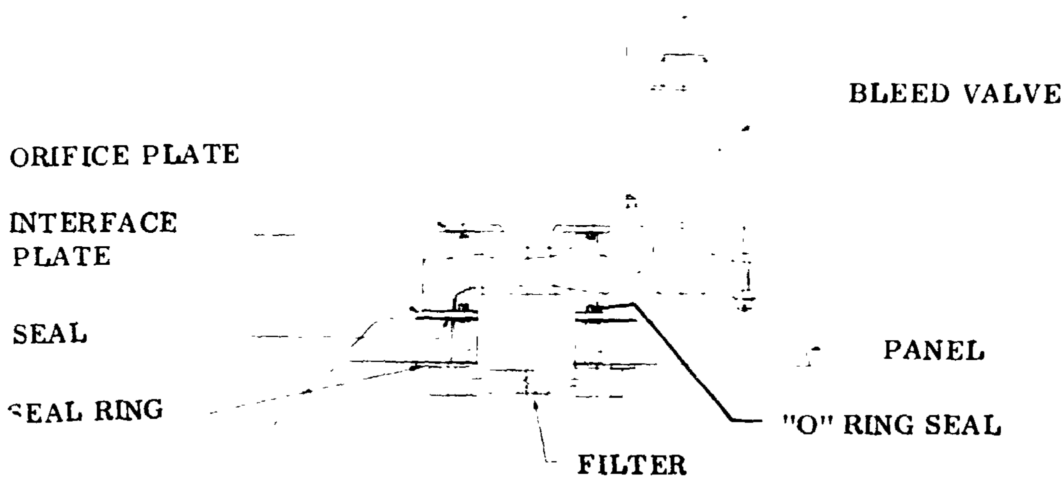

SECTION BB
BLEED VALVE INSTALLATION

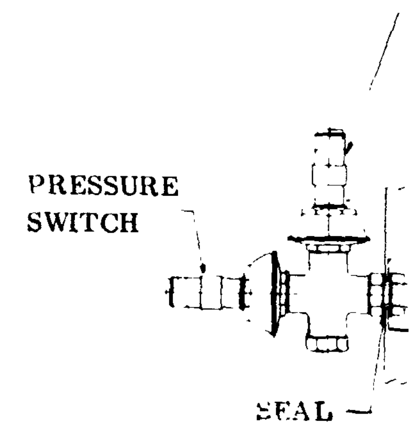

SECTION
PRESSURE SWITCH

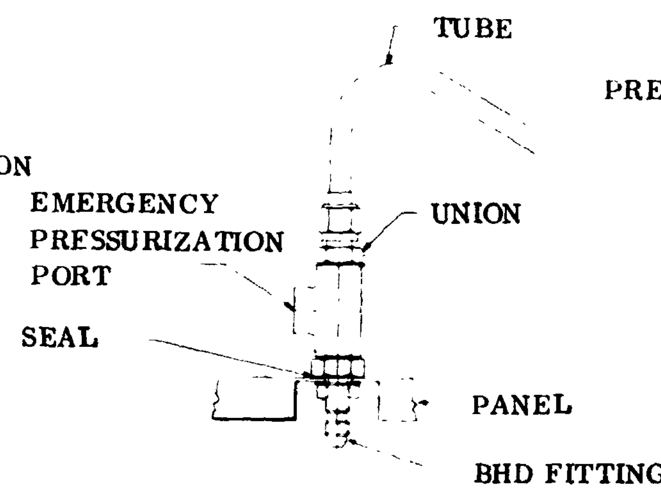

SECTION KK
(ROTATE 60° CCW)

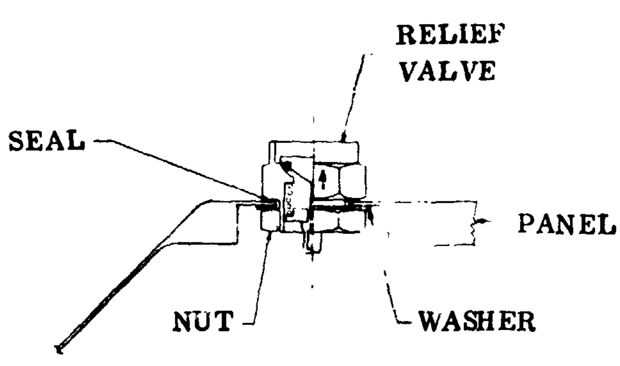

SECTION CC
RELIEF VALVE INSTALLATION

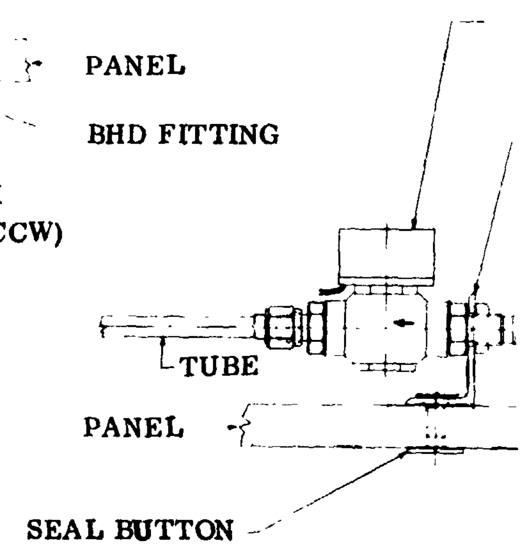

SECTION E
SUPPLY VALVE INST

FOLDOUT FRAME 2

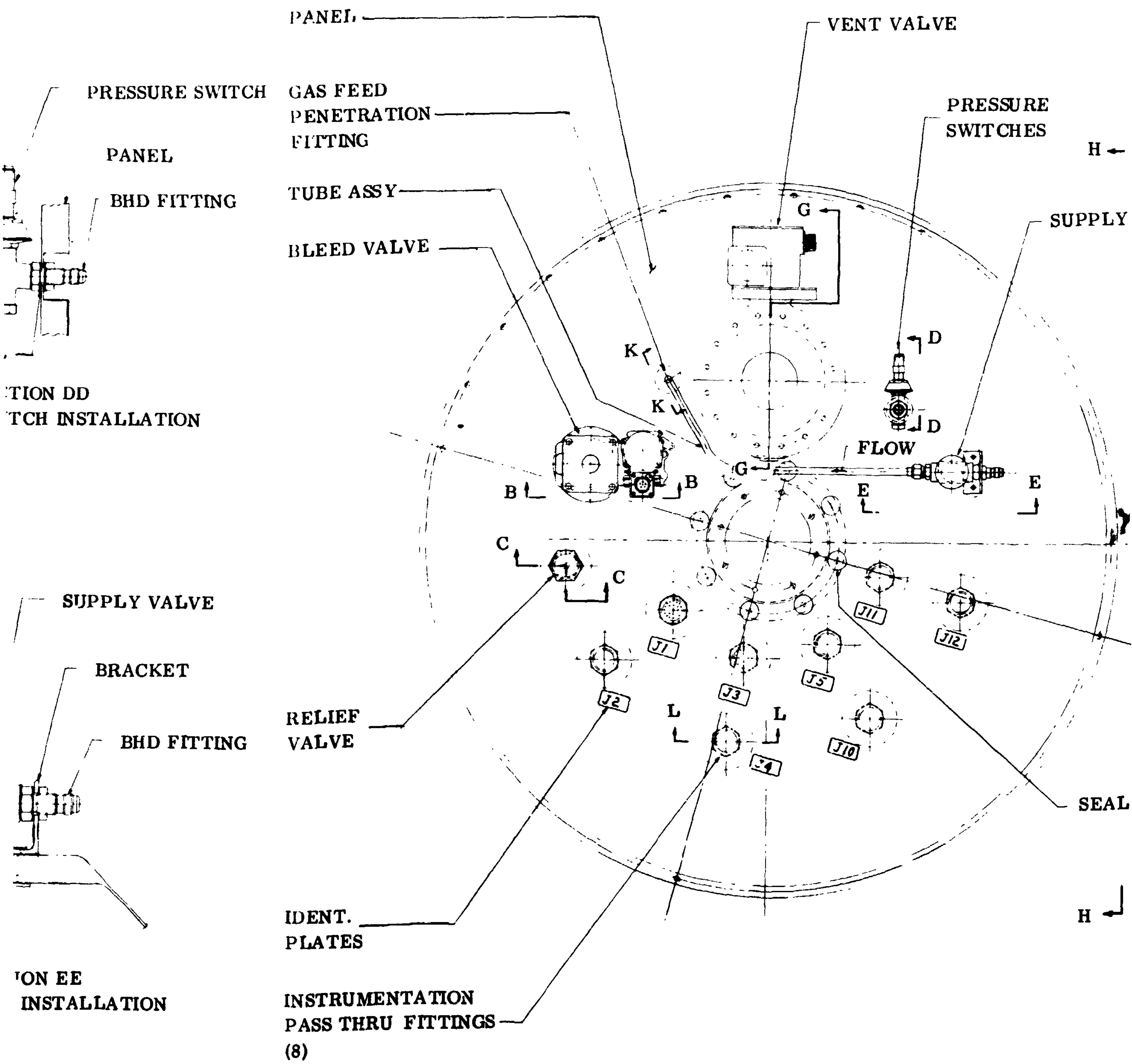

FOLDOUT FRAME 3

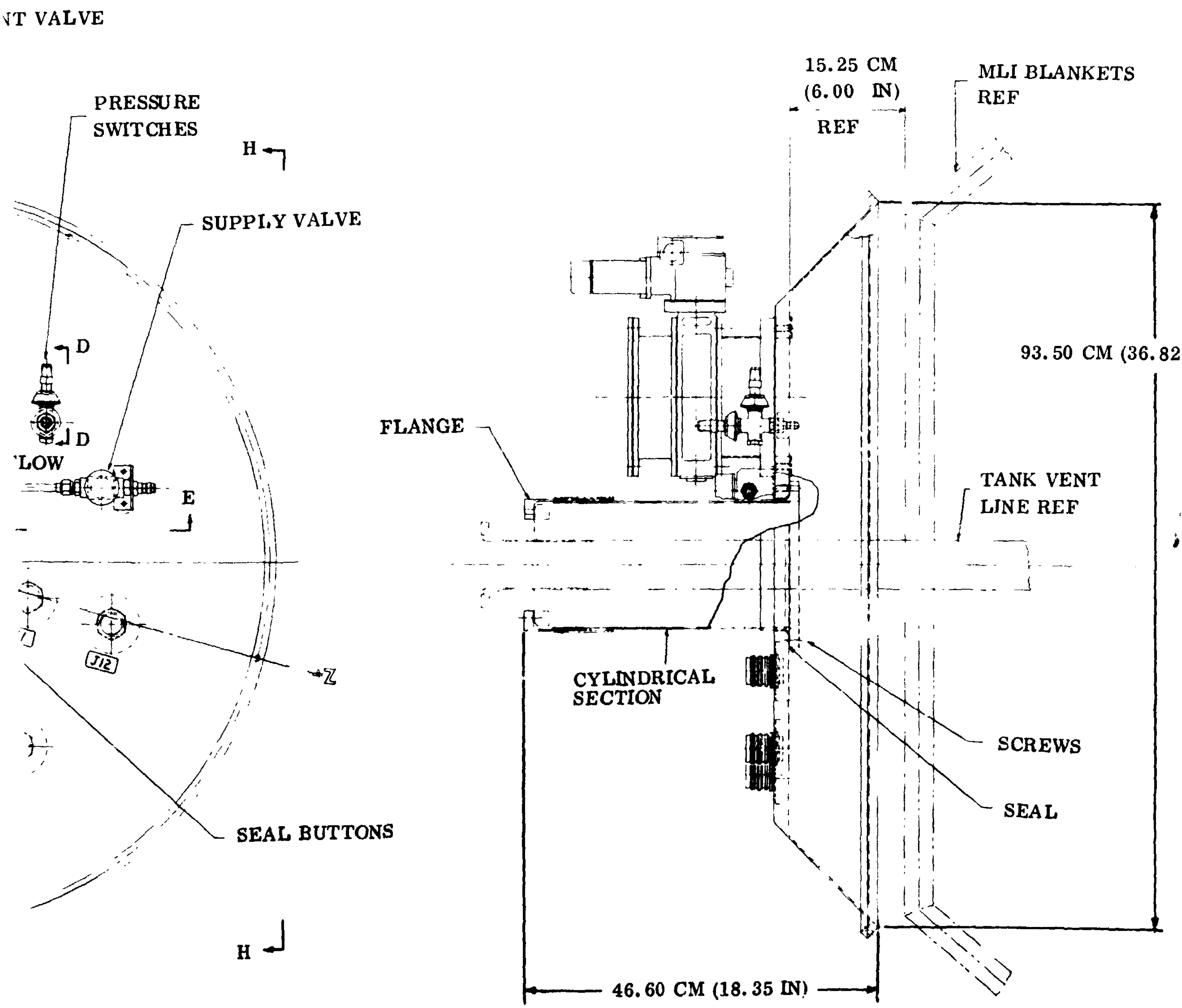

VIEW HH

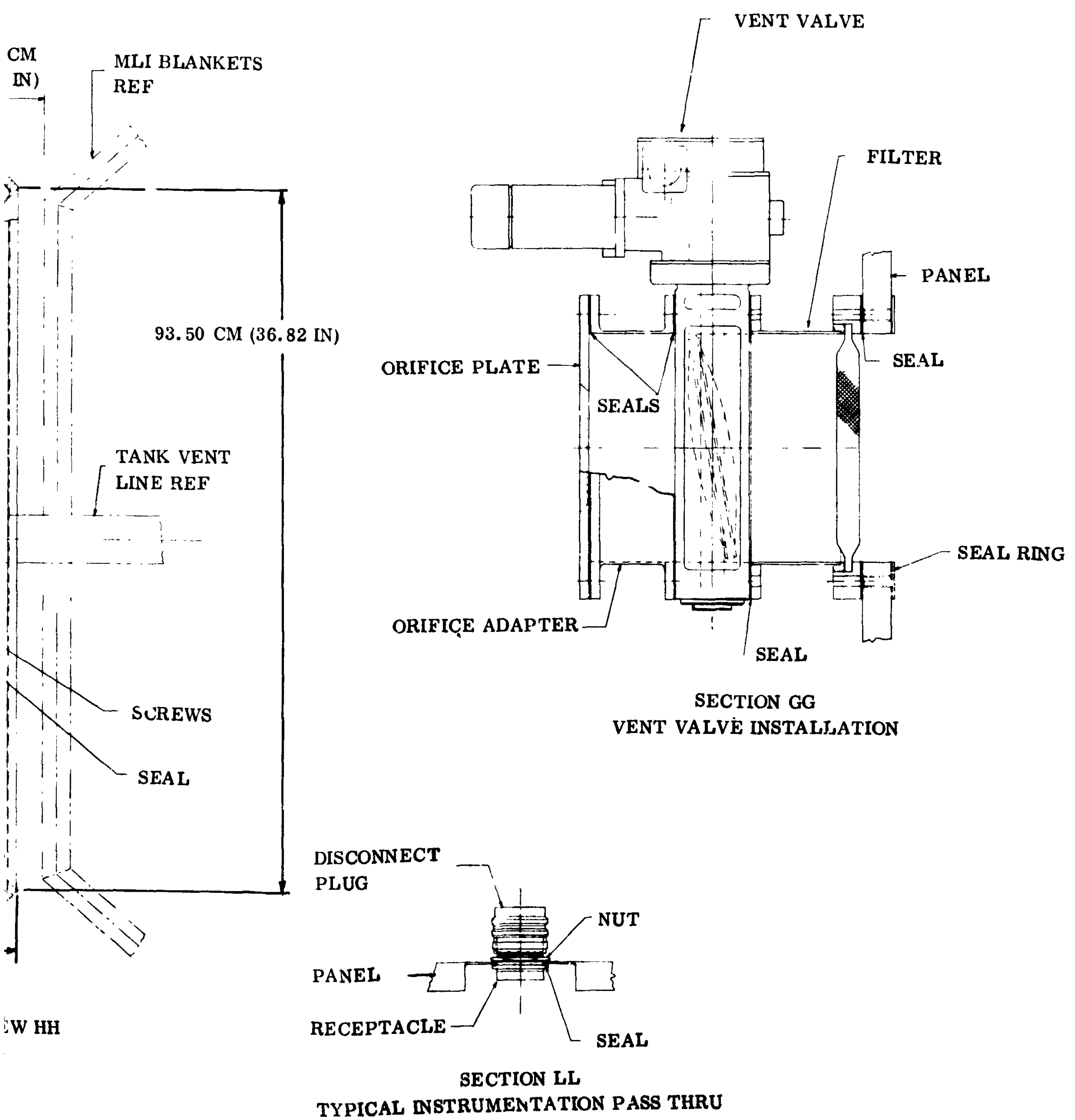

Figure 71. Penetration Panel Assembly

PRECEDING PAGE BLANK NOT FILMED

from epoxy/fiberglass, a comparative weight was determined using epoxy/PRD49 combination. A summary of the results is shown in Table 9. The system reflects flight designs where possible and incorporates flight proven fluid loop hardware. The existing fairing system for the test tank requires new structural addition in the flat panel sections to withstand the repressurization loads. The weight of the fairings is therefore unrealistically high for a flight type tankage system due to these flat sections.

Weight reductions of 15.7% for the bag/penetration panel areas and 23% for the fairings can be expected when using DuPont's New High-Modulus Fiber PRD49. This is conservative since gage reductions were not considered in the penetration panel or fairings. The wall thickness for the bag would not be reduced since two ply is the minimum acceptable gage thickness.

The increased strength, greater stiffness and lower density of PRD49 cloth compared to fiberglass offers several distinct advantages for its use in an application such as the purge bag and fairing system. The material however, is still in the experimental stage and has a limited availability and high cost when compared to fiberglass. For this reason the PRD49 was not selected as a substitute material for the 181 Style fiberglass. The PRD49, however, shows definite promise for future usage as an improved state of the art material.

3.3.9 TEST ARTICLE ASSEMBLY. The complete test article includes instrumentation, purge distribution system, MLI lay-up, forward and aft bag sections, tank supports,

Table 9. Weight Summary

	Weight Using Epoxy/Style 181 Fiberglass		Weight Using Epoxy PRD 49	
Item	Kilograms	Pounds	Kilograms	Pounds
Forward Bag Section	13.10	28.88	9.95	21.91
Aft Bag Section	13.35	29.44	10.30	22.79
Penetration Panel	15.65	34.50	11.80	26.04
Bag Assembly Hardware	1.13	2.49	1.02	2.25
Purge and Pressurization System Hardware	11.20	24.65	11.20	24.65
MLI Lay-up	12.90	28.35	12.90	28.35
MLI Fasteners and Supports	1.10	2.43	0.96	2.13
Purge Distribution Hardware	0.92	2.03	0.89	1.95
Total for Bag, Panel, MLI and Purge System	69.35	152.77	59.02	130.07
Forward Fairing	11.90	26.26	9.45	20.82
Girth Fairing	8.30	18.30	6.03	13.30
Aft Fairing	9.25	20.45	7.05	15.53
Total for Fairings	29.45	65.01	22.53	49.65

penetration panel, pressurization system, and fill/drain/vent assembly. The completed test article is installed in an enclosure which simulates vehicle structure. The assembly sequence is shown in Figure 72.

With the tank suspended from the vent tube, the assembly starts with the MLI blankets and instrumentation (external to the fairings) as shown in Step 1. Prior to Step 1, the tank wall instrumentation, fairings, and purge distribution tubing is installed. All electrical leads inside the fairing have also been bundled and sealed to the pass through fitting in the flat panel section of the fairing. The following procedure is used in Step 1.

a. Engage the MLI gore blankets with the support pins on the fairing (one at a time) and check the overall fit.

b. Install the twin pin fasteners.

c. After all gore blankets are installed, holes through the blankets are cut for the support struts, and the fit between strut and hole checked.

d. Insulate the struts and check the fit between the strut insulation and the blankets.

e. Install the forward and aft MLI cap blankets.

f. Insulate the vent line.

g. Install the MLI components for the purge gas and electrical penetrations.

The instrumentation leads for the MLI and the fairing are bundled at the forward flat cap area and prepared for connection to the pass through fittings in the penetration panel.

Step 2 consists of positioning and holding the aft bag section, engaging the struts with the tank fittings, and checking the fit between the MLI on the strut and the gore blankets. During this maneuver, the instrumentation leads for the struts and the cables for the interstitial gas pressure gages are threaded through the sealing coll[illegible] on two of the struts.

For Step 3, the assembly is transferred to a handling fixture which incorporates clips for maintaining the aft bag position. The tank is now supported by the struts which attach to the handling fixture.

The forward bag section is positioned in Step 4, and the girth joint assembled including the [illegible] accessories.

In Step 5 the penetration panel is positioned and held forward of the assembly while the electrical leads are connected to the pass through fittings on the panel.

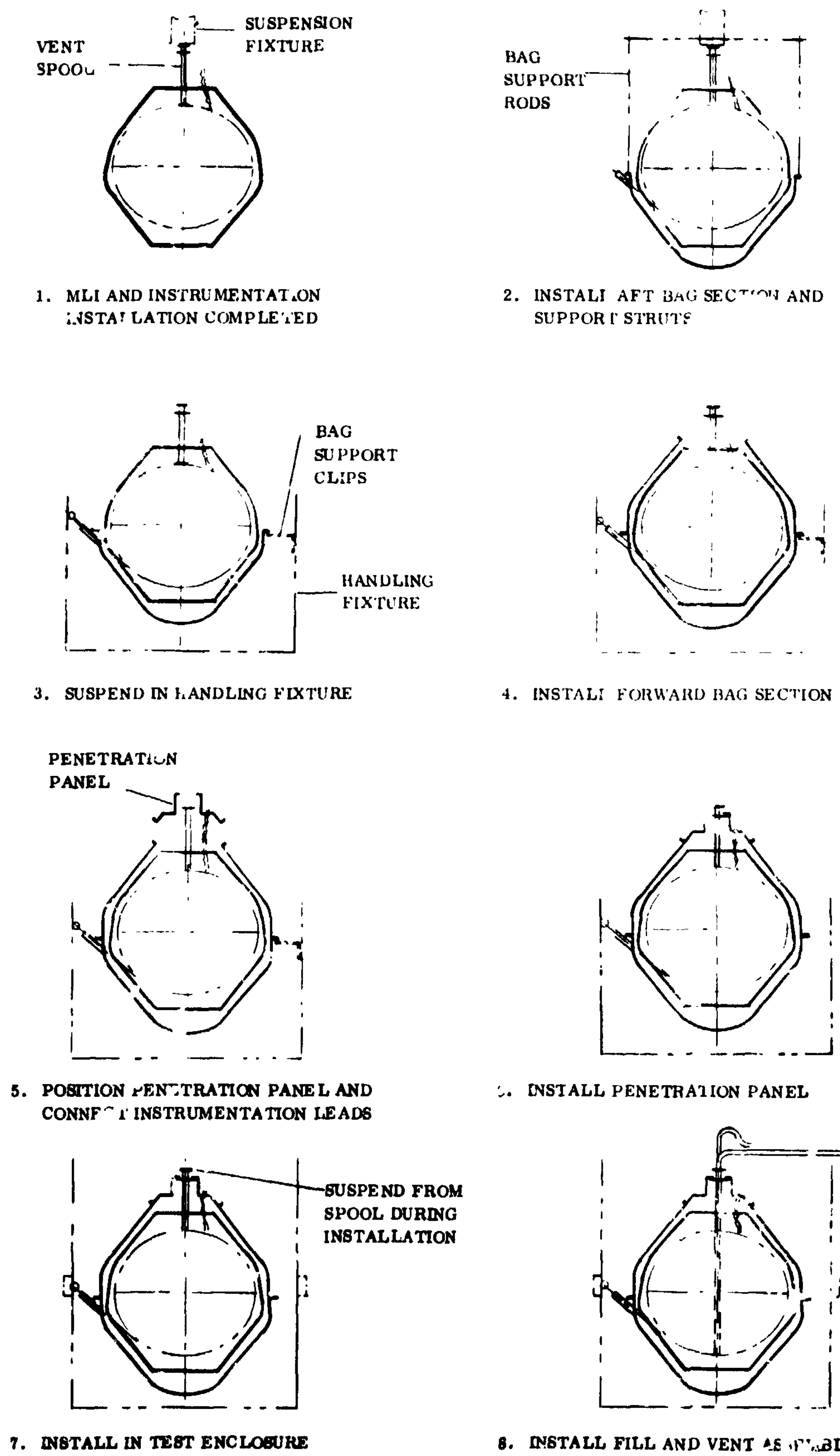

Figure 72. Assembly Sequence

The penetration panel is lowered into position in Step 6 and connected to the forward bag section and to the hub on the vent tube. The total bag assembly is now supported from the penetration panel. The wiring bundles are inspected and the final purge line connection made using the 15.25 cm (6 in) vent hole in the panel as on access port. The remaining pressurization system components are installed, the boots sealed to the struts, and a leak check performed.

In Step 7, the assembly is removed from the fixture and installed in the test enclosure.

The test article is completed in Step 8 by installing and insulating the fill/drain/vent line assembly.

4

REFERENCES

1. Walburn, A. B., et al, "Design and Development of Pressure and Repressurization Purge System for Reusable Space Shuttle Multilayer Insulation Systems, Second Quarterly Progress Report," Contract NAS8-27419, GD/CA Report 632-1-3, 18 February 1972.

2. Walburn, A. B., et al, "Design and Development of Pressure and Repressurization Purge System for Reusable Space Shuttle Multilayer Insulation Systems, First Quarterly Progress Report," Contract NAS8-27419, GD/CA Report 584-4-708, 1 December 1971.

3. Krause, D. R., et al, "Development of Lightweight Material Composites to Insulate Cryogenic Tanks for 30-Day Storage in Outer Space," Contract No. NAS8-26006, MDC G2742, Final Report, June 1972.

4. Telephone Conversation Between G. Fredrickson of McDonnell Douglas and R. Jennings of General Dynamics Convair Aerospace, July 1972.

5. O'Neill, R. F., "Convair Thermal Analyzer," GD/CA Computer Program No. P4560, GD/CA Report No. GDC-BTD69-005, 29 May 1969.

6. "Investigations Regarding Development of a High Performance Insulation System," Contract No. NAS8-20758, Final Report, Lockheed Missiles and Space Co., Report No. K-17-68-5, 25 July 1968.

7. Betts, W. S. and G. A. Howell, "An Analytical Solution for Determining the Heat Leakage to the 87.6 Inch Tank," GD/CA Report No. 584-4-416, 23 October 1969.

8. Leonhard, K. E., et al, "Development of a New Superinsulation for Cryogenic Space Tankage," ASME Aviation and Space Division Conference, June 1968.

9. Leonhard, K. E., et al, "Cryogenic Insulation Development," Final Report, Contract No. NAS8-26129, Report No. GD/CA-DDB72-004, 28 July 1972.

10. Burton, K. R., "Amps Propellant Tank Heat Transfer," GD/CA Report No. 584-4-149, 2 April 1968.

11. Corruccini, R. J., "Gaseous Heat Conduction at Low Pressures and Temperatures," Vacuum, Vol. VII and VIII, 1957-1958, published April 1959.

12. Leonhard, K. E., W. S. Betts, F. O. Bennett, R. E. Tatro, "Cryogenic Tank Test Program," GDC-ERR-1419, December 1969.

13. Leonhard, K. E. and Hyde, E. H., "Flightworthy, High Performance Insulation Development," Cryogenic Technology, Vol. 7, Nos. 1 and 2, Jan-Feb and Mar-Apr 1971.

APPENDIX A

THERMAL AND PHYSICAL PROPERTY TABLES USED IN THERMAL ANALYSIS

Table 1. D-G-K MLI Overall Interchange Factor ($\mathcal{F}$) - 12 MLI Shields

Source: Computed from specification parameters per para. 3.2.4.1

Temperature (R)	$\mathcal{F}$
40.	0.0012
600.	0.0012

Table 2. Superfloc Dacron Needle Thermal Conductivity

Source: Reference 9

Temperature (R)	K (Btu/hr-ft-R)
0.	0.807×10^{-6}
200.	0.884×10^{-6}
400.	0.970×10^{-6}
600.	1.050×10^{-6}

Table 3. Polyphenylene Oxide (PPO) Thermal Conductivity

Source: Reference 9

Temperature (R)	K (Btu/hr-ft-R)
40.	0.033
80.	0.050
150.	0.069
300.	0.086
800.	0.137

Table 4. Fiberglass Thermal Conductivity

Source: Reference 9

Temperature (R)	K (Btu/hr-ft-R)
25.	0.085
100.	0.137
200.	0.200
250.	0.226
300.	0.249
350.	0.266
400.	0.278
450.	0.285
500.	0.288
550.	0.290

Table 5. Purge Bag to Shroud Overall Radiation Interchange Factor ($\mathcal{F}$)

Source: Computed

Temperature (R)	$\mathcal{F}$
0.	0.693
1000.	0.693

Table 6. Aluminum Thermal Conductivity

Source: Reference 13

Temperature (R)	K (Btu/hr-ft-R)
40.	38.
60.	40.
110.	50.
170.	60.
260.	72.
410.	88.
660.	102.

Table 7. D-G-K Overall Radiation Interchange Factor ($\mathcal{F}$) 45 Slides

Source: Reference 7

Temperature (R)	$\mathcal{F}$
50.	0.000247
100.	0.000274
200.	0.000309
300.	0.000327
400.	0.000332
500.	0.000330
600.	0.000327

Table 8. D-A-M Fill and Drain Line Insulation Overall Radiation Interchange Factor ($\mathcal{F}$) - 45 Shields

Source: Reference 7

Temperature (R)	$\mathcal{F}$
287.5	0.000403
317.5	0.000399
347.5	0.000395
377.5	0.000392

Table 9. D-A-M Instrumentation and Vent Line Insulation Overall Radiation Interchange Factor ($\mathcal{F}$) - 45 Shields

Source: Reference 7

Temperature (R)	$\mathcal{F}$
287.5	0.000435
317.5	0.000427
347.5	0.000420
377.5	0.000418

Table 10. Thermocouple Effective Thermal Conductivity

Source: Computed

Temperature (R)	K (Btu/hr-ft-R)
0.	0.
50.	557.
100.	286.
200.	171.
300.	155.
600.	155.

Table 11. MLI Interstitial Gas Pressure

Source: Specified Parameter

Time (sec)	Pressure (Torr)
0.	1×10^{-5}
1000.	1×10^{-5}

Table 12. Titanium Thermal Conductivity

Source: Reference 7

Temperature (R)	K (Btu/hr-ft-R)
10.	0.30
60.	1.6
110.	2.25
160.	2.70
210.	2.90
260.	3.00
310.	3.20
360.	3.50
410.	3.80
460.	4.15
510.	4.45
550.	4.70

Table 13. Strut Internal MLI Overall Radiation Interchange Factor ($\mathcal{F}$) - 31 Shields

Source: Reference 7

Temperature (R)	$\mathcal{F}$
100.	0.00078
150.	0.00079
200.	0.00080
250.	0.00082
300.	0.00083
400.	0.00087
500.	0.00090
550.	0.00092

Table 14.. CRES Thermal Conductivity

Source: Reference 7

Temperature (R)	K (Btu/hr-ft-R)
0.	0.
60.	2.3
110.	4.0
160.	5.2
210.	6.0
260.	6.6
310.	7.05
360.	7.55
410.	8.0
460.	8.4
510.	8.9
535.	9.05

Table 15. Outer Face Sheet-to-Purge Bag Overall Radiation Interchange Factor ($\mathcal{F}$)

Source: Computed

Time (sec)	$\mathcal{F}$
0.	0.273
100.	0.273